Chloroplast Retrograde Signaling via GUN1 and Organellar Responses to Drought Stress in *Arabidopsis*

Dissertation

zum Erwerb des Doktorgrades der Naturwissenschaften

(Dr. rer. nat)

Dissertation der Fakultät für Biologie

der Ludwig-Maximilians-Universität München

vorgelegt von

Qian Tang

München, 04.12.2024

Die Dissertation wurde unter der Leitung von PD Dr. Kleine, Tatjana
an der Fakultät für Biologie
der Ludwig-Maximilians-Universität München (LMU)

angefertigt

Gutachter:	PD Dr. Tatjana Kleine
Zweitgutachter:	Prof. Dr. Wolfgang Frank
Tag der Abgabe:	04.12.2024
Tag der mündlichen Prüfung:	25.02.2025

Eidesstattliche Erklärung:

Ich versichere hiermit an Eides statt, dass die vorgelegte Dissertation von mir selbstständig und ohne unerlaubte Hilfe angefertigt wurde. Des Weiteren erkläre ich, dass ich nicht anderweitig ohne Erfolg versucht habe, eine Dissertation einzureichen oder mich der Doktorprüfung zu unterziehen. Die folgende Dissertation liegt weder ganz noch in wesentlichen Teilen einer anderen Prüfungskommission vor.

_____

Qian Tang

München, 04.12.2024

Statutory declaration

I declare that I have authored this thesis independently, that I have not used other than the declared sources/resources. Furthermore, I declare that I have not submitted a dissertation without success or failed to pass the oral examination. The present dissertation (neither the entire dissertation nor parts) has not been presented to another examination board.

_____

Qian Tang

München, 04.12.2024

Content

Abbreviations

ABA	Abscisic acid
ABI4	ABSCISIC ACID INSENSITIVE 4
accD	Acetyl-CoA carboxylase beta subunit
APX	Ascorbate peroxidase
Arabidopsis	Arabidopsis thaliana (L.) Heynh
AS	Alternative splicing
bp	Base pairs
CA	CARBONIC ANHYDRASE
Ca^{2+}	Calcium ion
CHLH	H subunit of Mg-chelatase
cpDNA	Chloroplast DNA
EMB2217	EMBRYO DEFECTIVE 2217
EMSA	Electrophoretic mobility shift assay
FC1	Ferrochelatase 1
FLM	FLOWERING LOCUS M
GUN1	GENOMES UNCOUPLED1
IR	Inverted repeat
LHCB	Light-harvesting chlorophyll a/b-binding proteins of photosystem II
LIN	Lincomycin
LSC	Large single copy
MgProto	Mg protoporphyrin IX
MS	Murashige and Skoog medium
NDH	NADH dehydrogenase-like
NEP	Nuclear-encoded RNA polymerase
NF	Norflurazon
NIP	Nucleotide immunoprecipitation
NPQ	Non-photochemical quenching
O^{2-}	Superoxide
P	Proline

Abbreviations

PEP	Plastid-encoded RNA polymerase
PhANGs	Photosynthesis-associated nuclear genes
PLS	PPR-like subfamily
PPR	Pentatricopeptide repeat protein
PS	Photosystem
psbA	D1 protein of photosystem II
pTAC2	PLASTID TRANSCRIPTIONALLY ACTIVE 2
PTM	Plant homeodomain (PHD) transcription factor
Rubisco	Ribulose 1,5-bisphosphate carboxylase/oxygenase
rbcL	Rubisco large subunit
rbcS	Rubisco small subunit
RBPs	RNA-binding proteins
RIP-seq	RNA immunoprecipitation sequencing
ROS	Reactive oxygen species
SMR	Small MutS-related
SOD	Superoxide dismutase
SOT1	SUPPRESSOR OF THYLAKOID FORMATION 1
SSC	Small single copy
SVR7	SUPPRESSOR OF VARIEGATION 7
TCA	Tricarboxylic acid
TIC	Translocon at the inner chloroplast membrane
TOC	Translocon at the outer chloroplast membrane
tRFs	tRNA-derived RNA fragments
UTRs	Untranslated regions

Declaration of contribution as a co-author

Chapter 1:

Tang, Q., Xu, D., Lenzen, B., Brachmann, A., Yapa, M. M., Doroodian, P., Schmitz-Linneweber, C., Masuda, T., Hua, Z., Leister, D., & Kleine, T. (2024). GENOMES UNCOUPLED PROTEIN1 binds to plastid RNAs and promotes their maturation. Plant Communications, 101069. https://doi.org/10.1016/j.xplc.2024.101069

Conceptualization: Q.T., D.X., and T.K.; formal analysis and supervision: T.K.; investigation: Q.T., D.X., A.B., B.L., M.M.Y., T.M., Z.H. and T.K.; writing – original draft: T.K. with input from Z.H., C.S.-L. and D.L.; – review and editing: all authors; funding acquisition: C.S.-L., Z.H., D.L., and T.K.

Chapter 2:

Xu, D., **Tang, Q.**, Xu, P., Schäffner, A. R., Leister, D., & Kleine, T. (2023). Response of the organellar and nuclear (post)transcriptomes of *Arabidopsis* to drought. Frontiers in Plant Science, 14. https://doi.org/10.3389/fpls.2023.1220928

Conceptualization, TK and DX; Methodology, DX, QT, PX, and TK; Validation, DX and QT; Formal Analysis, TK; Investigation, DX, QT, and TK; Resources, DL, AS and TK; Writing – Original Draft, TK; Writing – Review & Editing, QT, DX, DL, AS and TK; Funding Acquisition, DL and TK Supervision, TK. All authors contributed to the article and approved the submitted version

Summary

Although plants are sessile organisms, they have developed sophisticated mechanisms to adapt and evolve, securing their ecological niches against a wide range of threats. A crucial aspect of this adaptation is retrograde signaling, a communication process from chloroplasts to the nucleus. GENOMES UNCOUPLED1 (GUN1) is the key regulator in the retrograde signaling pathway. **Chapter 1** of this thesis presents new insights into GUN1's function. The study of *gun1* seedlings with white and pale cotyledons demonstrates that GUN1 deficiency significantly alters the entire plastid transcriptome, with the absence of plastid rRNAs and a reduction in nearly all plastid transcripts explaining the chlorophyll-deficient phenotype. Reevaluation of GUN1 as a potential PPR protein, hypothesized to bind RNA, was conducted using *in silico* PPR motif-based predictions, validated by *in vivo* RNA immunoprecipitation sequencing (RIP-seq) experiments, and confirmed by *in vitro* gel electrophoresis mobility shift assays (EMSA). These analyses reveal GUN1 as a bona fide RNA-binding protein. Moreover, this work identifies several putative GUN1 targets, including tRNAs and RNAs derived from *ycf1.2*, *rpoC1*, *rpoC2*, and the *ndhH-ndhA-ndhI-ndhG-ndhE-psaC-ndhD* gene cluster. These findings lay a foundation for further investigation into GUN1's function and its critical role in retrograde signaling.

In addition to their adaptive mechanisms, plants have developed strategies to cope with drought, involving significant changes in nuclear and organellar gene expression. **Chapter 2** employed RNA-sequencing after ribosomal RNA depletion to track (post)transcriptional changes over a series of time points during drought exposure in *Arabidopsis* Col-0, with a particular focus on both organellar and nuclear (post)transcriptomes. Chloroplast transcript levels were globally reduced, accompanied by a noticeable decrease in RNA editing efficiency, though splicing remained largely unaffected. In contrast, mitochondrial transcripts exhibited a slight increase, with no significant changes in editing or splicing. The study also revealed extensive alternative splicing (AS) events, affecting nearly 1,500 nuclear genes, 42% of which were regulated exclusively at the level of AS. This included 927 isoform switching events, suggesting a critical role for AS in enhancing proteome diversity as a response to drought stress. Notably, the research identified several key

candidates, such as carbonic anhydrase mutants (*ca1* and *ca2*), which exhibited increased drought tolerance. Additionally, the data suggest that the accumulation of a nonfunctional *FLM* (*FLOWERING LOCUS M*) isoform, rather than the ratio of *FLM-ß* and -*δ* isoforms, may be responsible for the early flowering phenotype observed under long-day drought conditions. These findings provide new insights into the complex molecular mechanisms that plants use to adapt to drought, offering potential strategies for improving crop resilience to such stresses.

Zusammenfassung

Obwohl Pflanzen sessile Organismen sind, haben sie hochentwickelte Mechanismen entwickelt, um sich anzupassen und weiterzuentwickeln und so ihre ökologischen Nischen gegen eine Vielzahl von Bedrohungen zu sichern. Ein wesentlicher Aspekt dieser Anpassung ist retrograde Signaltransduktion, ein Kommunikationsprozess von den Chloroplasten zum Zellkern. GENOMES UNCOUPLED1 (GUN1) ist der Schlüsselregulator des retrograden Signals. Kapitel 1 dieser Arbeit präsentiert neue Erkenntnisse über die Funktion von GUN1. Die Untersuchung von *gun1*-Keimlingen mit weißen und blassen Keimblättern zeigt, dass der Mangel an GUN1 das gesamte Plastiden-Transkriptom signifikant verändert. Das Fehlen von Plastiden-rRNAs und die Reduktion fast aller Plastiden-Transkripte erklären den chlorophyll-defizienten Phänotyp. Eine Neubewertung von GUN1 als mögliches PPR-Protein, das RNA binden könnte, wurde mittels *in silico* PPR-motivbasierter Vorhersagen durchgeführt, validiert durch *in vivo* RNA-Immunopräzipitationssequenzierung (RIP-seq) Experimente und bestätigt durch *in vitro* Gelelektrophorese-Mobilitätsverschiebungstests (EMSA). Diese Analysen bestätigen, dass GUN1 tatsächlich RNA bindet. Darüber hinaus identifiziert diese Arbeit mehrere mutmaßliche Zieltranskripte von GUN1-, darunter tRNAs und RNAs, die von *ycf1.2*, *rpoC1*, *rpoC2* und dem *ndhH-ndhA-ndhI-ndhG-ndhE-psaC-ndhD*-Gencluster stammen. Diese Erkenntnisse legen eine Grundlage für weitere Untersuchungen zur Funktion von GUN1 und seiner wichtigen Rolle im retrograden Signalweg.

Neben ihren Anpassungsmechanismen haben Pflanzen Strategien entwickelt, um mit Trockenheit umzugehen, die bedeutende Veränderungen in der Zellkern- und Organellen-Genexpression beinhalten. Kapitel 2 verwendete RNA-Sequenzierung nach der Depletion von ribosomaler RNA, um (post)transkriptionelle Veränderungen über eine Reihe von Zeitpunkten während der Trockenheitsexposition in *Arabidopsis* Col-0 zu verfolgen, mit besonderem Fokus auf sowohl Organellen- als auch Zellkern-(post)transkriptomen. Die Transkriptlevel in Chloroplasten waren global reduziert, begleitet von einem deutlichen Rückgang der RNA-Editierungseffizienz, während das Spleißen weitgehend unbeeinflusst blieb. Im Gegensatz dazu zeigten mitochondriale Transkripte einen leichten Anstieg, ohne signifikante Veränderungen in der Editierung oder dem Spleißen. Die Studie zeigte auch

umfangreiche alternative Spleißereignisse (AS), die fast 1.500 zellkernkodierte Gene betrafen, von denen 42 % ausschließlich auf der Ebene des alternativen Spleißens reguliert wurden. Dazu gehörten 927 Isoform-Wechselereignisse, was auf eine wichtige Rolle des alternativen Spleißens bei der Erhöhung der Proteomvielfalt als Reaktion auf Trockenstress hindeutet. Besonders hervorzuheben sind einige Schlüsselgene, wie Karboanhydrase-Mutanten (*ca1* und *ca2*), die eine erhöhte Trockenheitstoleranz zeigten. Darüber hinaus legen die Daten nahe, dass die Anhäufung einer nicht funktionellen *FLM* (*FLOWERING LOCUS M*)-Isoform, und nicht das Verhältnis der *FLM-ß*- und -*δ*-Isoformen, für den unter langtägigen Trockenheitsbedingungen beobachteten frühblühenden Phänotyp verantwortlich sein könnte. Diese Erkenntnisse bieten neue Einblicke in die komplexen molekularen Mechanismen, die Pflanzen zur Anpassung an Trockenheit nutzen, und bieten potenzielle Strategien zur Verbesserung der Resilienz von Nutzpflanzen gegenüber solchen Belastungen.

1 Introduction

1.1 Origin of chloroplasts

Plants are sessile organisms that utilize organelles called plastids to carry out various essential functions. Among the different types of plastids, the chloroplast is the specialized form responsible for oxygenic photosynthesis. Chloroplasts are double membrane-bound organelles, that not only can be found in plants, but also in algae, and cyanobacteria. They originate from an endosymbiotic event, in which a eukaryotic cell with mitochondria absorbed a bacterium resembling cyanobacteria with photosynthetic capabilities (Archibald, 2015). This bacterium was integrated permanently into the cell, a process that was possibly assisted by *Chlamydiae*, as described by Ball et al. (2016). The development of chloroplasts provided cells with the novel capability to perform photosynthesis, marking a milestone in the evolution from heterotrophic to autotrophic life.

From the endosymbiotic progenitor into the modern chloroplast organelle, horizontal gene transfer happened between plastids and the nucleus, leading to gradual loss of most of the plastid genes towards the nucleus (Stegemann et al., 2012). The consequence is that only a small set of fundamental and highly conserved genes remained in the plastid genome (referred to as plastome hereafter). Ultimately, approximately 100 proteins were preserved in the plastome (Sun et al., 2023). Those proteins include crucial parts of the photosynthetic electron transport mechanisms and the ribulose 1,5-bisphosphate carboxylase/oxygenase (Rubisco) large subunit (rbcL) (Sato, 1999). A chloroplast phylogeny study (Martin et al., 2002) revealed that around 18% of the protein-coding genes in the *Arabidopsis thaliana (L.) Heynh* (referred as *Arabidopsis* hereafter) nuclear genome originated from the cyanobacterial ancestor of chloroplasts and were gradually transferred to the nucleus during the evolutionary adaptation process. This includes essential genes for gene expression machinery, the photosynthetic apparatus, and other biological processes of the chloroplasts, leading to its dependency on the nucleus.

1.2 The plastome feature

Typically, plant cells contain between 1000 to 1700 chloroplast nucleoids on average (Oldenburg and Bendich, 2015). In the case of a mesophyll cell from *Arabidopsis*, one

chloroplast may have about 20 to 35 copies of chloroplast DNA (cpDNA). However, the number of cpDNA can vary significantly throughout the plant's development. In the model plant *Arabidopsis*, the complete chloroplast genome of the Col-0 ecotype was sequenced in 1999 (Sato, 1999). This genome has a total length of 154,478 base pairs (bp), featuring a large single copy (LSC) region of 84,170 bp and a small single copy (SSC) region of 17,780 bp. These regions are separated by inverted repeat (IR) regions, each being 26,624 bp in length (Sato, 1999).

The *Arabidopsis* chloroplast genome comprises approximately 128 genes, including 87 protein-coding genes, 37 tRNA genes, and four rRNA genes (*rrn23S*, *rrn16S*, *rrn5S*, and *rrn4.5S*) (Sato, 1999). The protein-coding genes can be grouped by function based on their roles in chloroplast processes. A significant portion of these genes is involved in gene expression, such as the RNA polymerase subunits (*rpoA*, *rpoB*, *rpoC1*, *rpoC2*) and ribosomal proteins (*rpl* and *rps* genes), which are essential for transcription and translation (Bock, 2007; Zoschke and Bock, 2018). Another major group includes genes related to photosynthesis, encoding components of the photosynthetic apparatus: Photosystem I (e.g., *psaA*, *psaB*, *psaC*), Photosystem II (e.g., *psbA*, *psbB*, *psbC*, *psbD*), the cytochrome b_6f complex (e.g., *petA*, *petB*, *petC*), and ATP synthase subunits (e.g., *atpA*, *atpB*, *atpE*) (Green, 2011). Additionally, there are genes involved in metabolic processes, such as those for fatty acid synthesis like acetyl-CoA carboxylase beta subunit (*accD*) and the large subunit of Rubisco *rbcL*, which are essential for biosynthesis and energy production (Green, 2011). The coordinated expression of chloroplast and nuclear genes is critical for these processes, as nuclear-encoded proteins complement the chloroplast's gene expression machinery. This close cooperation between the nucleus and chloroplast ensures efficient regulation of chloroplast function and reflects the intricate interplay required to sustain normal cellular processes (Richter et al., 2023).

1.3 Plastid gene expression

Arabidopsis plastid gene expression relies on the plastid-encoded RNA polymerase (PEP), which is structurally similar to bacterial RNA polymerase, and the nuclear-encoded RNA polymerase (NEP) (Ji et al., 2021). PEP is primarily responsible for transcribing photosynthesis-related genes, such as those coding for proteins involved in the

photosynthetic apparatus and chlorophyll biosynthesis. NEP, on the other hand, transcribes genes essential for housekeeping functions, including those coding for ribosomal RNAs, transfer RNAs, and other components required for plastid maintenance and some non-photosynthetic processes (Hajdukiewicz et al., 1997). Both polymerases can have overlapping functions, especially during developmental transitions and under certain environmental conditions (Hwang et al., 2022).

The core subunit genes for PEP, such as *rpoA*, *rpoB*, *rpoC1*, and *rpoC2*, are retained within the plastid genome, reflecting its prokaryotic ancestry (Yagi and Shiina, 2014). However, the genes encoding sigma factors, which are crucial for promoter recognition and PEP specificity, have been transferred to the nuclear genome (Yagi and Shiina, 2014).

Plastid and cytosolic protein expression differ significantly in both their mechanisms and structural components. Plastid mRNAs, unlike cytosolic mRNAs, typically lack a 5' cap and a poly-A tail, which are features that confer stability and translational efficiency in the cytosol. Instead, plastid mRNAs contain untranslated regions (UTRs) and possess a Shine-Dalgarno sequence to facilitate ribosome binding, mimicking bacterial gene expression processes (Barkan, 2011). Moreover, plastid gene expression is organized in an operon-like system, where multiple genes are transcribed together as a polycistronic mRNA, similar to prokaryotes. In contrast, cytosolic gene expression in eukaryotes involves individually regulated monocistronic mRNAs, each encoding a single protein (Sugiura, 1992).

1.3.1 RNA editing and splicing in chloroplasts

To achieve accurate translation in chloroplasts, transcripts undergo specific post-transcriptional modifications. RNA editing and splicing are essential post-transcriptional processes in chloroplasts, critical for producing functional mRNAs and ensuring proper gene expression. In *Arabidopsis* and other plants, chloroplast RNA editing primarily involves C-to-U conversions at specific sites within transcripts, which often leads to the restoration of conserved amino acid sequences in protein-coding regions or generation of new translation starting site (Hirose, 2001). For example, RNA editing at position 117166 in the chloroplast genome of the *ndhD* transcript creates the AUG initiation codon, necessary for the assembly of the chloroplast NADH dehydrogenase-like complex, which

is a key component in the electron transport chain and supports photosynthesis (Boussardon et al., 2012). This editing is significantly inhibited under heat stress, as it requires the cooperative association between the RNA-binding proteins CRR4 and DYW1, with the latter showing reduced expression under heat stress (Castandet et al., 2016). This suggests that RNA editing in chloroplasts may be dynamically regulated in response to environmental conditions, potentially contributing to stress adaptation.

Another crucial post-transcriptional process in chloroplasts is splicing. In Arabidopsis, there are 20 chloroplast genes contain group II introns (Zeng et al., 2022), which need to be excised for the proper maturation of mRNAs (de Longevialle et al., 2010). This splicing is often mediated by nuclear-encoded splicing factors, which assist in the removal of introns to ensure correct expression of chloroplast-encoded genes (de Longevialle et al., 2010). An example of this process is the splicing of the *atpF* gene, which encodes a subunit of the ATP synthase complex in chloroplasts, contains a group II intron that requires splicing for proper mRNA maturation (Jenkins et al., 1997). This process is facilitated by the nuclear-encoded splicing factor CRS1, which binds specifically to the *atpF* intron (Ostersetzer et al., 2005). Accurate splicing is essential for the correct translation and function of the ATP synthase complex, which plays a pivotal role in photosynthetic energy production (Ostersetzer et al., 2005).

Together, RNA editing and splicing are fundamental to chloroplast gene expression, enabling the production of correctly processed and functional mRNAs necessary for chloroplast biogenesis and function.

1.3.2 Chloroplast and cytosolic protein expression

Proteins located in the chloroplast can be synthesized in either the cytosol or the chloroplast itself. Chloroplast-encoded proteins, such as the D1 protein of photosystem II (psbA) and rbcL, are synthesized directly within the chloroplast on its own ribosomes (Sugiura, 1992). In contrast, the vast majority of chloroplast proteins are encoded by nuclear genes and synthesized in the cytosol, such as proteins of the 70s ribosome (Tiller and Bock, 2014). The ribosomes within chloroplasts resemble prokaryotic 70S ribosomes, composed of a 50S large subunit and a 30S small subunit, (Yamaguchi and Subramanian, 2000). While some ribosomal proteins, such as RPS12 and RPL2, are encoded by the chloroplast genome,

many others like RPS9 and RPL11 are encoded by nuclear genes (Tiller and Bock, 2014). These nuclear-encoded ribosomal proteins are synthesized in the cytosol and imported into the chloroplast, reflecting the evolutionary origin of chloroplasts (Tiller and Bock, 2014). Further examples for key chloroplast proteins encoded by the nucleus are Rubisco small subunit (rbcS), ferredoxin (FD), and components of the protein import machinery like translocase subunits (TIC/TOC proteins) (Jarvis, 2008). Once these nuclear-encoded proteins are synthesized in the cytosol, they are post-translationally targeted to the chloroplast, where they are imported and localized to their specific functional compartments, such as the thylakoid membrane for photosynthetic proteins or the stroma for metabolic enzymes (Jarvis, 2008). The spatial separation of synthesis and function requires tight coordination between the nuclear and chloroplast genomes to ensure correct protein localization and timing of expression (Li and Chiu, 2010).

1.3.3 Protein import into chloroplasts

Since most chloroplast proteins are synthesized in the cytosol, they need to be imported into the chloroplast. The import of nuclear-encoded proteins into the chloroplast involves an intricate process that utilizes transit peptides as targeting signals (Jarvis, 2008; Li and Chiu, 2010). For example, the enzyme rbcS contains a transit peptide that guides it to the chloroplast (Van den Broeck et al., 1985). Upon reaching the chloroplast envelope, this precursor protein is recognized by receptor complexes on the outer membrane, such as Toc159 and Toc34, which are part of the translocon at the outer chloroplast membrane (TOC complex) (Bédard and Jarvis, 2005). The protein is then translocated across the envelope through a channel formed by the Toc75 complex and enters the stroma, facilitated by the translocon at the inner membrane (TIC complex), which includes proteins like Tic110 (Bédard and Jarvis, 2005). Once in the stroma, the transit peptide is cleaved by a stromal processing peptidase, and the mature protein is then folded and directed to its functional destination within the chloroplast (Richter and Lamppa, 1998). Some proteins like plastocyanin are further targeted to the thylakoid lumen using an additional thylakoid-targeting signal (Cline and Henry, 1996). This coordinated import system is crucial for plastid biogenesis and function, and highlights the complex regulation needed for the proper functioning of chloroplasts (Bédard and Jarvis, 2005).

1.4 Interplay between nuclear and chloroplast genomes

As a consequence of the endosymbiotic event and horizontal gene transfer, it is estimated that approximately 1,500 proteins of cyanobacterial origin are encoded by the nuclear genome in *Arabidopsis*, with roughly half directed to the chloroplast (Abdallah et al., 2000). Approximately 3,000 proteins encoded by the nuclear genome are translated in the cytosol and subsequently imported into plastids (Baruah et al., 2009). Proper plant growth requires coordination between the nuclear and plastid genomes, which involves both anterograde and retrograde signaling.

The processes of signaling during plastid biogenesis and the responses of mature chloroplasts to environmental changes are referred to as "biogenic" and "operational" controls, respectively (Pogson et al., 2008). Nucleus and plastids can sense environmental and developmental stimuli. When the nucleus perceives these signals, it generates messages that are transmitted to chloroplasts, prompting adjustments in chloroplast biogenesis to support adaptation. This process is known as anterograde signaling. Conversely, signals generated within the chloroplasts can be conveyed to the nucleus, resulting in alterations in the expression of nuclear genes, particularly those *Photosynthesis-Associated Nuclear Genes* (*PhANGs*). This process is known as retrograde signaling (Jan et al., 2022). Retrograde signaling coordinates nuclear gene expression in response to the functional state of the chloroplast. This feedback mechanism plays a crucial role in regulating the expression of nuclear-encoded plastid proteins and maintaining cellular homeostasis (Chan et al., 2016).

1.4.1 Discovery of *gun* mutants

Retrograde signaling becomes essential when chloroplast biogenesis is impaired. To mimic this perturbation, scientists utilize chemical reagents like norflurazon (NF) and lincomycin (Lin) to study *genomes uncoupled* (*gun*) mutants. Norflurazon treatment blocks chloroplast biogenesis by inhibiting the accumulation of carotenoids. Lincomycin is a chloroplast specific translation inhibitor (Mulo et al., 2003), it targets the peptidyl transferase domain V of the 23S rRNA within the 50S ribosomal subunit, which is crucial for peptide bond formation, thereby perturbating chloroplast biogenesis (Hong et al., 2014).

Approximately three decades ago, a mutant screen utilizing *Arabidopsis* led to the identification of a class of *gun* mutants (Susek et al., 1993). These mutants display de-repression of *PhANGs* expression in seedlings exposed to norflurazon, specifically the marker gene *LHCB* which encodes light-harvesting chlorophyll a/b-binding proteins of photosystem (PS) II. Initial forward genetics approach (Susek et al., 1993) identified five-*gun* mutants (*gun1-gun5*), and later, the overexpression of plastid ferrochelatase 1 (FC1) in *gun6-1D* was shown to produce a "*gun*" phenotype, later defined as *gun6* (Woodson, Perez-Ruiz, and Chory, 2011).

1.4.2 GUN2-GUN6 in tetrapyrrole (tetpy) biosynthesis

GUN2 - GUN6 have demonstrated their significant roles in tetrapyrrole (tetpy) biosynthesis (Richter et al., 2023). These genes encode key enzymes and regulators essential for the production of heme, chlorophyll, and other metabolites (Terry and Smith, 2013). Specifically, GUN2 encodes heme oxygenase that converts heme into biliverdin iXα (Davis et al., 1999). GUN3 encodes phytochromobilin synthase that reduces biliverdin iXα to phytochromobilin (Kohchi et al., 2001), and GUN5 encodes the H subunit of Mg-chelatase (CHLH), which is a key enzyme in chlorophyll branch of tetpy biosynthesis (Mochizuki et al., 2001). GUN4, on the other hand, is a regulator of Mg-chelatase activity, influencing the flux of the pathway towards chlorophyll production (Adhikari et al., 2011).

These proteins contribute to the regulation of retrograde signaling through the modulation of tetrapyrrole intermediates. It is anticipated that disruption of normal tetpy synthesis could lead to the overaccumulation of intermediates, which can serve as signals that shuttle to the nucleus and trigger retrograde signaling. Actually, Mg protoporphyrin IX (MgProto) and heme have been proposed as such signaling molecular (Vasileuskaya et al., 2005). However, deeper studies, such as those by Mochizuki et al. (2008), have shown that MgProto is not a determinant of retrograde signaling in *Arabidopsis*. This conclusion was drawn by quantifying the steady-state levels of MgProto in *Arabidopsis* plants with altered plastid signaling responses, monitored through the expression of the *Lhcb1*, *rbcS*, *HEMA1*, *BAM3*, and *CA1* genes.

Subsequently, heme has been proposed as a potential signaling component originating from the chloroplast (Woodson, Perez-Ruiz, and Chory, 2011). It is suggested to act as a retrograde signal that communicates the status of tetrapyrrole metabolism to the nucleus, thereby influencing the expression of genes involved in chloroplast development and function (Woodson, Perez-Ruiz, and Chory, 2011). Later study provided evidence indicating that a specific heme pool or a heme-derived metabolite generated via FC1 activity might serve as a positive retrograde signal promoting genes required for chloroplast development (Terry and Smith, 2013).

1.4.3 Insights of GUN1 on chloroplast-nuclear interactions

Since the initial discovery of GUN1 as a key component in retrograde signaling, intensive research has been undertaken to elucidate its mode of action. Given its complexity and critical role as an integrator of multiple biological processes, findings in the field often present conflicting views. Despite these discrepancies, significant progress has been made in understanding GUN1's functions through continued investigation and debate.

1.4.3.1 Adaptive hypothesis of *gun* mutants

Initially, the uncoupled expression of *PhANGs* in *gun* mutants has been debated due to the hypothesis that these mutants might exhibit increased tolerance to chloroplast-disturbing factors, thereby reducing the impact on *PhANGs* expression. This idea suggests that *gun* mutants have an adaptive advantage under conditions that disrupt chloroplast function, leading to less pronounced changes in the nuclear gene expression related to photosynthesis (Wu et al., 2018; Mochizuki, Susek, and Chory, 1996). Later findings provided solid evidence that *gun1* mutants are actually hyposensitive to lincomycin and norflurazon (Zhao, Huang, and Chory, 2018). Except for less accumulation of anthocyanin compared to the wild type, the *gun1-9* mutant exhibited bleached cotyledons similar to the wild type under strong inhibition from 5 μM NF or 220 μg/mL Lin. However, when the concentration of NF was lowered to 20 nM, the *gun1-9* mutant displayed a visible pale yellow or white and smaller cotyledon phenotype compared to the wild type, indicating that *gun1-9* was actually hypersensitive to NF (Zhao, Huang, and Chory, 2018). This study confirmed that the uncoupled expression of *PhANGs* in dysfunctional plastids is not a result of increased tolerance to oxidative stress or altered chloroplast development.

1.4.3.2 GUN1-ABI4-PTM hypothesis

It was suggested that GUN1 integrates chloroplast retrograde signals to the nucleus, with the plant homeodomain (PHD) transcription factor (PTM) containing transmembrane domains identified as a downstream component (Sun et al., 2011). Here, PTM, initially in the chloroplast outer membrane, is cleaved in response to GUN1 signals, relocating to the nucleus to regulate *ABSCISIC ACID INSENSITIVE 4* (*ABI4*), which represses *PhANG*s (Koussevitzky et al., 2007). Both *ptm* and *abi4* mutants show a *gun1*-like phenotype in *PhANG*s expression, though milder, suggesting other factors in GUN1 signaling (Brunkard and Burch-Smith, 2018; Hernández-Verdeja and Strand, 2018). Later studies questioned PTM's and ABI4's roles, showing inconsistent results. This contradiction was ended by Kacprzak et al. (2019) through the analysis of *gun* phenotypes in multiple *abi4* alleles across different laboratories. The authors showed that *abi4* mutants failed to restore the expression of a set of *PhANG*s after norflurazon and lincomycin treatment.

1.4.4 Regulation and dynamics of the GUN1 protein in *Arabidopsis*

Interestingly, despite the crucial role of GUN1 in *Arabidopsis*, *gun1* mutants have been previously described as exhibiting a wild-type-like phenotype, except for the occasionally observed chlorophyll-deficient cotyledons (Ruckle, DeMarco, and Larkin, 2008). In addition, the GUN1 protein is hardly detectable by proteomic approaches (Plant Proteome DataBase; http://ppdb.tc.cornell.edu/). The abundance of proteins relies on the balance between their rate of synthesis and their degradation rate. Wu et al. (2018) demonstrated that the GUN1 protein accumulates to detectable levels only during the very early stages of leaf development, where intensive biogenesis occurs. In more mature leaves, although *GUN1* mRNA expression remains high, the protein itself is present at very low abundance with a rapid turnover rate, estimated to have a half-life of approximately 4 hours (Wu et al., 2018). This rapid turnover is primarily controlled by the chaperone ClpC1, suggesting that GUN1 is degraded by the Clp protease (Wu et al., 2018).

1.5 GUN1 is a pentatricopeptide repeat protein (PPR)

Plant organellar RNA metabolism is controlled by numerous nuclear-encoded RNA-binding proteins (RBPs), which regulate RNA stability, processing, and degradation (Small et al., 2023). In chloroplasts and mitochondria, these processes are crucial for synthesizing

the machinery required for photosynthesis and respiration, making them vital for organelle biogenesis and plant viability (Small et al., 2023). Among the RBPs, PPR proteins play significant roles in RNA editing, splicing, and stabilization (Kupsch et al., 2012; Meierhoff et al., 2003; Shields and Wolfe, 1997). Though PPR proteins are found across eukaryotes, they are much more abundant in plants (Saha et al., 2007), with over 450 identified in *Arabidopsis* and 477 in rice (*Oryza sativa*), compared to just six in humans and five in yeast (O'Toole et al., 2008).

Among the many PPR proteins in *Arabidopsis*, GUN1 stands out due to its involvement in the retrograde signaling pathway. Interestingly, GUN1 is the only PPR protein classified as a "*gun*" mutant, highlighting its distinctive role within the anterograde-retrograde signaling axis and its function in chloroplast biogenesis and stress response.

1.5.1 Classification and function of PPR proteins

PPR proteins are classified into two subfamilies based on their domain architecture (Qin et al., 2021): the P subfamily, which features tandem arrays of 35-amino-acid PPR motifs typically ending with a proline (P), and the PPR-like (PLS) subfamily, which includes alternating canonical P-type motifs along with variant "long" (L: 35–36 amino acids) and "short" (S: ~31 amino acids) motifs (Ban et al., 2013; Manna, 2015). The PLS subfamily is further divided into five subgroups according to the domain assembly at the C-terminus of the PPR protein: PLS, E1, E2, E+, and DYW (Cheng et al., 2016; Xing et al., 2018). Generally, P-class PPR proteins mediate various aspects of RNA processing in plant organelles, whereas PLS-class PPR proteins primarily function in RNA editing (Schmitz-Linneweber and Small, 2008).

Unlike PPR proteins in the PLS-class subfamily, most P-class PPR proteins lack additional domains. However, a few P-class subfamily members contain small MutS-related (SMR) domains following an array of P-class PPR motifs. These P-class PPR proteins with SMR domains are known as PPR-SMR proteins. Among the large number of PPR proteins, *Arabidopsis* contains a total of eight PPR-SMR proteins, with five predicted to be localized within chloroplasts (Zhang and Lu, 2019). These proteins include PLASTID TRANSCRIPTIONALLY ACTIVE 2 (pTAC2), SUPPRESSOR OF VARIEGATION 7 (SVR7), EMBRYO DEFECTIVE 2217 (EMB2217), SUPPRESSOR OF THYLAKOID

FORMATION 1 (SOT1), and GUN1 (Honkanen and Small, 2022).

The structure of PPR proteins determines their RNA-binding specificity. Each PPR motif contains two alpha helices (Wang et al., 2021). PPR-RNA binding occurs in a "one-repeat, one-nucleotide" manner, where each motif aligns with a specific nucleotide. The specificity of this interaction is determined by the amino acids at positions 5 and 35 within each PPR motif (Barkan and Small, 2014). With varying numbers of PPR motifs, this modular recognition allows PPR proteins to bind to specific RNA sequences (**Figure 1**), thereby facilitating essential RNA processing activities, including editing, splicing, and stabilization. As a P-type PPR protein, GUN1 is potentially involved in RNA metabolism through its RNA-binding ability, making this association a valuable area for further investigation.

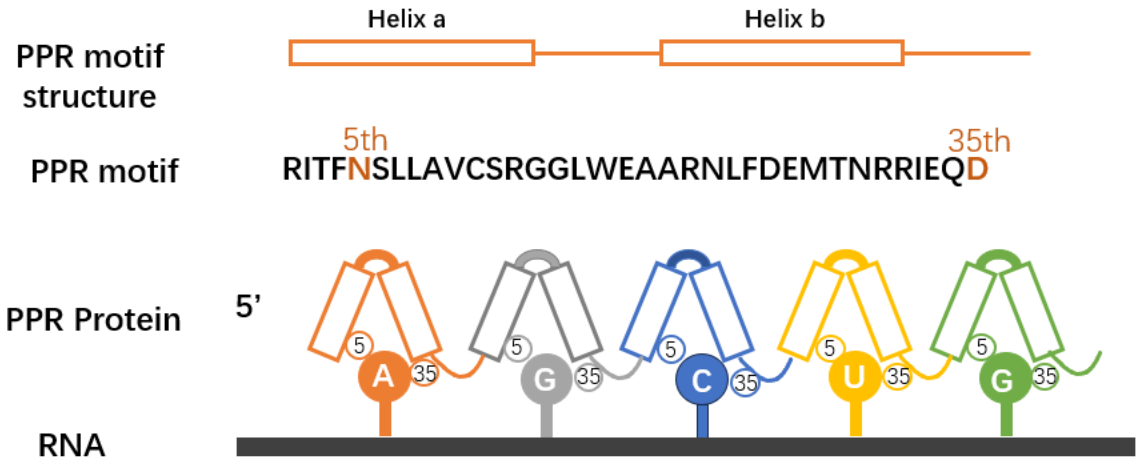

Figure 1: Schematic representation of PPR motif structure and its interaction with RNA. The PPR motif consists of two α-helices (Helix a and Helix b) that form a repeat structure. Each PPR motif recognizes a specific nucleotide on the RNA through interactions primarily determined by the amino acid residues at the 5th and 35th positions of the motif. PPR proteins recognize their specific RNA targets through a tandem array of these PPR motifs, allowing for sequence-specific binding.

1.6 Chloroplasts in response to drought stress

Chloroplasts and mitochondria are not only responsive to environmental changes but also act as primary targets for various stress factors including drought (Kleine et al., 2021). The

rising intensity and frequency of drought events pose significant threats to global agricultural productivity. Countries previously unaffected by drought stress are now experiencing its adverse impacts, and this drought threat is foreseen to continue into the future. As sessile organism, plants can only develop mechanisms to tolerant and adapt to the environment which can be divided into four basic types-drought avoidance, drought tolerance, drought escape, and drought recovery (Fang and Xiong, 2015). The drought stress response is complicated and largely studied due to its practical meaning.

1.6.1 Drought stress sensing

From a microscopic perspective, drought stress can result in increased accumulation of reactive oxygen species (ROS) through multiple pathways, acting as an alarm that initiates acclimatory or defense responses via specific signal transduction pathways, with H_2O_2 serving as a secondary messenger (de Carvalho, 2008). ROS signaling is intricately linked to abscisic acid (ABA) (Aslam et al., 2022), calcium ion (Ca^{2+}) fluxes (Corti et al., 2023), and sugar sensing (Zou et al., 2024), and it likely plays a role both upstream and downstream of ABA-dependent signaling pathways under drought conditions. However, if drought stress persists beyond a certain threshold, ROS production can overwhelm the antioxidant system's scavenging capacity, leading to extensive cellular damage and eventual cell death (de Carvalho, 2008).

The drought stress response encompasses a range of physiological processes, from the initial perception of water deficit conditions to the development of drought resistance at the whole-plant level (Kuromori et al., 2022). It is hypothesized that plants initially detect water deficits in their roots, prompting the transmission of various molecular signals from roots to shoots (Takahashi et al., 2020). Ultimately, ABA is synthesized primarily in the leaves and transported to other parts of the plant, where it triggers the expression of drought-responsive genes that enhance the plant's drought tolerance. ABA regulates stomatal closure to reduce water loss, thereby conserving water during drought conditions (Takahashi et al., 2020).

1.6.2 The role of chloroplasts in drought stress acclimation

Growing evidence reveals the pivotal role of chloroplasts in plant stress responses, emphasizing the interconnection between various stress responses and organellar signaling

pathways (Gläßer et al., 2014). It is well established that water deprivation accelerates the degradation of photosynthetic pigments, resulting from the deterioration of thylakoid membranes (Fang and Xiong, 2015). This damage will directly or indirectly influence the chlorophyll content. It has been reported that chlorophyll content has positive regulation with soil water content. Plants that can sustain higher chlorophyll levels under water stress conditions are thought to more efficiently manage absorbed light energy, thereby reducing ROS production, which is linked to enhanced drought resistance. (Guo et al., 2008; Kocheva et al., 2004; Shields and Wolfe, 1997). Another approach to managing excess light energy under drought conditions is through non-photochemical quenching (NPQ). NPQ dissipates surplus absorbed light energy as heat, thereby preventing the overproduction of ROS that could otherwise result in oxidative stress. This mechanism is essential for maintaining the stability of the photosynthetic apparatus during times of limited water availability (Nosalewicz et al., 2022).

In addition, during drought stress, the efficiency of photosynthesis can be compromised. Chloroplasts adjust their function to optimize carbon assimilation under water-limited conditions. By fine-tuning the light reactions and Calvin cycle processes (Hu et al., 2023), chloroplasts help sustain energy production and minimize photoinhibition, thus supporting the plant's survival during drought.

In summary, chloroplasts play a pivotal role in managing drought stress by fine-tuning the balance between energy absorption and consumption, maintaining water levels through ABA-mediated stomatal closure, reducing ROS via chlorophyll adjustments and NPQ, and preventing photoinhibition damage by modifying light reactions and Calvin cycle processes. These interconnected biological processes within the chloroplast highlight its essential function in helping plants withstand drought stress.

Aims of the thesis

This thesis aims to provide a deeper characterization of the retrograde signaling integrator GUN1 and to explore the responses of organellar and nuclear (post)transcriptomes in *Arabidopsis* under drought conditions.

GUN1 is a PPR protein that functions as an integrator in retrograde signaling (Wu and Bock, 2021). In Chapter 1, the primary goal is to elucidate the molecular function of GUN1 and to address the long-standing questions surrounding its role in retrograde signaling. Leveraging a seed batch of three different *gun1* mutants, each exhibiting varying degrees of greening in their cotyledons, the function of GUN1 was analyzed independent of NF or LIN treatment. By examining these distinct *gun1* seedling pools (green, marbled, and white cotyledons) through RNA sequencing and integrating these findings with existing data, this study aims to uncover the molecular changes in the *gun1* mutants that lead to these variant phenotypes. The intriguing phenotypic variations prompted a deeper investigation into the molecular function of GUN1.

As a PPR protein, GUN1 is presumed to have RNA-binding ability. However, previous nucleotide immunoprecipitation (NIP)-chip analysis (Tadini et al., 2016) on chloroplast stroma extract from adult plants did not confirm this ability. Given that GUN1 expression is known to be high during the seedling stage, it is crucial to perform another RIP-seq analysis at this developmental stage to confirm its RNA-binding capacity and to further elucidate its role in the observed phenotypic differences. In addition, GUN1's RNA-binding ability is also assessed through *in silico* prediction of PPR motifs and *in vitro* binding assays using EMSA (Electrophoretic Mobility Shift Assay). These combined approaches provide a comprehensive understanding of GUN1's function and its involvement in retrograde signaling. The results of these investigations are shown in **Chapter 1**.

Plants have evolved various strategies to adapt to drought, which involve extensive changes in gene expression. While the alterations in transcription levels have been well-studied, the impact of post-transcriptional processing on nuclear and organellar transcripts remains largely unexplored. To address this, **Chapter 2** employed RNA sequencing following

ribosomal RNA depletion to monitor (post)transcriptional changes at different time points during drought exposure in *Arabidopsis* Col-0. This RNA-seq dataset was then used to analyze alternative splicing of nuclear transcripts, the accumulation of organellar (chloroplast and mitochondrial) transcripts, as well as the editing and splicing of organellar transcripts. The detailed findings are presented in **Chapter 2**.

Results

Chapter 1

GENOMES UNCOUPLED PROTEIN1 binds to plastid RNAs and promotes their maturation

Plant Communications
Research article

GENOMES UNCOUPLED PROTEIN1 binds to plastid RNAs and promotes their maturation

Qian Tang[1], Duorong Xu[1], Benjamin Lenzen[2], Andreas Brachmann[3], Madhura M. Yapa[4], Paymon Doroodian[4], Christian Schmitz-Linneweber[2], Tatsuru Masuda[5], Zhihua Hua[4], Dario Leister[1] and Tatjana Kleine[1,*]

[1]Plant Molecular Biology (Botany), Faculty of Biology, Ludwig-Maximilians-University München, 82152 Martinsried, Germany

[2]Molecular Genetics, Humboldt-University Berlin, Philippstr. 13, 10115 Berlin, Germany

[3]Biocenter of the LMU Munich, Genetics Section, Grosshaderner Str. 2-4, 82152 Planegg-Martinsried, Germany

[4]Department of Environmental and Plant Biology, Ohio University, Athens, OH 45701, USA

[5]Graduate School of Arts and Sciences, The University of Tokyo, Komaba, Meguro-ku 153-8902, Tokyo, Japan

*Correspondence: Tatjana Kleine (tatjana.kleine@lmu.de)

https://doi.org/10.1016/j.xplc.2024.101069

ABSTRACT

Plastid biogenesis and the coordination of plastid and nuclear genome expression through anterograde and retrograde signaling are essential for plant development. GENOMES UNCOUPLED1 (GUN1) plays a central role in retrograde signaling during early plant development. The putative function of GUN1 has been extensively studied, but its molecular function remains controversial. Here, we evaluate published transcriptome data and generate our own data from *gun1* mutants grown under signaling-relevant conditions to show that editing and splicing are not relevant for GUN1-dependent retrograde signaling. Our study of the plastid (post)transcriptome of *gun 1* seedlings with white and pale cotyledons demonstrates that GUN1 deficiency significantly alters the entire plastid transcriptome. By combining this result with a pentatricopeptide repeat code-based prediction and experimental validation by RNA immunoprecipitation experiments, we identified several putative targets of GUN1, including tRNAs and RNAs derived from *ycf1.2*, *rpoC1*, and *rpoC2* and the *ndhH–ndhA–ndhI–ndhG–ndhE–psaC–ndhD* gene cluster. The absence of plastid rRNAs and the significant reduction of almost all plastid transcripts in white *gun1* mutants account for the cotyledon phenotype. Our study provides evidence for RNA binding and maturation as the long-sought molecular function of GUN1 and resolves long-standing controversies. We anticipate that our findings will serve as a basis for subsequent studies on mechanisms of plastid gene expression and will help to elucidate the function of GUN1 in retrograde signaling.

Key words: GUN1, MORF2, plastid (post)transcriptome, retrograde signaling, RIP-seq, RNA binding protein

Tang Q., Xu D., Lenzen B., Brachmann A., Yapa M.M., Doroodian P., Schmitz-Linneweber C., Masuda T., Hua Z., Leister D., and Kleine T. (2024). GENOMES UNCOUPLED PROTEIN1 binds to plastid RNAs and promotes their maturation. Plant Comm. 5, 101069.

INTRODUCTION

Chloroplasts are the characteristic organelles of algae and plants, and it is generally accepted that they are derived from ancient cyanobacteria through endosymbiosis (Archibald, 2015). During evolution, most genes of the endosymbiont were transferred to the nuclear genome, resulting in only about 100 genes being present in current plastid genomes (Kleine et al., 2009) and at least 3000 plastid proteins being encoded in the nucleus (Christian et al., 2020). As a result, most plastid multiprotein complexes, such as the plastid gene expression (PGE) machinery and the photosynthetic apparatus, are formed by a mixture of plastid- and nuclear-encoded proteins, requiring coordination of the expression of both genomes. Because most plastid proteins are encoded in the nucleus, this organelle exerts anterograde control over the plastids. For example, the process of PGE necessitates the involvement of diverse nuclear-encoded proteins that promote the transcription, splicing, trimming, and editing of RNA in organelles while simultaneously regulating their translation (Borner et al., 2015; Kleine and Leister, 2015; Small et al., 2023; Zhang et al., 2023). On the other hand,

Published by the Plant Communications Shanghai Editorial Office in association with Cell Press, an imprint of Elsevier Inc., on behalf of CSPB and CEMPS, CAS.

nuclear gene expression, such as expression of the so-called photosynthesis-associated nuclear genes (PhANGs), is controlled by plastid-to-nucleus retrograde signaling (Kleine and Leister, 2016; Liebers et al., 2022), which is thought to be mediated by multiple factors and sources. For instance, in seedlings treated with norflurazon (NF) or lincomycin (LIN), mRNA levels of *PhANGs* are repressed (Oelmuller et al., 1986). NF is an inhibitor of carotenoid biosynthesis (Oelmuller et al., 1986), whereas LIN targets peptidyl transferase domain V of the 23S ribosomal RNA (rRNA) of the 50S ribosomal subunit, which is the site of peptide bond formation, thereby preventing peptide bond formation (Hong et al., 2014). A mutant screen with *Arabidopsis thaliana* (*Arabidopsis* hereafter) identified a group of *genomes uncoupled* (*gun*) mutants three decades ago (Susek et al., 1993). In these mutants, expression of the *PhANG*s, in particular the marker gene *LHCB1.2*, which encodes a light-harvesting chlorophyll a/b-binding protein of photosystem (PS) II, is de-repressed in seedlings treated with an inhibitor (Susek et al., 1993). The original gun screens (Susek et al., 1993; Woodson et al., 2011) led to discovery of six *gun* mutants, five of which, *gun2* to *gun6*, are impaired in the tetrapyrrole biosynthesis pathway. The *gun1* mutant exhibits a distinct *gun* phenotype when treated with LIN, distinguishing it from the other mutants (summarized in Richter et al., 2023). *GUN1* encodes a chloroplast pentatricopeptide repeat (PPR) protein (Koussevitzky et al., 2007). PPR proteins belong to a large family, with an estimated 106 of these proteins targeted to chloroplasts (Small et al., 2023). They participate in various PGE steps, including RNA cleavage, splicing, editing, stabilization, and translation (Small et al., 2023; Zhang et al., 2023). Thus far, no other *ppr* mutant has been identified as a *gun* mutant, indicating that GUN1 is a special component of an anterograde–retrograde axis.

GUN1 is an ancient protein that evolved within the streptophyte clade of the algal ancestors of land plants before the first plants colonized land more than 470 million years ago. It has been suggested that the primary role of GUN1 is to act in PGE and that its involvement in retrograde signaling probably evolved more recently (Honkanen and Small, 2022). In fact, GUN1 contains two domains known to interact with nucleic acids, the PPR domain and a MutS-related (SMR) domain (Koussevitzky et al., 2007). Among a large number of PPR proteins, *Arabidopsis* contains only eight PPR-SMR proteins, five of which are predicted to be localized in chloroplasts (Zhang and Lu, 2019), including PLASTID TRANSCRIPTIONALLY ACTIVE 2, SUPPRESSOR OF VARIEGATION 7 (SVR7), EMBRYO DEFECTIVE 2217, SUPPRESSOR OF THYLAKOID FORMATION 1 (SOT1), and GUN1. Mutants of the first four show severe molecular and/or visible phenotypes, but only SOT1 has been shown to have an RNA-binding function (Zhou et al., 2017; Zhang and Lu, 2019). Mainly by studying *gun1* seedlings grown on inhibitors or in combination with other mutants, GUN1 has been implicated in a variety of processes in chloroplasts, such as regulation of tetrapyrrole biosynthesis (Shimizu et al., 2019), protein homeostasis (Tadini et al., 2016), ribosome maturation (Paieri et al., 2018), accumulation of certain chloroplast transcripts, and chloroplast import (Tadini et al., 2020), to name a few. Recently, GUN1 has been proposed to cooperate with MULTIPLE ORGANELLAR RNA EDITING FACTOR 2 (MORF2)/DIFFERENTIATION AND GREENING-LIKE 1 to regulate RNA editing under NF conditions (Zhao et al., 2019). In the suggested mechanism, GUN1 would not bind directly to the target RNAs. Rather, it would facilitate differential editing through its interaction with MORF2. Although GUN1 has been suggested to interact with DNA *in vitro* (Koussevitzky et al., 2007), no function in nucleic acid binding has yet been demonstrated *in vivo*, although the hypothesis that GUN1 exerts its function by binding RNA has recently been illuminated (Loudya et al., 2024). Furthermore, apart from occasional observations of pale cotyledons in a proportion of seedlings (e.g., in Ruckle et al., 2007), no clear severe phenotype has been observed.

In this study, we revisit the editing functions of GUN1 and MORF2 during retrograde signaling, define a distinct *gun1* phenotype with white cotyledons but green true leaves, examine the *gun1* (post)transcriptome in detail, and perform RNA immunoprecipitation (RIP) and electrophoretic shift experiments that strongly suggest an RNA-binding function of GUN1.

RESULTS

GUN1 does not play a significant role in plastid RNA editing or splicing during retrograde signaling

On the basis of Sanger sequencing data analysis, GUN1 has been proposed to regulate plastid RNA editing during retrograde signaling (Zhao et al., 2019). Previously, RNA sequencing after rRNA depletion (long non-coding RNA sequencing [lncRNA-seq]) data covering both nuclear and organellar transcripts were generated for wild-type (WT) and *gun1-102* seedlings grown on Murashige and Skoog (MS) and NF (Habermann et al., 2020). The benefit of the lncRNA-seq technique is that its workflow involves library preparation after depletion of rRNAs rather than enrichment of mRNAs, the latter approach having been used in Zhao et al. (2019) and many other studies analyzing *gun1* mutants. Analysis of the sequences generated by Habermann et al. (2020) for splicing and editing changes revealed no significant alterations between WT and *gun1-102* when grown on MS (Supplemental Figures 1A and 1B). NF had a significant (secondary) effect on plastid splicing, which was similarly reduced in WT and *gun1-102* (Supplemental Figure 1C). Also, no major differences in editing (C-to-U base substitutions) efficiencies were observed between *gun1-102* and WT grown on MS (Supplemental Figure 1D), consistent with previous findings (Zhao et al., 2019). Editing was reduced at multiple sites in NF-treated WT (Figure 1A), confirming that editing is altered under stress exposure (Kakizaki et al., 2009; Zhao et al., 2019). According to Zhao et al. (2019), GUN1-mediated editing is particularly important under inhibitor treatment. They found that RNA editing levels in *gun1-8* and *gun1-9* increased for *clpP-559*, *ndhB-467/-836*, *ndhD-878*, and *rps12-i-58* but decreased for *rpoC1-488*, *ndhF-290*, *psbZ-50*, and *rpoB-338/-551/-2432* compared with the WT when grown on NF. We confirmed increased editing levels in *gun1-102* for the same sites (Figure 1A) but observed only a moderate reduction in RNA editing at two sites, *psbZ-50* (87% in WT, 82% in *gun1-102*) and *rpoB-338* (87% in WT, 79% in *gun1-102*). To account for the different growth and analysis conditions, we repeated the experiment in two different laboratories using the growth conditions employed by

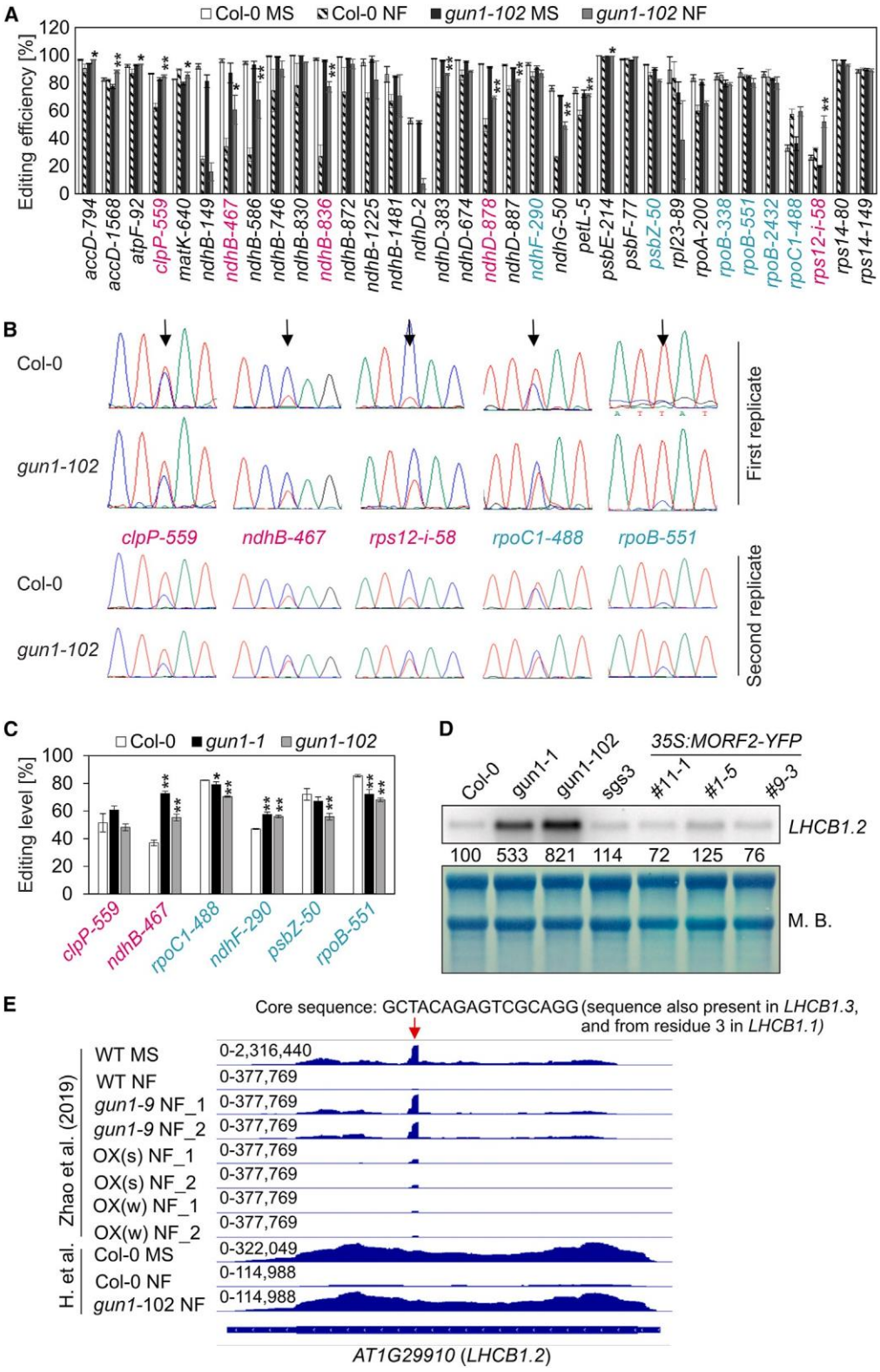

Figure 1. GUN1 does not play a significant role in plastid RNA editing or splicing during retrograde signaling.

(A) RNA editing efficiencies of 4-day-old Col-0 and *gun1-102* seedlings grown on MS and norflurazon (NF) were determined using previously published RNA-seq data (Habermann et al., 2020). These sequencing data were generated to allow for the detection of organellar transcripts. Mean values ± standard deviations were obtained from three independent experiments. Statistically significant differences between Col-0 NF and *gun1-102* NF are indicated (post hoc Tukey's HSD [honestly significant difference] test; **P* < 0.05 and ***P* < 0.01). A graph showing the statistical differences between Col-0

(legend continued on next page)

Zhao et al. (2019). Laboratory 1 used *gun1-102* in Sanger sequencing experiments (Figure 1B), and laboratory 2 included both *gun1-1* and *gun1-102* in amplicon sequencing experiments (Figure 1C). These experiments revealed no reproducible differences in editing efficiency between W T and *gun1* under NF conditions except for a slight reduction in *rpoC1-488* and *rpoB-551* editing.

To summarize, the presence of only mild editing and splicing differences between WT and *gun1* upon NF treatment argue against a major impact of these processes in GUN1 signaling.

Overexpression of MORF2 does not result in a significant *gun* phenotype

Previously, two MORF2 overexpression lines, *MORF2OX(s)* and *MORF2OX(w)*, were constructed (Zhao et al., 2019). *MORF2OX(s)* exhibited a *gun* phenotype, as its mRNA levels of nuclear-encoded photosynthesis genes, including *LIGHT HARVESTING CHLOROPHYLL A/B BINDING PROTEIN1.2* (*LHCB1.2*), were higher than those of the WT when the seedlings were treated with NF (Zhao et al., 2019). We found that overexpression of *MORF2* in the Col-0 background induced co-suppression of *MORF2* and led to variegation phenotypes in both early seedlings and adult plants (Yapa et al., 2023), similar to those observed for *MORF2OX(s)* (Zhao et al., 2019). To prevent potential post-transcriptional co-suppression-mediated gene silencing, we introduced a *35S:MORF2-YFP* construct into *suppressor of gene silencing 3-1* (*sgs3-1*) plants (Peragine et al., 2004) (Supplemental Figure 2). At the cotyledon stage, lines *35S-MORF2-YFP #1-5* and *#11-1* exhibited phenotypes similar to those of Col-0 and *sgs3-1*. However, line *#9-3*, which had the highest induction of *MORF2* levels (Supplemental Figure 2A), displayed a reduction in the maximum quantum yield of PSII (measured as the parameter Fv/Fm) (Supplemental Figure 2B). The determination of editing levels for *ndhF-290*, *psbZ-50*, *rpoB-338*, and *rpoB-551*, sites that have been described as less edited in both *MORF2OX(s)* and *gun1–9* seedlings under NF treatment (Zhao et al., 2019), indicated that, interestingly, the editing levels of *ndhF-290* And *psbZ-50* were also compromised in our strongest *MORF2 overexpressor (#9-3)* (Supplemental Figure 3A) compared with its parent plant, *sgs3-1* (Supplemental Figure 3B).

To examine the *gun* phenotype of *35S:MORF2-YFP* lines, RT–qPCR was performed on retrograde marker genes. As expected, mRNA levels of the marker genes *LHCB1.2*, *CARBONIC ANHYDRASE 1*, and *PLASTOCYANIN* were higher in the *gun1* alleles. Although *LHCB1.2*, *CARBONIC ANHYDRASE 1*, and *PLASTOCYANIN* mRNA levels were slightly elevated in line *#9-3*, they remained significantly lower than in *gun1* mutants and similar to those in *sgs3-1* (Supplemental Figure 3C). Also, northern blot analysis showed high levels of *LHCB1.2* in *gun1* alleles but WT-like levels in the *35S:MORF2-YFP* lines (Figure 1D). We reanalyzed RNA-seq data generated for WT, *gun1-9*, *oeMORF2(s)*, and *oeMORF2(w)* (Zhao et al., 2019) and sequencing data from Habermann et al. (2020) and plotted the reads across the *LHCB1.2* gene. Whereas the data from Habermann et al. (2020) showed an even distribution of reads across *LHCB1.2*, the reads generated by Zhao et al. (2019) exhibited a prominent peak of 16 nucleotides (Figure 1E). It is predominantly this peak that is found in MORF2 overexpressors after NF treatment (Zhao et al., 2019), whereas there are almost no reads for the remainder of the *LHCB1.2* gene.

Overall, this evidence suggests that overexpression of MORF2 does not result in a significant *gun* phenotype.

The nuclear transcriptome of white and marbled *gun1* seedlings is significantly affected

During experiments examining the role of GUN1 in NF-mediated editing changes, we observed the appearance of *gun1* seedlings with white (*gun1W*) and marbled (*gun1M*) cotyledons among the green *gun1* (*gun1G*) seedlings grown on MS medium without inhibitors (Figure 2A). This phenomenon has also been reported previously (Ruckle et al., 2007), but at lower frequencies, which we will discuss later. The phenotype was most pronounced in *gun1-102* seedlings but

MS and *gun1-102* MS can be found in Supplemental Figure 1. The efficiency of editing sites labeled in magenta and turquoise was found to be elevated and reduced, respectively, by Zhao et al. (2019). We also identified an unexpected increase in editing of *rpoC1* in both WT and *gun1-102* under NF treatment. Our results may vary due to the use of different analysis methods—Sanger sequencing versus lncRNA-seq data analysis—as well as discrepancies in growth media and conditions. Notably, Zhao et al. (2019) cultivated 5-day-old seedlings on MS plates without sucrose, whereas Habermann et al. (2020) used MS plates with 1.5% sucrose. Thus, to account for these variations, we repeated the experiment for selected editing sites in two distinct laboratories as shown in (B) and (C).

(B) Col-0 and *gun1-102* seedlings were grown in laboratory 1 for 5 days under continuous light conditions as reported by Zhao et al. (2019). The editing efficiency of the selected sites was visualized by Sanger sequencing for two biological replicates.

(C) Col-0, *gun1-1*, and *gun1-102* seedlings were grown in laboratory 2 for 5 days under continuous light conditions as reported by Zhao et al. (2019). The editing efficiency of the selected sites was determined by amplicon sequencing. Mean values with their standard deviations are shown. Statistically significant differences between Col-0 and *gun1* seedlings are indicated (post hoc Tukey's HSD test; $*P < 0.05$ and $**P < 0.01$).

(D) Overexpression of MORF2 does not result in a significant *gun* phenotype. Steady-state levels of *LHCB1.2* transcripts in 5-day-old seedlings grown under NF conditions are shown. Col-0 serves as the WT control for *gun1* and *sgs3-1* as a control for oeMORF2 (*35S:MORF2-YFP*) lines. For each genotype, the total RNA was fractionated on a formaldehyde-containing denaturing gel, transferred to a nylon membrane, and probed with [α-^{32}P]dCTP-labeled complementary DNA (cDNA) fragments specific for the transcripts encoding *LHCB1.2*. rRNA was visualized by staining the membrane with methylene blue (M.B.) and served as a loading control. Quantification of signals relative to the WT (=100) is provided below each lane.

(E) Snapshots of reanalyzed RNA-seq data published by Zhao et al. (2019) and Habermann et al. (2020). The read depths were visualized with the Integrated Genome Browser. Whereas reads from Habermann et al. (2020) are evenly distributed across *LHCB1.2*, reads generated by Zhao et al. (2019) exhibit a prominent peak of 16 nucleotides (red arrow). The sequence of the peak (5′-GCTACAGAGTCGCAGG-3′) is also present in *LHCB1.3* and from the third nucleotide in *LHCB1.1*. The sequence of this peak coincides with the sequence of the ''LHB1.2'' forward primer (actually detecting *LHCB1.3* in combination with the given reverse primer) used by Zhao et al. (2019) for RT–qPCR.

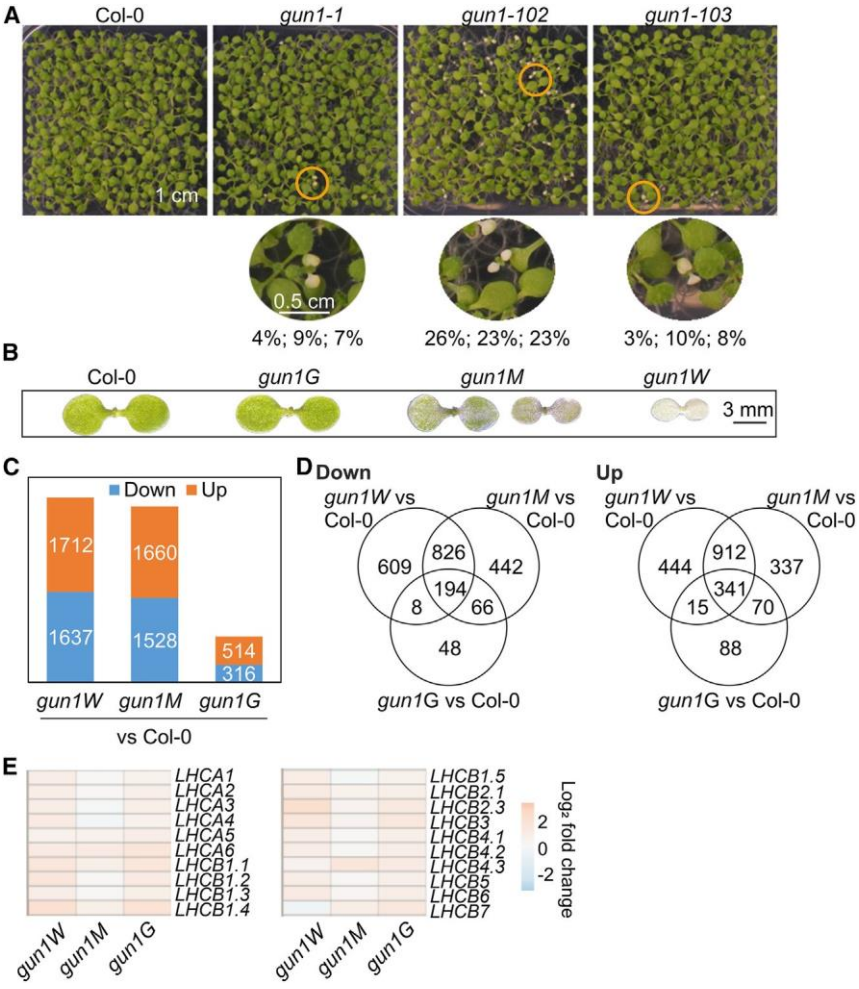

Figure 2. The nuclear transcriptome of white and marbled *gun1* seedlings is significantly affected.

(A) Phenotypes of 10-day-old Col-0, *gun1-1*, *gun1-102*, and *gun1-103* seedlings grown on MS without inhibitor supplementation under 16-h light/8-h dark conditions. Zoomed-in images were taken of white seedlings, denoted by the circles below the overview pictures. The percentages of abnormal seedlings (white and marbled cotyledons) were calculated for three different seed batches.

(B) Phenotypes of Col-0, *gun1G*, *gun1M*, and *gun1W* seedlings (derived from *gun1-102*).

(C) Analysis of transcriptome changes in white (*gun1W*), marbled (*gun1M*), and green (*gun1G*) *gun1-102* mutant seedlings. The numbers represent genes with at least a two-fold reduction (down) or elevation (up) compared with the Col-0 WT control.

(D) Venn diagrams depicting the degree of overlap between the sets of genes whose expression levels were altered at least two-fold in *gun1W*, *gun1M*, and *gun1G* compared with the Col-0 control.

(E) Heatmap showing transcript accumulation of genes encoding chlorophyll *a*/*b* binding proteins.

was also observed in *gun1-1* and *gun1-103* seedlings. The emerging true leaves turned green, suggesting that GUN1 has a specific role in chloroplast development in the cotyledons, consistent with the particular accumulation of GUN1 protein at early stages of cotyledon development (Wu et al., 2018). To obtain a general overview of RNA expression patterns in these prominent *gun1* seedlings, RNA isolated from 4-day-old Col-0 and *gun1W*, *-M*, and *-G* mutant seedlings (Figure 2B) was subjected to lncRNA-seq. Absence of transcription in a portion of exon 2 and subsequent exons of the *GUN1* gene was verified in all *gun1* mutant seedlings (Supplemental Figure 4), confirming the presence of the transfer DNA insertion in all *gun1* seedlings and validating the RNA-seq data. The strong phenotype of *gun1W* seedlings in particular suggests that the post(transcriptome) may be pleiotropically affected. The severity of the *gun1* phenotype was correlated with an increased number of de-regulated genes (Figure 2C). The expression of 3349 genes (including chimeras) changed significantly in *gun1W seedlings compared with* Col-0 (>two-fold, $P < 0.05$; Supplemental Table 1). Among these genes, 1637 showed decreased expression and 1712 showed increased expression, and the numbers of de-regulated genes in *gun1M* and *gun1G* were 3188 and 830, respectively (Figures 2C and 2D). mRNA expression of the marker gene *LHCB1.2* showed only a mild decrease compared with the significant reduction in Col-0 seedlings treated with LIN or NF. This pattern was evident for nearly all of the *LHC* members (Figure 2G).

In summary, the lack of GUN1 in *gun1W* and *gun1M* seedlings has a substantial effect on the nuclear transcriptome, but expression of *LHC* transcripts is only mildly decreased.

GUN1 deficiency has a significant impact on the entire chloroplast transcriptome

Both NF- and LIN-treated seedlings are bleached to the same degree as *gun1W* seedlings. Therefore, the following analyses involve data previously generated from NF-treated (Habermann et al., 2020) and LIN-treated (Xu et al., 2020) seedlings to account for putative pleiotropic effects in *gun1W* seedlings. Reads from these published data sets were analyzed using the same methodology as that used for our own data (Supplemental Tables 2 and 3). For the plastid transcriptome, we aimed to identify loci for which the relative ratio of editing or splicing was lower in *gun1W*/Col-0, progressively rescued in *gun1M*/Col-0 and *gun1G*/Col-0, and WT-like in NF/MS or LIN/MS. We concluded that the absence of GUN1 does not result in significant changes in chloroplast splicing or editing events (Supplemental Figures 5 and 6). However, plastid transcript levels of 91 out of 133 transcripts (including tRNAs, rRNA, and inverted repeats) were significantly reduced in *gun1W* compared with WT, and no transcripts were significantly induced (Supplemental Table 2). Transcription of chloroplast genes relies on plastid-encoded polymerases (PEPs) and

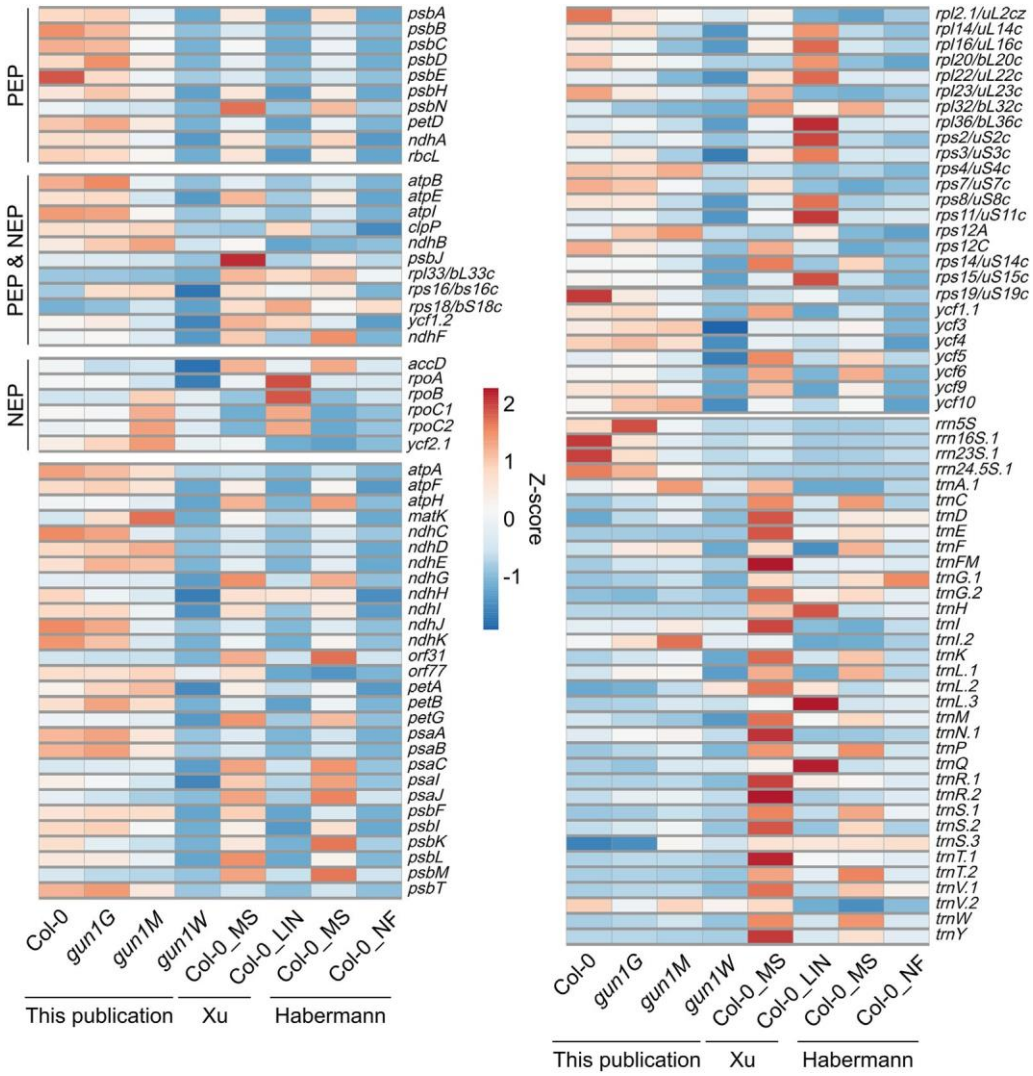

Figure 3. Heatmap illustrating the impact of GUN1 deficiency and NF and LIN treatment on plastid-encoded transcripts (*Z scores*).

Low to high expression is represented by the blue to red transition. Note that *Z* scores are calculated for each individual transcript over the different genotypes. NEP is a single-subunit enzyme, whereas PEP consists of core subunits that are encoded by the plastid genes *rpoA*, *rpoB*, *rpoC1*, and *rpoC2* (which are transcribed by NEP) and additional protein factors (sigma factors and polymerase-associated proteins [PAPs]) encoded by the nuclear genome (Borner et al., 2015; Liebers et al., 2018). The general picture has been that only PEP transcribes photosystem I and II genes (*psa* and *psb*), most other genes have both NEP and PEP promoters, and NEP alone transcribes a few housekeeping genes (*rpoB*, *accD*, *ycf2*) (Hajdukiewicz et al., 1997). However, more recent analyses have shown that the division of labor between NEPs and PEPs is more complex (Legen et al., 2002; Borner et al., 2015), and no clear conclusion can be drawn about PEP- or NEP-dependent transcription in *gun1W*: the so-called PEP-dependent genes had lower expression in *gun1W* than in Col-0, as did the genes transcribed by PEP and NEP, although to a lesser extent. NEP-dependent gene expression was also reduced or in the range of Col-0. The transcriptome changes in lincomycin (LIN)-treated (Xu et al., 2020) and NF-treated (Habermann et al., 2020) seedlings were reanalyzed in the same way as the sequencing data generated for this publication. NEP, nuclear-encoded RNA polymerase; PEP, plastid-encoded RNA polymerase.

nuclear-encoded polymerases (NEPs) (Borner et al., 2015; Liebers et al., 2018). No clear conclusion can be drawn about PEP- or NEP-dependent transcription in *gun1W*: expression of the so-called PEP-dependent genes was lower in *gun1W* than in Col-0, as was that of the genes transcribed by PEP and NEP, although to a lesser extent. NEP-dependent gene expression was also reduced or in the range of Col-0 (Figure 3; Supplemental Table 2). Note that in the following, our focus is on protein-coding genes, as tRNAs and rRNAs are not reliably detected by the RNA-seq protocol used. When we examined transcript accumulation of protein-coding genes in *gun1W* and NF- and LIN-treated Col-0 seedlings in parallel, we observed, remarkably, that 16 transcripts (excluding transcripts from inverted repeat B) were exclusively decreased in *gun1W* (Figure 4A; Supplemental Figure 7A; Supplemental Tables 2 and 3). This may be due to the use of different growth conditions. Whereas we used 4-day-old seedlings grown under long-day conditions, the NF-treated (Habermann et al., 2020) and LIN-treated (Xu et al., 2020) seedlings were grown under continuous light conditions for 4 and 5 days, respectively. We therefore performed an RT–qPCR experiment using seedlings grown under the same growth conditions (4-day-old seedlings

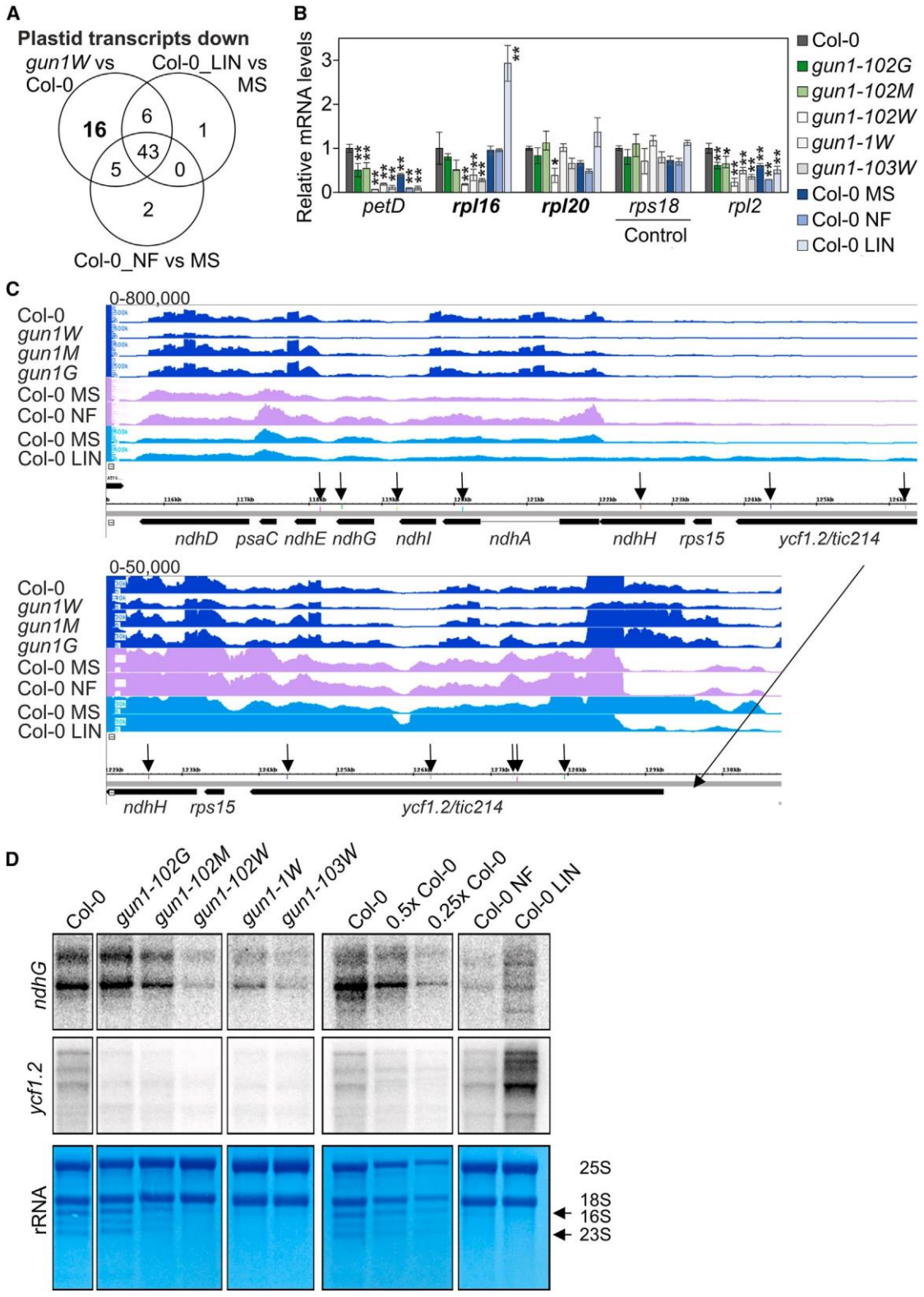

Figure 4. GUN1 deficiency has a significant impact on the chloroplast transcriptome.

(A) Venn diagrams depicting the degree of overlap between the sets of plastid protein-coding genes whose RNA expression levels were reduced by at least two-fold in *gun1W* relative to Col-0, as well as in LIN- and NF-treated seedlings compared with Col-0 grown on medium without inhibitor (MS). The

(legend continued on next page)

grown under long days) and confirmed the transcript accumulation behavior of *rpl16* and *rpl20* (Figure 4B). Apart from a few genes, most plastid genes belong to polycistronic units and are co-transcribed (Shahar et al., 2019). A closer look at transcripts exclusively reduced in *gun1W*, gradually increased in *gun1M*, and WT-like in *gun1G* drew our attention to a large polycistron containing *rpoA* along with several *rps* and *rpl* genes (Supplemental Figure 7B). Inspection of the coverage plots and transcript accumulation data revealed a comparable behavior for *ycf1.2*, *rps15*, and the *ndhH–ndhA–ndhI–ndhG–ndhE–psaC–ndhD* gene cluster (Figure 4C). The downregulation of transcripts was verified by northern blot detection of *ndhG* and *ycf1.2* (Figure 4D). It is noteworthy that although *ndhG* transcripts did not appear to be reduced in the RNA-seq data of Habermann et al. (2020), the transcript pattern and abundance in *gun1W* plants looked the same as those in Col-0 NF plants under our growth conditions, and therefore, a secondary effect of reduced *ndhG* transcripts in *gun1* seedlings cannot be excluded at this stage. By contrast, *ycf1.2* transcripts appear to be specifically reduced in *gun1W* compared with inhibitor-treated WT. In addition, during the quality control of RNA for sequencing, we observed strong rRNA depletion in *gun1W*, which was gradually rescued in *gun1M* and completely restored in *gun1G* (Figure 4D; Supplemental Figure 8A). The rRNA depletion phenotype was similar to that of Col-0 seedlings treated with NF or LIN (Figure 4D). Therefore, also for this pattern, a secondary effect cannot be excluded at this stage.

In conclusion, the plastid (post)transcriptome is significantly affected by GUN1 deficiency in *gun1W* and *gun1M* seedlings.

Re-evaluation of a putative RNA-binding function of GUN1

Many of the significant changes observed in the chloroplast (post) transcriptomes of *gun1W* and *gun1M* could explain their seedling phenotypes. But what is the primary cause? GUN1 is a P-type PPR protein, suggesting that it may be associated with RNA cleavage, splicing, and stabilization (Barkan and Small, 2014), and this led us to revisit a putative direct RNA-binding function of GUN1. PPR motifs bind to RNA in a one-repeat and one-nucleotide manner, and PPR motifs recognize specific RNA bases through amino acids at positions 5 and 35. Using this code, the binding sites of several PPR proteins can be predicted very well (Shen et al., 2016; Miranda et al., 2018; Yan et al., 2019). Because the correct PPR code is crucial for determining the binding sequence, we investigated the structural configuration of the GUN1 protein by modeling with PyMOL and found that the 12 PPR domains of GUN1 predicted by ScanProsite should be shifted by one amino acid (Supplemental Figure 9). We therefore adjusted the repeat annotation to better fit the predicted structure and description of canonical PPR tracts (Yan et al., 2019; Honkanen and Small, 2022). Prediction of putative RNA target sites (Yan et al., 2019) yielded the following ambiguous 11-nucleotide sequence: 5′-AA(U>C>G)(U>C>G)(C>U) (G>>C) (U>C>G) (C>U)(G>>C)A(C>U>A)-3' (Figure 5A). Using this ambiguous sequence and considering location in inverted repeat regions, 78 potential target sites can be identified within the chloroplast genome, distributed over 41 gene loci (Supplemental Table 4). The application of strict and very strict sequence-matching criteria, as explained in the figure legend to Figure 5A, yields 25 and 9 possible targets, respectively. On the basis of our previous analysis, two regions are noteworthy. One is the *ycf1.2–rps15–ndhH–ndhA–ndhI–ndhG–ndhE–psaC–ndhD* gene cluster (see Figure 4C), which contains ten potential targets. Among these targets, *ndhE* and 3′*ndhI* are also identified with the strict target sequence and *ndhG* with the very strict target sequence (Figure 5B; Supplemental Table 4). The second region is the *rrn23S* gene (Supplemental Figure 10), which contains four predicted target sequences: 23S_104766, 23S_104856, 23S_106002, and 23S_106558 (numbered according to the nucleotide position in the plastid genome). 23S_104856 and 23S_106558 fall within the strict possible targets. To gain insight into the accumulation of reads across the rRNA operon, we performed lncRNA-seq again without rRNA depletion. This analysis confirmed that plastid rRNAs are significantly reduced in *gun1W* and *gun1M* seedlings (Supplemental Figure 10). Upon closer examination of the first two binding sites and adjustment of the plots for differences in expression, a disproportionately high number of reads were found to map 5′ to the *rrn23S* gene, which is not present in *gun1G* (Supplemental Figure 10). In addition, a distinct coverage pattern of *rrn23S* was observed in the region of binding site 23S_106558, although a secondary effect on 23S rRNA still cannot be excluded.

GUN1 binds to chloroplast RNAs *in vivo* and *in vitro*

To investigate whether GUN1 is involved in RNA binding *in vivo*, RNA Co-IP was performed using a GPF-tagged GUN1 line (*GUN1–GFP*) (Tadini et al., 2016) with Col-0 as a control. The success of the IP experiment was demonstrated by detection of the tagged proteins in the respective eluates by western blotting (Supplemental Figure 11). Four predicted target regions

transcripts of inverted repeat B have been omitted. Note that for the transcripts downregulated by LIN or NF, the adjusted *P* value may also be higher than 0.05.

(B) RT–qPCR was used to determine expression levels of selected chloroplast transcripts. The results were normalized to the expression of *AT4G36800*, which encodes a RUB1-conjugating enzyme (RCE1). Expression values are reported relative to the corresponding transcript levels in Col-0, which were set to 1. Mean values ± SE were derived from three independent experiments, each performed with three technical replicates per sample. Statistically significant differences (post hoc Tukey's HSD test; **P* < 0.05 and ***P* < 0.01) between Col-0 (batch grown together with *gun1* seedlings), *gun1* mutants, and Col-0 seedlings grown on MS, NF, or LIN are indicated by black asterisks. Transcripts marked in bold were downregulated exclusively in *gun1W* but not under NF or LIN treatment.

(C) Coverage plots depict the accumulation of reads across the *ycf1.2–rps15–ndhH–ndhA–ndhI–ndhG–ndhE–psaC–ndhD* gene cluster. Vertical arrows point to predicted GUN1 binding sites (see Figure 6; Supplemental Table 6).

(D) Analysis of *ndhG* and *ycf1.2* transcript accumulation by northern blotting. Total RNA was isolated from 4-day-old Col-0 and *gun1-102* white, marbled, and green seedlings, as well as from Col-0 seedlings grown on medium supplemented with NF or LIN. The samples were run on the same gel but rearranged for clarity. As a loading control and for visualization of rRNAs, the membrane was stained with M.B. The arrows point to bands representing chloroplast rRNAs.

A

PPR repeat #	1	2	3	4	5	6	7	8	9	10	11	12	
Amino acid code	ST	SN	**ND**	ND	**NN**	**SD**	**ND**	**NN**	**SD**	**SN**	**NS**	SY	# of targets
Pred. RNA seq.	A	A	**U>C>G**	U>C>G	**C>U**	**G>>C**	**U>C>G**	**C>U**	**G>>C**	**A**	**C>U>A**	?	(wo IR):
First nucleotide only	A	A	**U**	U	**C**	**G**	**U**	**C**	**G**	**A**	C		0
U and C (Y) allowed	A	A	**Y**	Y	**Y**	**G**	**Y**	**Y**	**G**	**A**	**Y**		9
All allowed, still strict G	A	A	**B**	B	**Y**	**G**	**B**	**Y**	**G**	**A**	**H**		25
All nucleotides allowed	A	A	**B**	B	**Y**	**S**	**B**	**Y**	**S**	**A**	**H**		78

B

Target #	Start position	End position	Matched sequence for AYYYGYYGAY	Strand	Description
1	17952	17962	AACCCGCCGAC	Plus	*rpoC2*
2	22797	22807	AAUUUGUUGAU	Minus	*rpoC1*
3	31827	31837	AAUCCGUCGAU	Plus	BLRP of *psbD*
4	35646	35656	AAUCCGUUGAU	Minus	95 bp 5' of *ycf9*
5	47443	47453	AAUCCGUUGAC	Plus	Second exon of *trnL.1*
6	53800	53810	AACCCGUUGAU	Minus	*atpB*
7	71411	71421	AAUUUGUUGAC	Minus	First intron of *clpP*
8	118454	118464	AAUCUGUUGAU	Plus	*ndhG*
9	138429	138439	AAUUUGUCGAU	Minus	3' of *trnV.3*

Figure 5. Predicted GUN1 binding sites.

(A) Predicted ambiguous GUN1 target sequence. The numbers in the first row depict the PPR motif number, whereas the second row displays the amino acids in each PPR motif that are crucial for prediction of target nucleotides. For some amino acid combinations, the predicted target nucleotide is unique (such as ST and SN), whereas for others (such as ND), multiple nucleotides are predicted with descending preference. Subsequent rows indicate the prospective target sequences dependent on the stringency applied to the predicted nucleotides. For example, using only the first nucleotide of each of the predicted nucleotides results in 0 target sites. Allowing U, C, or G for the ambiguous B and G or C for "G>>C" results in 78 potential target sites. Allowing U, C, or G for the ambiguous B and only G for "G>>C" results in 25 potential target sites (here and in the following, marked in magenta). Allowing only U or C for the ambiguous Y and only G for "G>>C" results in 9 potential target sites (here and in the following, marked in blue). Highly conserved regions in GUN1 are highlighted in bold letters, according to Honkanen and Small (2022). In addition, representative predicted binding sites at *ndhG*, *ndhE*, and *rrn23S* are shown. wo IR, without inverted repeat.

(B) Table showing the nine sites in the "U and C (Y)" category.

of the notable regions described above (*ndhG*, *ycf1.2*, and two regions of *23S* rRNA; Figure 6A) along with negative controls were tested in RT–qPCRs of input and immunoprecipitated RNA, and the input/immunoprecipitated ratio was calculated. In GUN1 IPs, *ndhG*, *ycf1.2*, and a target in *23S* rRNA comprising binding sites 104766 and 104856 demonstrated significant enrichment in the pellet compared with the control (Figure 6B). By contrast, there was no significant enrichment of RNAs that lacked predicted target sites. Also, binding of GUN1 to *23S*_106558 was not statistically significant. However, the identification of *ndhG*, *ycf1.2*, and *23S* rRNA as true targets must be considered with caution. First, all RNAs tested gave a stronger signal in the GUN1 IP than in the control. Second, all negative controls contained a sample with extremely large error bars.

To determine whether GUN1 can directly bind to the identified target sites, we used electrophoretic mobility shift assays (EMSAs). It is difficult to obtain full-length GUN1 by overexpression in *E. coli*, possibly owing to the highly disordered domain in the N-terminal region (Shimizu et al., 2019). Therefore, we overexpressed a GUN1–PS construct encompassing all PPR and SMR motifs (PS) spanning amino acids 232 to 918 (Shimizu et al., 2019) in *E. coli* (Figure 6C) and used GUN1–PS for EMSAs. Four different Cy5-labeled RNA oligonucleotides were designed, representing the putative binding sites at *ndhG*, *23S*_104856, and *trnG.1* and an unrelated sequence. All probes were 25 bp long. The secondary structure of the non-specific probe was represented by a hairpin loop similar in structure to the *ndhG* probe, whereas the *trnG.1* probe formed a more stable hairpin loop, and the *23S* probe formed a predominantly circular loop. When 100, 200, 400, and 600 nM of purified GUN1–PS protein was added to the Cy5-labeled probes and the mixtures electrophoresed, band shifts were observed, especially for the *ndhG* and *trnG.1* probes. The shift was more pronounced at a higher protein concentration and was not detected when no protein or probe was added, indicating that the RNA probes formed complexes with the protein (Figure 6D). A slight shift could also be detected for *23S_104856*. However, the non-specific probe produced a similar shift pattern.

The intensity of the shifted *ndhG* and *trnG.1* bands progressively decreased upon addition of increasing concentrations of the respective unlabeled single-stranded RNAs but not upon addition of increasing concentrations of unlabeled, unrelated single-stranded RNA (Figure 6E). However, the intensity of the *23S* shift decreased upon addition of both the specific and the nonspecific competitor. This suggests that GUN1 binds

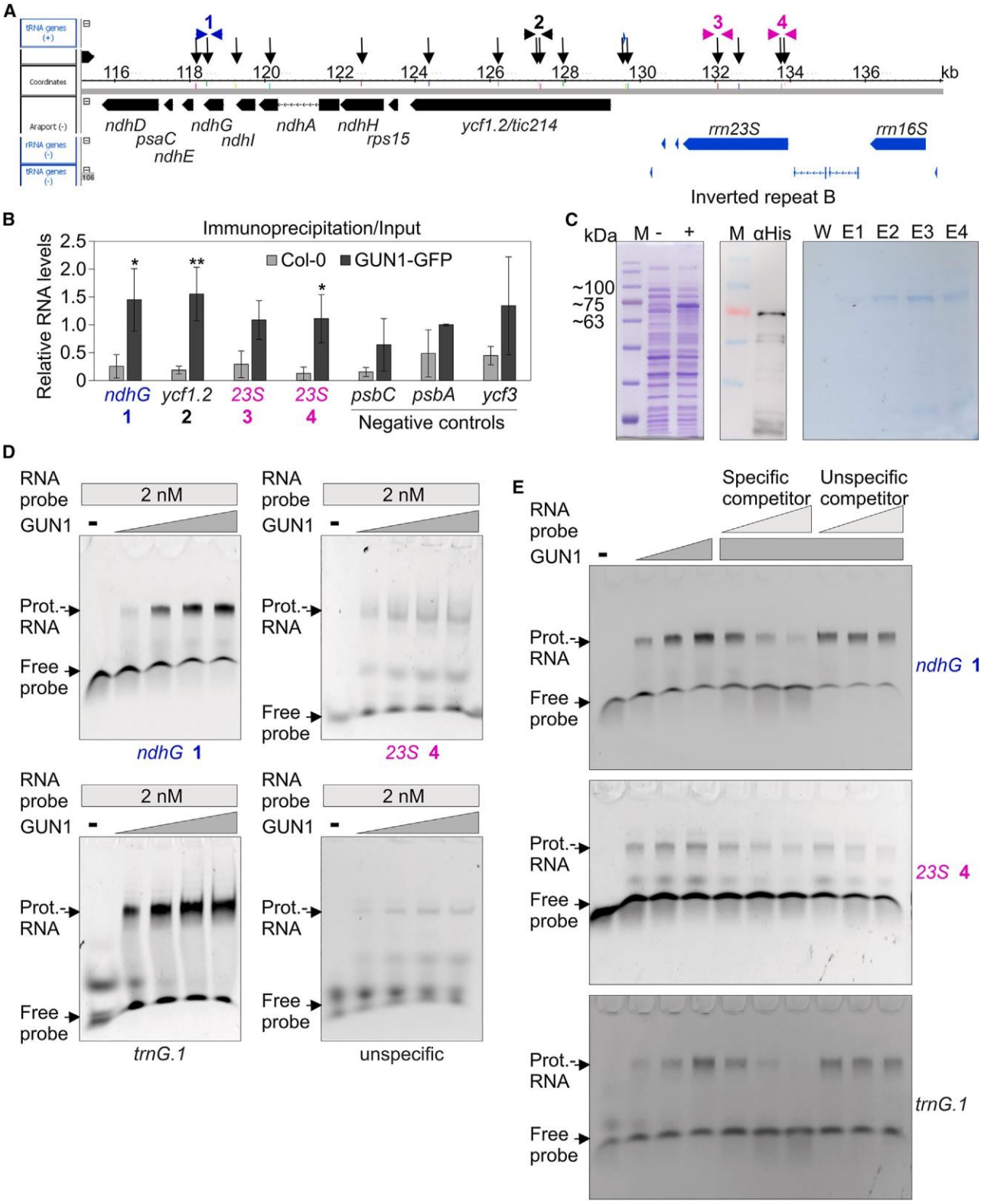

Figure 6. GUN1 binds to RNAs *in vivo* and *in vitro*.

(A) Schematic presentation of predicted RNA binding sites (indicated by black vertical arrows) in *ycf1.2*, the *rps15–ndhH–ndhA–ndhI–ndhG–ndhE–psaC–ndhD* polycistron, and the *rrn23S* gene. Positions of primers used in (B) are depicted with arrowheads using the color code explained in the legend to Figure 5.

specifically to the *ndhG* and *trnG.1* target sites but does not bind, or does so only weakly or nonspecifically, to *23S_104856*.

To obtain a broader view of the RNA targets of GUN1, libraries prepared from immunoprecipitated RNAs of the GUN1–GFP line and Col-0 were subjected to RNA-seq (RIP-seq). In addition to Col-0, another unrelated GFP-tagged line (PP7L–GFP; Xu et al., 2019) served as a control. Supplemental Table 5 shows the normalized read depths at each position in the chloroplast genome. Coverage files were generated using the bamCoverage tool, set to reads per kilobase per million, and reads were plotted across the entire chloroplast genome. This procedure revealed several read peaks in the GUN1 libraries that were not observed as strongly in plots of the control libraries (Figure 7A). These included, for example, *trnK*/*matK*, *trnG.1*, and *ndhB.1*. One predicted GUN1 target is the blue light responsive promoter (*BLRP*) of *psbD* (see Supplemental Table 4); *psbD* transcript levels are reduced to 11% in *gun1W* relative to the WT (see Supplemental Table 2), and RIP–qPCR and EMSA experiments recently suggested that GUN1 binds to the *BLRP* (Cui et al., 2023). However, our RIP-seq analysis did not show any enrichment of reads at the *BLRP* (Figure 7B), perhaps due to different growth conditions. We used 4-day-old seedlings grown under long-day conditions, whereas Cui et al. (2023) used seedlings grown in the dark for 2.5 days, which were then transferred to light (100 mmol m^{-2} s^{-1}) for 6 h. Furthermore, it has been shown that *BLRP* transcripts are strongly reduced in *gun1 p35S*::*GUN1–GFP* seedlings under the above-mentioned light-transfer growth conditions or in 5-day-old seedlings grown under continuous light (Cui et al., 2023), a result that we confirmed for the latter growth condition (Figure 7C). Therefore, failure to detect a peak in the *BLRP* region in our RIP-seq data may be due to insufficient levels of *BLRP* transcript input. To further investigate GUN1 binding to the *BLRP* region, we performed EMSA experiments with our *23S_104856*, *trnG.1*, and *ndhG* probes and the RNA1 and RNA3 probes designed by Cui et al. (2023). RNA1 includes the *BLRP* GUN1 binding site, and RNA3 is a probe with 10 mutation sites in the *BLRP* binding region. Addition of 800 nM purified GUN1 protein to 2 nM of each probe resulted in shifts of the *trnG.1* and *ndhG* probes, a weaker shift of the *23S_104856* probe, and a faint shifted smear of the RNA1 and RNA3 probes (Figure 7D). Two additional independent experiments produced similar results (Supplemental Figure 12A). Because we performed the binding reactions at 23ºC and ran them at 4ºC, we repeated the EMSA experiments twice using the conditions of Cui et al. (2023), who performed the binding reactions at 37ºC and ran them at room temperature, again showing similar results (Supplemental Figure 12B). There was no clear shift of the RNA1 probe, and the binding reaction with the RNA3 probe—which contained the mutation sites—behaved similarly to that with RNA1, although a shift was visible for *trnG.1* and *ndhG*. Therefore, under our RIP-seq and EMSA conditions with our GUN1–PS protein, we did not observe a shift of the *BLRP* GUN1 target. It should be noted that our GUN1–PS comprises amino acids 232 to 918, whereas the GUN1 protein expressed by Cui et al. (2023) contained 100 additional amino acids: it encompassed amino acids 132 to 918, and we cannot exclude the possibility that these 100 additional amino acids are required for *BLRP* binding.

Enrichment analysis at the exon level compared with RNAs identified in the control lines showed that 22 transcripts were significantly enriched in GUN1–GFP (Figure 7E; Supplemental Table 6); 13 of them contained at least one predicted GUN1 target region, covering a total of 26 predicted targets. This was a significant enrichment according to three different statistical tests, the chi-squared (P = 0.019), hypergeometric (P = 0.019), and binomial (P = 0.021) tests. The enriched transcripts harboring a predicted GUN1 target site included *ycf1.2*, *ycf2*, *rps2*, *rps12C* and *rpl20*, *rpoC1* and *rpoC2*, *ndhB*, the *ndhH–ndhA–ndhI–ndhG–ndhE–psaC–ndhD* gene cluster, and tRNAs such as *trnK*, *trnG.1*, and *trnI.2* (Figure 7E and 7F).

It is important to note that we did not sequence input libraries, and we only confirmed significant IP/input ratios for three targets (see Figure 6B). Overall, however, these experiments provide evidence for an RNA-binding function of GUN1 and suggest candidates for further testing.

DISCUSSION

Although the functions of other GUN proteins are well established, the specific molecular function of GUN1 has remained largely unclear. Most conclusions regarding GUN1 have been made by examining *gun1* mutants in combination with inhibitor treatments or in conjunction with the generation of double mutants (Richter et al., 2023). Our observation of *gun1W* and *gun1M* seedlings is independent of NF or LIN treatment. In these seedlings, the emerging true leaves turned green, suggesting a specific role for GUN1 in chloroplast development

(B) Demonstration of co-purification of selected RNAs with GUN1. RNAs that were isolated from the pellet after Co-IP experiments with Col-0 and a GUN1 overexpression line (GUN1–GFP) (IP) and the respective input RNAs (Input) were amplified by RT–qPCR. Ratios of immunoprecipitated versus input RNA levels are reported relative to the corresponding levels in the first Col-0 replicate, which were set to 1. Mean values ± SD were derived from three independent experiments, each performed with three technical replicates per sample. Statistically significant differences (post hoc Tukey's HSD test; *P < 0.05 and **P < 0.01) between GUN1–GFP and Col-0 lines are indicated by black asterisks.

(C) Overexpression and purification of a His-tagged GUN1–PS protein in *E. coli*. GUN1–PS encompasses all PPR and SMR motifs (PS) spanning amino acids 232 to 918. Left: SDS–PAGE before (—) and after (+) 20 h of induction at 18ºC; middle: western blot of the induced protein with an anti-His antibody; right: SDS–PAGE after purification. W, wash fraction with a buffer containing 20 mM imidazole; E1 and E2, elution fractions with a buffer containing 250 mM imidazole; E3 and E4, elution fractions with a buffer containing 500 mM imidazole.

(D) The GUN1 protein interacts *in vitro* with RNA sequences located in *ndhG* and *trnG*. EMSAs were performed with purified His-tagged GUN1 protein that was produced in *E. coli*. Aliquots (0, 100, 200, 400, and 600 nM) of purified GUN1 protein were incubated with Cy5-labeled single-stranded RNA (ssRNA) probes representing the putative target sequences and a nonspecific ssRNA probe. Binding reactions were performed at 23ºC, followed by electrophoresis on non-denaturing TBE polyacrylamide gels at 4ºC.

(E) Aliquots (0, 200, and 400 nM) of purified GUN1 protein were incubated with Cy5-labeled ssRNA probes in the presence of increasing concentrations (53, 253, 503; indicated by the light gray triangle) of the same unlabeled ssRNA (specific) or a nonlabeled ssRNA of unrelated sequence (nonspecific) as competitors. Binding reactions were then subjected to electrophoresis on non-denaturing TBE-polyacrylamide gels as performed in **(D)**.

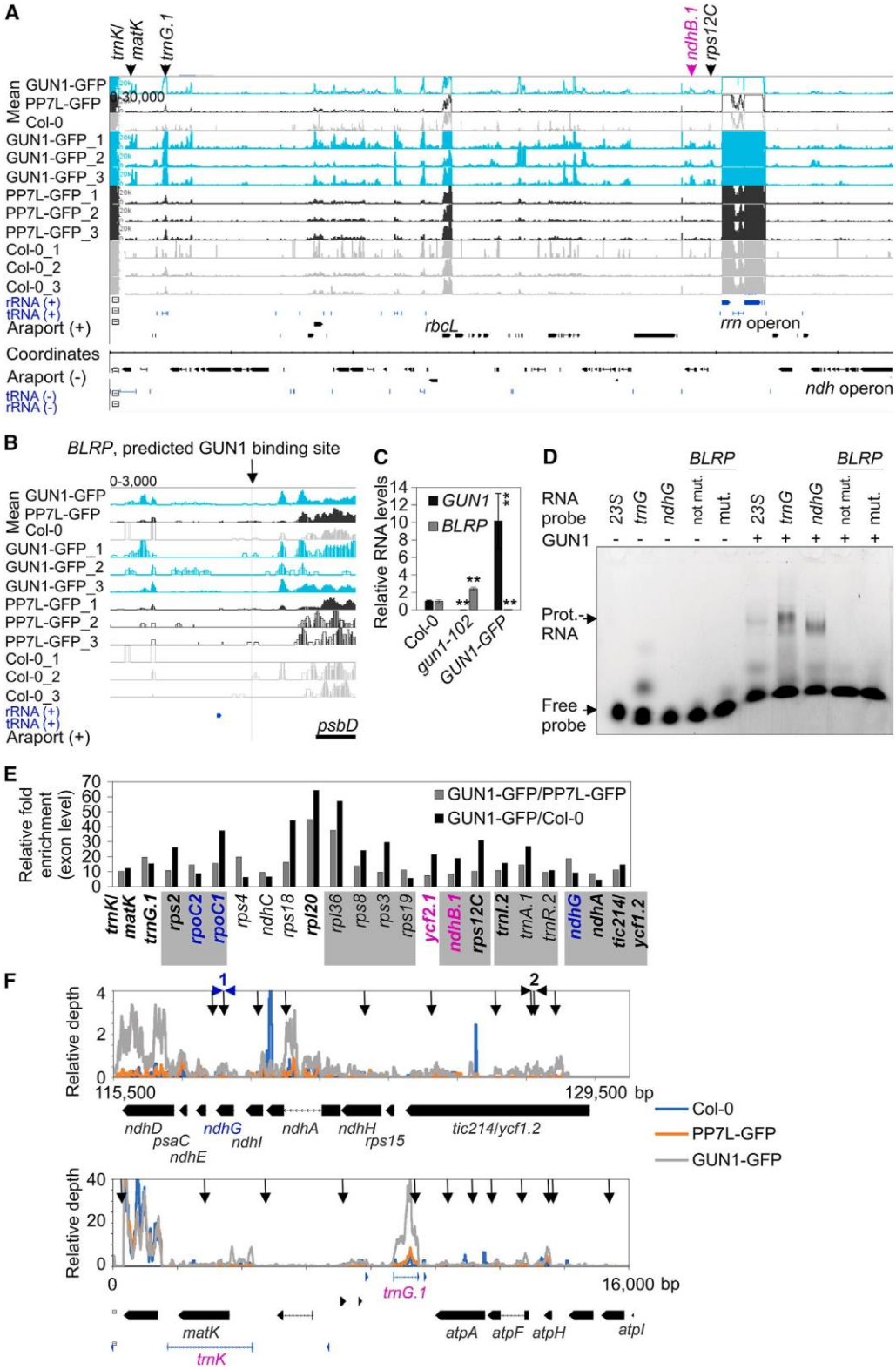

Figure 7. Identification of putative GUN1 targets by RIP-seq analysis.

(A) Libraries were prepared from RNAs co-immunoprecipitated from a GPF-tagged GUN1 line (GUN1–GFP) and, as controls, from a PP7L–GFP line and Col-0 and then sequenced. The experiment was performed with three biological replicates. Coverage plots of reads per kilobase per million (RPKM) values show the accumulation of reads across the chloroplast genome, here shown without inverted repeat B. Vertical arrows indicate examples of

in cotyledons. This is consistent with the particular accumulation of GUN1 at early stages of cotyledon development (Wu et al., 2018).

''Same genotype, different phenotype'' phenomenon

The prevailing view of *gun1* mutants is that adult plants exhibit no noteworthy phenotypes under normal growth conditions, apart from earlier flowering (Wu et al., 2018; Marino et al., 2019). Most inferences related to GUN1 were made when the *gun1* mutant was examined under stressful conditions, in combination with inhibitor treatments, or in conjunction with the creation of double mutants (see the introduction). We observed the appearance of *gun1* seedlings with white (*gun1W*) or marbled (*gun1M*) cotyledons when plants were grown under normal growth conditions and without inhibitor supplementation (see Figure 2). Previous reports also noted the sporadic presence of variegated (observed in *gun1-1* and *gun1-101*; Ruckle et al., 2007) or paler (observed in *gun1-101*; Wu et al., 2018) cotyledons. It is interesting to note that seedlings with the same genotype can exhibit various phenotypes. This phenomenon, described as incomplete penetrance and variable expressivity, is widely discussed in the animal field because of its relevance for diseases (Kingdom and Wright, 2022). Epigenetic modifications and environmental effects are potential factors that could contribute to this phenomenon. Environmental effects on mutants impaired in PGE have been observed, as in the case of *gun1* mutants, which exhibit a defect in cold acclimation (Marino et al., 2019). However, we can exclude a purely environmental cause for the appearance of *gun1W* seedlings, as they were interspersed among green *gun1* seedlings on the same plate. Epigenetic changes, specifically DNA methylation and histone modifications, can affect gene expression without modifying the DNA sequence. Again, these changes can be influenced by environmental factors and can result in distinct phenotypes despite identical genotypes. The *gun1W* seedlings were observed in diverse laboratories with different generations and *gun1* alleles, including complete knockouts (*gun1-101* and *gun1-102*). Therefore, epigenetics is also unlikely to be the primary/sole contributing factor. A comparable scenario to that of *gun1* mutants was described for the *immutants* and *variegated2* mutants. Nevertheless, these mutants exhibited green and white sectors within the same leaf. Discussion of these mutants revolves around the compensatory mechanisms and the concept of plastid autonomy for both mutants. However, although redundant gene products are suggested to be involved in *variegated2*, they are not implicated in *immutants*. The hypothesis is that the attainment of certain activity thresholds is required for the proper development of chloroplasts (Yu et al., 2007), and this may also apply for the *gun1* mutant. A threshold effect would also explain the sensitivity of *gun1* mutants to LIN, NF (Song et al., 2018; Zhao et al., 2018), and abscisic acid (Cottage et al., 2010) during early seedling development. Recently, a *gun1* molecular phenotype was identified under non-stressful conditions. This phenotype included lower activities of both superoxide dismutase and ascorbate peroxidase and, consequently, higher superoxide anion concentrations and lipid peroxidation compared with the WT, suggesting that GUN1 may protect chloroplasts from oxidative damage (Fortunato et al., 2022). The phenotype could also be influenced by the presence of modifier genes that can suppress or enhance the mutant phenotype, as observed for floral trait variation, which is highly dependent on ecotype (Juenger et al., 2000). In the absence of GUN1, compensatory mechanisms may be activated during seedling development, and the failure of compensation in only a subset of the population is likely dependent on the intensity or specific nature of environmental stresses experienced by the parent plants. This, in turn, may indicate that there are critical thresholds of environmental factors beyond which the compensation is inadequate, leading to phenotypic variability within the population. In addition, GUN1 protein accumulates at the early stages of cotyledon development, and the timing of gene expression during development is known to influence penetrance (Kingdom and Wright, 2022). However, further analysis is needed and may include how stochastic factors—such as segregation of organelle genomes through development and reproduction (Broz et al., 2024) — in conjunction with environmental factors and transgenerational effects contribute to the development of individual phenotypes (Burga and Lehner, 2012).

Functions of GUN1 in plastid transcript maturation

GUN1 was previously suggested to regulate plastid RNA editing during NF treatment of seedlings (Zhao et al., 2019). The proposed mechanism involved the interaction of GUN1 with

regions with higher read accumulation in GUN1–GFP compared with PP7L–GFP and Col-0 and that also contain a match to the predicted GUN1 target code (see Supplemental Tables 4 and 6). The color code is explained in the legend to Figure 5.

(B) Coverage plot of RPKM values across the blue light responsive promoter (*BLRP*) of *psbD* encompassing the predicted GUN1 binding site.

(C) RT–qPCR to determine expression levels of *GUN1* and the *BLRP* region covering the predicted GUN1 binding site. Seedlings were grown under continuous light (100 mmol m^{-2} s^{-1}) for 5 days. The results were normalized to *AT4G36800*, which encodes a RUB1-conjugating enzyme (RCE1). Expression values are reported relative to the corresponding transcript levels in Col-0, which were set to 1. Mean values ± SE were derived from three independent experiments, each performed with three technical replicates per sample. Statistically significant differences (post hoc Tukey's HSD test; $*P < 0.05$ and $**P < 0.01$) between Col-0 and the transgenic lines are shown.

(D) Under our conditions, the GUN1 protein does not interact *in vitro* with the predicted GUN1 binding site located in the *BLRP*. EMSAs were performed with purified His-tagged GUN1 protein that was produced in *E. coli*. Aliquots (0 and 800 nM) of purified GUN1 protein were incubated with 2 nM Cy5-labeled ssRNA probes representing the putative target sequences and a *BLRP* probe containing 10 mutated sites (mut.). Binding reactions were performed at 23°C, followed by electrophoresis on non-denaturing TBE polyacrylamide gels at 4°C.

(E) Libraries were prepared from RNAs isolated from the Co-IP experiments described in **(A)**. Relative enrichment ratios (calculated at the exon level) of GUN1–GFP relative to Col-0 and GUN1–GFP relative to PP7L–GFP are shown. Gray shading indicates genes located in a polycistron. Transcripts that also contain a match to the predicted GUN1 target code (see Supplemental Tables 4 and 6) are written in bold. The color code is explained in the legend to Figure 5.

(F) Plot of RIP-seq data over two example regions. Relative depth was calculated at each nucleotide (nt) position by relating the number of reads to the total depth of the sequencing output. Black vertical arrows indicate predicted UN1 RNA-binding sites.

MORF2 and did not require the direct interaction of GUN1 with the target transcript, which was a logical explanation because no *in vivo* RNA-binding function of GUN1 had been demonstrated to date. However, the role of GUN1 in editing and its contribution to GUN signaling have not yet been satisfactorily resolved for several reasons. First, the oeMORF2 *gun* phenotype has been postulated for NF treatment but not LIN treatment. Second, the slight differences in editing performance between Col-0 and *gun1* during NF treatment (see Figure 1) are unlikely to be the trigger for retrograde signaling. Third, editing of relevant sites was more or equally suppressed in oeMORF2 compared with *gun1-9*. One would therefore expect oeMORF2 lines to be even stronger *gun* mutants than *gun1* itself, but this was not the case for both our data and data generated by Zhao et al. (2019) (see Figure 1). Here, it should be noted that our oeMORF2 lines had lower *MORF2* mRNA expression levels than those generated by Zhao et al. (2019). However, other studies have also not found any involvement of GUN1 in editing changes in other retrograde signaling processes (Kakizaki et al., 2012; Loudya et al., 2020). Furthermore, GUN1 is classified as a member of the P-type PPR proteins, which rarely have a direct role in editing (Small et al., 2020).

GUN1 is one of the five PPR-SMR chloroplast-located proteins, all of which have essential functions in chloroplast development (see Figure 2; Zhang and Lu, 2019). Interestingly, GUN1 protein is present at very low levels and is barely detectable by proteomic approaches, whereas the other PPR-SMR proteins are particularly abundant compared with most PPR proteins (Liu et al., 2013). This fact, together with the distinct (post) transcriptome of *gun1* mutants (see Figure 3), may be important for the unique function of GUN1 in GUN signaling, as *svr7* and *sot1* mutants are not *gun* mutants (Wu et al., 2016). Interestingly, plastid rRNA accumulation is impaired in mutants of the three proteins SVR7, SOT1, and GUN1. Whereas SOT1 (Wu et al., 2016; Zhou et al., 2017) binds directly to the (precursor) *23S* rRNA, this is not clear for SVR7 and is questionable for GUN1 (see Figure 6). Therefore, the defect in rRNA accumulation in the *svr7* mutant and *gun1W* and *gun1M* seedlings may be a secondary effect. However, the primary function of SVR7 is to ensure correct expression of the ATP synthase (Zoschke et al., 2013). For SOT1, specifically its function in rRNA maturation has been investigated, and it has been shown that the SMR domain has endonuclease activity (Wu et al., 2016; Zhou et al., 2017), but other targets are, to date, unknown. Interestingly, in contrast to those in the *gun1* mutant, the plastid transcripts of protein-coding genes (except *ndhA*) in *sot1* tend to be slightly upregulated (Yan et al., 2019), whereas the *gun1* (post)transcriptome is greatly affected, and we identified a plethora of enriched RNA sites in our RIP-seq experiment (see Figure 7).

The significantly reduced plastid rRNA levels (Scharff and Bock, 2014) would be sufficient to explain the *gun1W* phenotype, although this reduction is likely to be a secondary effect. The determination of theoretical targets of GUN1 on the basis of its PPR code and enriched targets by RIP-seq analysis suggests that *ycf1.2*, *ycf2*, *rps2*, *rps12C* and *rpl20*, *rpoC1* and *rpoC2*, *ndhB*, *ndhA* and *ndhG*, *matK*, and tRNAs such as *trnK*, *trnG.1*, and *trnI.2* are putative targets. Moreover, EMSA analysis suggests *in vitro* binding of GUN1 to two of these targets, *ndhG* and *trnG.1*. However, whether *ndhG* and *trnG.1* are authentic physiological targets of GUN1 still remains to be determined. NdhG is a component of the NAD(P)H dehydrogenase (NDH) complex. As discussed above, GUN1 is needed for cold acclimation (Marino et al., 2019), and GUN1 may protect chloroplasts from oxidative damage (Fortunato et al., 2022). This protection may be achieved by stabilization of the NDH complex to ensure chloroplast function, especially under oxidative stress conditions. However, here it has to be noted that the role of the NDH complex under different stress conditions remains controversial (Yamori and Shikanai, 2016). The *Arabidopsis* plastid genome contains two genes encoding precursor tRNAs specific for glycine: *trnG.1* for tRNA-Gly(UCC) and *trnG.2* for tRNA-Gly(GCC). Through Watson–Crick base pairing and by wobbling, tRNA-Gly(UCC) recognizes GGA and GGG codons, and tRNA-Gly(GCC) reads GGC and GGU triplets (Tiller and Bock, 2014). However, knockout of *trnG.2* in the tobacco plastid genome demonstrated that translation is maintained to some extent, but the trnG-UCC gene encoding tRNA-Gly(UCC) is essential. This suggests that tRNA-Gly(UCC), encoded by *trnG.1*, is sufficient to read all four glycine triplets (Rogalski et al., 2008). The *gun1W* phenotype is not lethal; therefore, an additional protein may be involved in *trnG.1* maturation, or the *gun1-102* mutant may still permit residual GUN1 expression. However, reduced maturation of *trnG.1* and possibly the predicted targets *trnK*, *trnI.2*, *rps2*, *rps12C*, and *rpl20* (all of which are essential) likely results in reduced protein translation, including that of chloroplast-encoded RNA polymerase subunits. This, or a direct effect of GUN1 on *rpoC1* and *rpoC2*, which contain predicted GUN1 target sites, may cause the widespread downregulation of chloroplast transcripts in *gun1W* seedlings.

Interestingly, GUN1 is predicted to bind to multiple sites in *ycf1.2*, and no *ycf1.2* maturation factors have been identified to date. Our data do not reveal precisely how GUN1 performs its function on plastid RNA, which may involve transcript stabilization or endonucleolytic cleavage through its SMR domain. In addition, we do not address how the molecular function of GUN1 relates to retrograde signaling. Nevertheless, we provide strong evidence that GUN1 binds to RNA and suggest target sites. We anticipate that our findings will serve as a foundation for subsequent studies exploring the role of GUN1 in plastid RNA metabolism and retrograde signaling.

METHODS

Plant material and growth conditions

The *gun1-1* mutant and the transfer DNA insertional mutants *gun1-102* (*SAIL_290_D09*) and *gun1-103* (*SAIL_742_A11*) are derived from the Col-0 ecotype and have been described previously (for example, Shimizu et al., 2019).

To detect editing levels via RT–PCR, surface-sterilized seeds were sown on MS plates containing 0.8% (m/v) agar. The seeds were then stratified for 4 days in the dark at 4°C. Seedlings were grown for 5 days at 22°C under continuous illumination (100 mmol photons m^{-2} s^{-1}) provided by white fluorescent lamps. For NF treatment, MS medium was supplemented with or without a 5 mM final concentration of NF (Sigma-Aldrich, 34364).

For RNA-seq and RIP experiments, surface-sterilized seeds were sown on half-strength MS plates containing 1% sucrose. The plates were then kept

in the dark at 4ºC for 2 days. Following stratification, the seedlings were grown under a 16-h light/8-h dark photoperiod at 22ºC with a light intensity of 100 mmol photons m^{-2} s^{-1} for 4 days. For the results shown in Figure 7C, seedlings were grown under continuous light (100 mmol m^{-2} s^{-1}) for 5 days after stratification.

Generation of oeMORF2 transgenic lines

The *35S:MORF2-YFP* transgene was constructed into the pFGC5941 binary transformation vector as described previously (Yapa et al., 2023). To avoid post-transcriptional co-suppression and to stabilize high expression of *MORF2-YFP*, *35S:MORF2-YFP* was transformed into the post-transcriptional gene silencing mutant *sgs3-1* (Butaye et al., 2004). Plants containing a single insertion of *35S:MORF2-YFP* were identified on the basis of a 3:1 (resistant/sensitive) segregation ratio of T2 plants grown on 1/2 MS medium containing 15 mg/L phosphinothricin. Homozygous transgenic plants were obtained in the T3 generation and further self-fertilized to generate T4 plants that were used for phenotypic analysis.

RNA preparation, cDNA synthesis, and RT–qPCR

Plant material (70 mg) was frozen in liquid nitrogen and then crushed using a TissueLyser (Retsch, model MM400). One milliliter of TRIZOL (Invitrogen, Carlsbad, CA, USA) and 200 ml of chloroform were used for RNA isolation according to the manufacturer's instructions. RNA was then precipitated from the aqueous phase using isopropyl alcohol, and the resulting RNA pellet was washed with 70% (v/v) ethanol and dissolved in RNase-free water. After DNase I treatment (New England Biolabs [NEB], Ipswich, MA, USA), 10 mg of RNA was further cleaned with the RNA Clean & Concentrator-5 Kit (Zymo Research, Irvine, CA, USA; R1016). The purified RNA (500 ng) was used to synthesize cDNA with the iScript cDNA Synthesis Kit (Bio-Rad). RT–qPCR analysis was performed on a Bio-Rad iQ5 real-time PCR instrument with iQ SYBR Green Supermix (Bio-Rad). The primers used for this assay are listed in Supplemental Table 7. Tukey's honestly significant difference test was performed using the following website: https://astatsa.com/OneWay_Anova_with_TukeyHSD/.

RNA editing analysis by amplicon sequencing

The same growth conditions used by Zhao et al. (2019) were applied. Total RNA was isolated from agar-plate-grown seedlings by acid guanidinium thiocyanate–phenol–chloroform-based extraction and purified from the aqueous phase using the Monarch RNA Clean Up Kit (NEB). Genomic DNA in the samples was removed using TURBO DNase (Thermo Fisher Scientific, Waltham, MA, USA), followed by purification with the Monarch RNA Clean Up Kit (NEB). RNA (1 mg per sample) was transcribed to cDNA with Protoscript II reverse transcriptase (NEB). *clpP*, *psbZ*, *rpoC1*, *rpoB*, *ndhB*, and *ndhF* amplicons were amplified from all samples with Q5 polymerase (NEB). Amplification specificity was assessed by agarose gel electrophoresis, and amplicons were then purified with the Monarch PCR & DNA Clean Up Kit (NEB). Resulting DNA concentrations were measured spectrophotometrically with a NanoDrop instrument. Equimolar amounts of all amplicons from a given sample were pooled and analyzed by the Amplicon-EZ service from Genewiz. The resulting 250-bp paired-end reads were mapped with the short-read aligner BBMap (https://sourceforge.net/projects/bbmap) to an amplicon-specific reference. RNA editing was assessed from the mapped reads as described previously (Royan et al., 2021).

RNA gel-blot analysis

Total RNA was isolated using TRIzol reagent (Thermo Fisher Scientific). RNA samples were digested with DNase I (NEB) to remove genomic DNA. Then, 2 mg of total RNA was electrophoresed on a denaturing formaldehyde gel, transferred to a nylon membrane (Hybond-XL; GE Healthcare, Freiburg, Germany), and cross-linked with UV light. Hybridizations were performed at 65ºC overnight according to standard protocols. The results were visualized using the Typhoon scanner (GE Healthcare).

RNA editing and splicing analysis of lncRNA-seq data

To ascertain the presence of edited and spliced transcripts from organelles from lncRNA-seq datasets, the Chloro-Seq pipeline (Malbert et al., 2018) was used with the modifications described in Xu et al. (2023).

RNA-seq and data analysis

Total RNA from plants was isolated with Trizol (Invitrogen), purified with Direct-zol RNA MiniPrep Plus columns (Zymo Research), and sequenced as described previously (Xu et al., 2019). RNA-seq reads were analyzed on the Galaxy platform (Afgan et al., 2016) essentially as described previously (Xu et al., 2019) except that reads were first mapped with the gapped-read mapper RNA STAR (Dobin et al., 2013) to generate the coverage plots in a subsequent step. The BAM files generated by RNA STAR were also used to determine the expression levels of chloroplast-encoded genes. To this end, reads were counted with featureCounts (Liao et al., 2014) using the gene annotation in Araport11 (https://www.arabidopsis.org/download/list?dir=Public_Data_Releases%2FTAIR_Data_20230630), allowing multimapping of reads to account for the inverted repeat regions. Differentially expressed genes were identified using DESeq2 (Love et al., 2014) with the fit type set to "parametric," a linear two-fold change cutoff, and an adjusted $P < 0.05$. To determine expression levels of nuclear-encoded genes, the reads were mapped with Salmon (Patro et al., 2017) to identify differentially expressed genes as described in Xu et al. (2023), except that the updated AtRTD3-QUASI high-resolution transcriptome (Zhang et al., 2022) was used as the reference transcriptome.

Protein expression and EMSAs

The pET48 AtGUN1–PS plasmid, encoding amino acids 232 to 918 of GUN1 with an N-terminal TRX-His tag, which was published in Shimizu et al. (2019), was obtained from Addgene (plasmid #136358). The plasmid was isolated and then transformed into BL21(DE3) cells (Thermo Fisher Scientific; EC0114) for protein expression. A positive colony was inoculated into Luria-Bertani medium containing 50 mg/ml ampicillin and grown overnight. The overnight culture was then diluted 1:100 and grown to an optical density 600 of 0.5. After cooling on ice for 30 min, 1 M IPTG was added to a final concentration of 1 mM to induce protein expression, and the culture was incubated at 18ºC for 20 h. After harvest of bacterial cells by centrifugation at 4ºC, the soluble tagged GUN1 protein was extracted and purified using Protino Ni-NTA agarose (Macherey-Nagel, Düren, Germany; #7450400-500) according to the manufacturer's instructions. Although the pET48 AtGUN1-PS construct tends to form inclusion bodies, purification was attempted from the supernatant to preserve the native state of the GUN1–PS protein. Detection with an anti-His antibody (Sigma-Aldrich, Taufkirchen, Germany; SAB1305538) confirmed the presence of the GUN1–PS protein. The protein concentration was determined using the Qubit protein assay kit (Invitrogen, Thermo Fisher Scientific; Q33211), and the protein was used fresh or stored at -80ºC for further use after addition of an equal volume of 50% glycerol.

For EMSA experiments, the indicated amounts of purified protein were used in the binding reactions. Each reaction consisted of 4 ml of 53 binding buffer (50 mM Tris–HCl [pH 7.5], 50 mM NaCl, 200 mM KCl, 5 mM $MgCl_2$, 5 mM EDTA, 5 mM DTT, 0.25 mg/ml BSA, and 5% glycerol), the specified amounts of protein, and 2 ml of a 1 nM Cy5-labeled probe. For competitor assays, the indicated amount of competitor was added to the binding reaction. The reactions were incubated for 30 min at 23ºC, followed by addition of 2 ml of 20% Ficoll 400 (v/v). The samples were then run on a 5% native polyacrylamide gel in a cold room at 4ºC. The gel was preconditioned for 1 h at 60 V in 0.53 TBE containing 2.5% glycerol to remove any residual ammonium persulfate. One well was loaded with 13 Orange G loading buffer as an indicator. Gel electrophoresis was performed at 60 V until adequate separation was achieved. The Cy5 signal was then detected using a FUSION FX scanner (VILBER LOURMAT GmbH, Eberhardzell, Germany).

RIP-seq and RT–qPCR

For RIP, we adapted a previously described method (Wang et al., 2022) with some modifications. Four-day-old seedlings grown on 1/2 MS medium were fixed with 1% formaldehyde for 15 min by vacuum infiltration. The fixation was stopped with 125 mM glycine for 5 min, again by vacuum infiltration. The seedlings were then washed four times with prechilled sterile ddH_20, ground to a fine powder with liquid nitrogen, and stored at —80°C for later use. Each ground plant sample (250 mg) was homogenized in 1 ml of RIP buffer. The composition of the RIP buffer was consistent with that of the original paper. Instead of preparing the beads–antibody conjugate, commercial GFP Trap Magnetic Agarose beads (gtma-20; ChromoTek) were used. Forty microliters of GFP-Trap was initially washed three times with 400 ml of RIP buffer and then incubated with 800 ml of cleared lysate for 2 h. The remaining steps for IP, RNA release, and extraction were performed following the previously outlined procedure (Wang et al., 2022). A western blot was performed for input, flow-through, and pull-down fractions of all samples with a GFP polyclonal antibody (Invitrogen; A6455). DNA contamination was removed using 2 U DNaseI (NEB; M0303S), and samples were then purified with the RNA Clean & Concentrator-5 Kit (Zymo).

For subsequent sequencing, the RNA was processed with the NEBNext Ultra II RNA Library Prep Kit from Illumina (NEB; E7770L). The libraries were then sequenced on an Illumina NextSeq 1000 system and analyzed on the Galaxy platform (Afgan et al., 2016). For RT–qPCR, 2 ml of purified RNA was reverse transcribed using the SuperScript IV Reverse Transcriptase Kit (Invitrogen, 18090050) with random hexamer priming. The cDNA synthesis reaction was performed under the following conditions: initial incubation at 23°C for 10 min, followed by reverse transcription at 55°C for 15 min for efficient cDNA synthesis. The reaction was then inactivated by heating at 80°C for 10 min. RT–PCR was performed on a Bio-Rad iQ5 real-time PCR instrument using SYBR Green Supermix (Bio-Rad; 1725274). All primer information is provided in Supplemental Table 7.

DATA AND CODE AVAILABILITY

Sequencing data have been deposited in NCBI's Gene Expression Omnibus (Edgar et al., 2002) and are accessible under GEO: GSE202931. Reads from experiments performed by Habermann et al. (2020), Zhao et al. (2019), and Xu et al. (2020) were retrieved from the NCBI Sequence Read Archive (SRA: PRJNA557616 and PRJNA432917, respectively) and Gene Expression Omnibus (GEO: GSE130337).

FUNDING

Funding was provided by the Deutsche Forschungsgemeinschaft to C.S.-L., D.L., and T.K. (TRR175, projects A02, C01, and C05). Research in the Hua laboratory was supported by a US NSF CAREER award (MCB-1750361).

ACKNOWLEDGMENTS

We thank David Meinke for critical discussions, Michael Färberböck and Katrin Straßer for excellent technical assistance, Irma Racic for library preparation for RIP-seq, Helmut Blum and Stefan Krebs for sequencing the RIP libraries, and Eslam Abdel-Salam for help with statistical questions. No conflict of interest is declared.

AUTHOR CONTRIBUTIONS

Conceptualization, Q.T., D.X., and T.K.; formal analysis and supervision, T.K.; investigation, Q.T., D.X., A.B., B.L., M.M.Y., T.M., Z.H., and T.K.; writing – original draft, T.K., with input from Z.H., C.S.-L., and D.L.; writing – review & editing, all authors; funding acquisition, C.S.-L., Z.H., D.L., and T.K.

SUPPLEMENTAL INFORMATION

Supplemental information is available at *Plant Communications Online*.

Received: February 14, 2024
Revised: August 5, 2024
Accepted: August 20, 2024

REFERENCES

Afgan, E., Baker, D., van den Beek, M., Blankenberg, D., Bouvier, D.,Č Čech, M., Chilton, J., Clements, D., Coraor, N., Eberhard, C. et al. (2016). The Galaxy platform for accessible, reproducible and collaborative biomedical analyses: 2016 update. Nucleic Acids Res. 44:W3–W10. https://doi.org/10.1093/nar/gkw343.

Archibald, J.M. (2015). Endosymbiosis and Eukaryotic Cell Evolution. Curr. Biol. 25:R911–R921. https://doi.org/10.1016/j.cub.2015.07.055.

Barkan, A., and Small, I. (2014). Pentatricopeptide repeat proteins in plants. Annu. Rev. Plant Biol. 65:415–442. https://doi.org/10.1146/annurev-arplant-050213-040159.

Borner, T., Aleynikova, A.Y., Zubo, Y.O., and Kusnetsov, V.V. (2015). Chloroplast RNA polymerases: Role in chloroplast biogenesis. Biochim. Biophys. Acta 1847:761–769. https://doi.org/10.1016/j.bbabio.2015.02.004.

Broz, A.K., Sloan, D.B., and Johnston, I.G. (2024). Stochastic organelle genome segregation through Arabidopsis development and reproduction. New Phytol. 241:896–910. https://doi.org/10.1111/nph.19288.

Burga, A., and Lehner, B. (2012). Beyond genotype to phenotype: why the phenotype of an individual cannot always be predicted from their genome sequence and the environment that they experience. FEBS J. 279:3765–3775. https://doi.org/10.1111/j.1742-4658.2012.08810.x.

Butaye, K.M.J., Goderis, I.J.W.M., Wouters, P.F.J., Pues, J.M.T.G., Delauré, S.L., Broekaert, W.F., Depicker, A., Cammue, B.P.A., and De Bolle, M.F.C. (2004). Stable high-level transgene expression in Arabidopsis thaliana using gene silencing mutants and matrix attachment regions. Plant J. 39:440–449. https://doi.org/10.1111/j.1365-313X.2004.02144.x.

Christian, R.W., Hewitt, S.L., Roalson, E.H., and Dhingra, A. (2020). Genome-Scale Characterization of Predicted Plastid-Targeted Proteomes in Higher Plants. Sci. Rep. 10:8281. https://doi.org/10.1038/s41598-020-64670-5.

Cottage, A., Mott, E.K., Kempster, J.A., and Gray, J.C. (2010). The Arabidopsis plastid-signalling mutant gun1 (genomes uncoupled1) shows altered sensitivity to sucrose and abscisic acid and alterations in early seedling development. J. Exp. Bot. 61:3773–3786. https://doi.org/10.1093/jxb/erq186.

Cui, C., Sun, S., Zhang, S., Zhang, Y., and Kim, C. (2023). GENOMES UNCOUPLED1: an RNA-binding protein required for early PSII biogenesis. Preprint at bioRxiv, 2023.09.21.558905. https://doi.org/10.1101/2023.09.21.558905.

Dobin, A., Davis, C.A., Schlesinger, F., Drenkow, J., Zaleski, C., Jha, S., Batut, P., Chaisson, M., and Gingeras, T.R. (2013). STAR: ultrafast universal RNA-seq aligner. Bioinformatics 29:15–21. https://doi.org/10.1093/bioinformatics/bts635.

Edgar, R., Domrachev, M., and Lash, A.E. (2002). Gene Expression Omnibus: NCBI gene expression and hybridization array data repository. Nucleic Acids Res. 30:207–210. https://doi.org/10.1093/nar/30.1.207.

Fortunato, S., Lasorella, C., Tadini, L., Jeran, N., Vita, F., Pesaresi, P., and de Pinto, M.C. (2022). GUN1 involvement in the redox changes occurring during biogenic retrograde signaling. Plant Sci. 320:111265. https://doi.org/10.1016/j.plantsci.2022.111265.

Habermann, K., Tiwari, B., Krantz, M., Adler, S.O., Klipp, E., Arif, M.A., and Frank, W. (2020). Identification of small non-coding RNAs responsive to GUN1 and GUN5 related retrograde signals

Arabidopsis thaliana. Plant J. 104:138–155. https://doi.org/10.1111/tpj.14912.

Hajdukiewicz, P.T., Allison, L.A., and Maliga, P. (1997). The two RNA polymerases encoded by the nuclear and the plastid compartments transcribe distinct groups of genes in tobacco plastids. EMBO J. 16:4041–4048. https://doi.org/10.1093/emboj/16.13.4041.

Hong, W., Zeng, J., and Xie, J. (2014). Antibiotic drugs targeting bacterial RNAs. Acta Pharm. Sin. B 4:258–265. https://doi.org/10.1016/j.apsb.2014.06.012.

Honkanen, S., and Small, I. (2022). The GENOMES UNCOUPLED1 protein has an ancient, highly conserved role but not in retrograde signalling. New Phytol. 236:99–113. https://doi.org/10.1111/nph.18318.

Juenger, T., Purugganan, M., and Mackay, T.F. (2000). Quantitative trait loci for floral morphology in Arabidopsis thaliana. Genetics 156:1379–1392. https://doi.org/10.1093/genetics/156.3.1379.

Kakizaki, T., Yazu, F., Nakayama, K., Ito-Inaba, Y., and Inaba, T. (2012). Plastid signalling under multiple conditions is accompanied by a common defect in RNA editing in plastids. J. Exp. Bot. 63:251–260. https://doi.org/10.1093/jxb/err257.

Kakizaki, T., Matsumura, H., Nakayama, K., Che, F.S., Terauchi, R., and Inaba, T. (2009). Coordination of plastid protein import and nuclear gene expression by plastid-to-nucleus retrograde signaling. Plant Physiol. 151:1339–1353. https://doi.org/10.1104/pp.109.145987.

Kingdom, R., and Wright, C.F. (2022). Incomplete Penetrance and Variable Expressivity: From Clinical Studies to Population Cohorts. Front. Genet. 13:920390. https://doi.org/10.3389/fgene.2022.920390.

Kleine, T., and Leister, D. (2015). Emerging functions of mammalian and plant mTERFs. Biochim. Biophys. Acta 1847:786–797. https://doi.org/10.1016/j.bbabio.2014.12.009.

Kleine, T., and Leister, D. (2016). Retrograde signaling: Organelles go networking. Biochim. Biophys. Acta 1857:1313–1325. https://doi.org/10.1016/j.bbabio.2016.03.017.

Kleine, T., Maier, U.G., and Leister, D. (2009). DNA transfer from organelles to the nucleus: the idiosyncratic genetics of endosymbiosis. Annu. Rev. Plant Biol. 60:115–138. https://doi.org/10.1146/annurev.arplant.043008.092119.

Koussevitzky, S., Nott, A., Mockler, T.C., Hong, F., Sachetto-Martins, G., Surpin, M., Lim, J., Mittler, R., and Chory, J. (2007). Signals from chloroplasts converge to regulate nuclear gene expression. Science 316:715–719. https://doi.org/10.1126/science. 1140516.

Liao, Y., Smyth, G.K., and Shi, W. (2014). featureCounts: An efficient general purpose program for assigning sequence reads to genomic features. Bioinformatics 30:923–930.

Legen, J., Kemp, S., Krause, K., Profanter, B., Herrmann, R.G., and Maier, R.M. (2002). Comparative analysis of plastid transcription profiles of entire plastid chromosomes from tobacco attributed to wild-type and PEP-deficient transcription machineries. Plant J. 31:171–188. https://doi.org/10.1046/j.1365-313x.2002.01349.x.

Liebers, M., Chevalier, F., Blanvillain, R., and Pfannschmidt, T. (2018). PAP genes are tissue- and cell-specific markers of chloroplast development. Planta 248:629–646. https://doi.org/10.1007/s00425-018-2924-8.

Liebers, M., Cozzi, C., Uecker, F., Chambon, L., Blanvillain, R., and Pfannschmidt, T. (2022). Biogenic signals from plastids and their role in chloroplast development. J. Exp. Bot. 73:7105–7125. https://doi.org/10.1093/jxb/erac344.

Liu, S., Melonek, J., Boykin, L.M., Small, I., and Howell, K.A. (2013). PPR-SMRs: ancient proteins with enigmatic functions. RNA Biol. 10:1501–1510. https://doi.org/10.4161/rna.26172.

Loudya, N, Okunola,T., He, J., Jarvis, P., and López-Juez, E. (2020). Retrograde signalling in a virescent mutant triggers an anterograde delay of chloroplast biogenesis that requires GUN1 and is essential for survival. Philos. Trans. R. Soc. Lond. B Biol. Sci. 375:20190400. https://doi.org/10.1098/rstb.2019.0400.

Loudya, N., Barkan, A., and López-Juez, E. (2024). Plastid retrograde signaling: A developmental perspective. Plant Cell 28:koae094. https://doi.org/10.1093/plcell/koae094.

Love, M.I., Huber, W., and Anders, S. (2014). Moderated estimation of fold change and dispersion for RNA-seq data with DESeq2. Genome Biol. 15:550. https://doi.org/10.1093/bioinformatics/btt656.

Malbert, B., Rigaill, G., Brunaud, V., Lurin, C., and Delannoy, E. (2018). Bioinformatic Analysis of Chloroplast Gene Expression and RNA Posttranscriptional Maturations Using RNA Sequencing. Methods Mol. Biol. 1829:279–294. https://doi.org/10.1007/978-1-4939-8654-5_19.

Marino, G., Naranjo, B., Wang, J., Penzler, J.F., Kleine, T., and Leister, D. (2019). Relationship of GUN1 to FUG1 in chloroplast protein homeostasis. Plant J. 99:521–535. https://doi.org/10.1111/tpj.14342.

Miranda, R.G., McDermott, J.J., and Barkan, A. (2018). RNA-binding specificity landscapes of designer pentatricopeptide repeat proteins elucidate principles of PPR-RNA interactions. Nucleic Acids Res. 46:2613–2623. https://doi.org/10.1093/nar/gkx1288.

Oelmuller, R., Levitan, I., Bergfeld, R., Rajasekhar, V.K., and Mohr, H. (1986). Expression of nuclear genes as affected by treatments acting on the plastids. Planta 168:482–492. https://doi.org/10.1007/BF00392267.

Paieri, F., Tadini, L., Manavski, N., Kleine, T., Ferrari, R., Morandini, P., Pesaresi, P., Meurer, J., and Leister, D. (2018). The DEAD-box RNA Helicase RH50 Is a 23S-4.5S rRNA Maturation Factor that Functionally Overlaps with the Plastid Signaling Factor GUN1. Plant Physiol. 176:634–648. https://doi.org/10.1104/pp.17.01545.

Patro, R., Duggal, G., Love, M.I., Irizarry, R.A., and Kingsford, C. (2017). Salmon provides fast and bias-aware quantification of transcript expression. Nat. Methods 14:417–419. https://doi.org/10.1038/nmeth.4197.

Peragine, A., Yoshikawa, M., Wu, G., Albrecht, H.L., and Poethig, R.S. (2004). SGS3 and SGS2/SDE1/RDR6 are required for juvenile development and the production of trans-acting siRNAs in Arabidopsis. Genes Dev. 18:2368–2379. https://doi.org/10.1101/gad.1231804.

Richter, A.S., Nägele, T., Grimm, B., Kaufmann, K., Schroda, M., Leister, D., and Kleine, T. (2023). Retrograde signaling in plants: A critical review focusing on the GUN pathway and beyond. Plant Commun. 4:100511. https://doi.org/10.1016/j.xplc.2022.100511.

Rogalski, M., Karcher, D., and Bock, R. (2008). Superwobbling facilitates translation with reduced tRNA sets. Nat. Struct. Mol. Biol. 15:192–198. https://doi.org/10.1038/nsmb.1370.

Royan, S., Gutmann, B., Colas des Francs-Small, C., Honkanen, S., Schmidberger, J., Soet, A., Sun, Y.K., Vincis Pereira Sanglard, L., Bond, C.S., and Small, I. (2021). A synthetic RNA editing factor edits its target site in chloroplasts and bacteria. Commun. Biol. 4:545. https://doi.org/10.1038/s42003-021-02062-9.

Ruckle, M.E., DeMarco, S.M., and Larkin, R.M. (2007). Plastid signals remodel light signaling networks and are essential for efficient chloroplast biogenesis in Arabidopsis. Plant Cell 19:3944–3960. https://doi.org/10.1105/tpc.107.054312.

Scharff, L.B., and Bock, R. (2014). Synthetic biology in plastids. Plant J. 78:783–798. https://doi.org/10.1111/tpj.12356.

Shahar, N., Weiner, I., Stotsky, L., Tuller, T., and Yacoby, I. (2019). Prediction and large-scale analysis of primary operons in plastids reveals unique genetic features in the evolution of chloroplasts.

Nucleic Acids Res. 47:3344–3352. https://doi.org/10.1093/nar/gkz151.

Shen, C., Zhang, D., Guan, Z., Liu, Y., Yang, Z., Yang, Y., Wang, X., Wang, Q., Zhang, Q., Fan, S., et al. (2016). Structural basis for specific single-stranded RNA recognition by designer pentatricopeptide repeat proteins. Nat. Commun. 7:11285. https://doi.org/10.1038/ncomms11285.

Shimizu, T., Kacprzak, S.M., Mochizuki, N., Nagatani, A., Watanabe, S., Shimada, T., Tanaka, K., Hayashi, Y., Arai, M., Leister, D., et al. (2019). The retrograde signaling protein GUN1 regulates tetrapyrrole biosynthesis. Proc. Natl. Acad. Sci. USA 116:24900– 24906. https://doi.org/10.1073/pnas.1911251116.

Small, I., Melonek, J., Bohne, A.V., Nickelsen, J., and Schmitz-Linneweber, C. (2023). Plant organellar RNA maturation. Plant Cell 35:1727–1751. https://doi.org/10.1093/plcell/koad049.

Small, I.D., Schallenberg-Rüdinger, M., Takenaka, M., Mireau, H., and Ostersetzer-Biran, O. (2020). Plant organellar RNA editing: what 30 years of research has revealed. Plant J. 101:1040–1056. https://doi.org/10.1111/tpj.14578.

Song, L., Chen, Z., and Larkin, R.M. (2018). The genomes uncoupled Mutants Are More Sensitive to Norflurazon Than Wild Type. Plant Physiol. 178:965–971. https://doi.org/10.1104/pp.18.00982.

Susek, R.E., Ausubel, F.M., and Chory, J. (1993). Signal transduction mutants of Arabidopsis uncouple nuclear CAB and RBCS gene expression from chloroplast development. Cell 74:787–799.

Tadini, L., Peracchio, C., Trotta, A., Colombo, M., Mancini, I., Jeran, N., Costa, A., Faoro, F., Marsoni, M., Vannini, C., et al. (2020). GUN1 influences the accumulation of NEP-dependent transcripts and chloroplast protein import in Arabidopsis cotyledons upon perturbation of chloroplast protein homeostasis. Plant J. 101:1198–1220. https://doi.org/10.1111/tpj.14585.

Tadini, L., Pesaresi, P., Kleine, T., Rossi, F., Guljamow, A., Sommer, F., Mühlhaus, T., Schroda, M., Masiero, S., Pribil, M., et al. (2016). GUN1 Controls Accumulation of the Plastid Ribosomal Protein S1 at the Protein Level and Interacts with Proteins Involved in Plastid Protein Homeostasis. Plant Physiol. 170:1817–1830. https://doi.org/10.1104/pp.15.02033.

Tiller, N., and Bock, R. (2014). The translational apparatus of plastids and its role in plant development. Mol. Plant 7:1105–1120. https://doi.org/10.1093/mp/ssu022.

Wang, L., Xu, D., Scharf, K., Frank, W., Leister, D., and Kleine, T. (2022). The RNA-binding protein RBP45D of Arabidopsis promotes transgene silencing and flowering time. Plant J. 109:1397–1415. https://doi.org/10.1111/tpj.15637.

Woodson, J.D., Perez-Ruiz, J.M., and Chory, J. (2011). Heme synthesis by plastid ferrochelatase I regulates nuclear gene expression in plants. Curr. Biol. 21:897–903. https://doi.org/10.1016/j.cub.2011.04.004.

Wu, G.Z., Chalvin, C., Hoelscher, M., Meyer, E.H., Wu, X.N., and Bock,R. (2018). Control of Retrograde Signaling by Rapid Turnover of GENOMES UNCOUPLED1. Plant Physiol. 176:2472–2495. https://doi.org/10.1104/pp.18.00009.

Wu, W., Liu, S., Ruwe, H., Zhang, D., Melonek, J., Zhu, Y., Hu, X., Gusewski, S., Yin, P., Small, I.D., et al. (2016). SOT1, apentatricopeptide repeat protein with a small MutS-related domain, is required for correct processing of plastid 23S-4.5S rRNA precursors in Arabidopsis thaliana. Plant J. 85:607–621. https://doi. org/10.1111/tpj.13126.

Xu, D., Dhiman, R., Garibay, A., Mock, H.P., Leister, D., and Kleine, T. (2020). Cellulose defects in the Arabidopsis secondary cell wall promote early chloroplast development. Plant J. 101:156–170. https://doi.org/10.1111/tpj.14527.

Xu, D., Tang, Q., Xu, P., Schäffner, A.R., Leister, D., and Kleine, T. (2023). Response of the organellar and nuclear (post)transcriptomes of Arabidopsis to drought. Front. Plant Sci. 14:1220928. https://doi.org/10.3389/fpls.2023.1220928.

Xu, D., Marino, G., Klingl, A., Enderle, B., Monte, E., Kurth, J., Hiltbrunner, A., Leister, D., and Kleine, T. (2019). Extrachloroplastic PP7L Functions in Chloroplast Development and Abiotic Stress Tolerance. Plant Physiol. 180:323–341. https://doi.org/10.1104/pp.19.00070.

Yamori, W., and Shikanai, T. (2016). Physiological functions of cyclic electron transport around photosystem I in sustaining photosynthesis and plant growth. Annu. Rev. Plant Biol. 67:81–106. https://doi.org/10.1146/annurev-arplant-043015-112002.

Yan, J., Yao, Y., Hong, S., Yang, Y., Shen, C., Zhang, Q., Zhang, D., Zou, T., and Yin, P. (2019). Delineation of pentatricopeptide repeat codes for target RNA prediction. Nucleic Acids Res. 47:3728–3738. https://doi.org/10.1093/nar/gkz075.

Yapa, M.M., Doroodian, P., Gao, Z., Yu, P., and Hua, Z. (2023). MORF2-mediated plastidial retrograde signaling is involved in stress response and skotomorphogenesis beyond RNA editing. Front. Plant Sci. 14:1146922. https://doi.org/10.3389/fpls.2023.1146922.

Yu, F., Fu, A., Aluru, M., Park, S., Xu, Y., Liu, H., Liu, X., Foudree, A., Nambogga, M., and Rodermel, S. (2007). Variegation mutants and mechanisms of chloroplast biogenesis. Plant Cell Environ. 30:350–365. https://doi.org/10.1111/j.1365-3040.2006.01630.x.

Zhang, R., Kuo, R., Coulter, M., Calixto, C.P.G., Entizne, J.C., Guo, W., Marquez, Y., Milne, L., Riegler, S., Matsui, A., et al. (2022). A high-resolution single-molecule sequencing-based Arabidopsis transcriptome using novel methods of Iso-seq analysis. Genome Biol. 23:149. https://doi.org/10.1186/s13059-022-02711-0.

Zhang, Y., and Lu, C. (2019). The Enigmatic Roles of PPR-SMR Proteins in Plants. Adv. Sci. 6:1900361. https://doi.org/10.1002/advs.201900361.

Zhang, Y., Tian, L., and Lu, C. (2023). Chloroplast gene expression: Recent advances and perspectives. Plant Commun. 4:100611. https://doi.org/10.1016/j.xplc.2023.100611.

Zhao, X., Huang, J., and Chory, J. (2018). genome uncoupled1 Mutants Are Hypersensitive to Norflurazon and Lincomycin. Plant Physiol. 178:960–964. https://doi.org/10.1104/pp.18.00772.

Zhao, X., Huang, J., and Chory, J. (2019). GUN1 interacts with MORF2 to regulate plastid RNA editing during retrograde signaling. Proc. Natl. Acad. Sci. USA 116:10162–10167. https://doi.org/10.1073/pnas.1820426116.

Zhou, W., Lu, Q., Li, Q., Wang, L., Ding, S., Zhang, A., Wen, X., Zhang, L., and Lu, C. (2017). PPR-SMR protein SOT1 has RNA endonuclease activity. Proc. Natl. Acad. Sci. USA 114:E1554–E1563. https://doi.org/10.1073/pnas.1612460114.

Zoschke, R., Qu, Y., Zubo, Y.O., Börner, T., and Schmitz-Linneweber,C. (2013). Mutation of the pentatricopeptide repeat-SMR protein SVR7 impairs accumulation and translation of chloroplast ATP synthase subunits in Arabidopsis thaliana. J. Plant Res. 126:403–414. https://doi.org/10.1007/s10265-012-0527-1.

.

Chapter 2

Response of the organellar and nuclear (post)transcriptomes of *Arabidopsis* to drought

frontiers | Frontiers in Plant Science

TYPE Original Research
PUBLISHED 17 July 2023
DOI 10.3389/fpls.2023.1220928

OPEN ACCESS

EDITED BY
Josefa M. Alamillo,
University of Cordoba, Spain

REVIEWED BY
Piotr Gawroński,
Warsaw University of Life Sciences, Poland
Hunseung Kang,
Chonnam National University, Republic of Korea

*CORRESPONDENCE
Tatjana Kleine
tatjana.kleine@lmu.de

RECEIVED 11 May 2023
ACCEPTED 28 June 2023
PUBLISHED 17 July 2023

CITATION
Xu D, Tang Q, Xu P, Schäffner AR, Leister D and Kleine T (2023) Response of the organellar and nuclear (post)transcriptomes of Arabidopsis to drought.
Front. Plant Sci. 14:1220928.
doi: 10.3389/fpls.2023.1220928

Response of the organellar and nuclear (post)transcriptomes of Arabidopsis to drought

Duorong Xu [1], Qian Tang [1], Ping Xu [2], Anton R. Schäffner[2], Dario Leister[1] and Tatjana Kleine [1]*

[1]Plant Molecular Biology, Faculty of Biology, Ludwig-Maximilians-University Munich, Planegg-Martinsried, Germany, [2]Department of Environmental Sciences, Institute of Biochemical Plant Pathology, Helmholtz Zentrum München, München, Germany

Plants have evolved sophisticated mechanisms to cope with drought, which involve massive changes in nuclear gene expression. However, little is known about the roles of post-transcriptional processing of nuclear or organellar transcripts and how meaningful these changes are. To address these issues, we used RNA-sequencing after ribosomal RNA depletion to monitor (post) transcriptional changes during different times of drought exposure in Arabidopsis Col-0. Concerning the changes detected in the organellar transcriptomes, chloroplast transcript levels were globally reduced, editing efficiency dropped, but splicing was not affected. Mitochondrial transcripts were slightly elevated, while editing and splicing were unchanged. Conversely, alternative splicing (AS) affected nearly 1,500 genes (9% of expressed nuclear genes). Of these, 42% were regulated solely at the level of AS, representing transcripts that would have gone unnoticed in a microarray-based approach. Moreover, we identified 927 isoform switching events. We provide a table of the most interesting candidates, and as proof of principle, increased drought tolerance of the carbonic anhydrase *ca1* and *ca2* mutants is shown. In addition, altering the relative contributions of the spliced isoforms could increase drought resistance. For example, our data suggest that the accumulation of a nonfunctional *FLM* (*FLOWERING LOCUS M*) isoform and not the ratio of *FLM-ß* and -δ isoforms may be responsible for the phenotype of early flowering under long-day drought conditions. In sum, our data show that AS enhances proteome diversity to counteract drought stress and represent a valuable resource that will facilitate the development of new strategies to improve plant performance under drought.

KEYWORDS

alternative splicing, carbonic anhydrase, chloroplast, drought, *FLOWERING LOCUS M* (FLM), mitochondria, nucleus, (post)transcriptome

1. Introduction

Land plants must cope with all sorts of environmental conditions, since, as sessile organisms, they cannot evade them. Owing to climate change, the frequency and amplitude of extreme conditions are increasing, and this seriously threatens crop yields worldwide (Zhao et al., 2017). Drought is the most important abiotic stress (Singh et al., 2018), and responses to drought are influenced by developmental stage, plant species and degree of stress (Hu and Xiong, 2014). The primary strain during drought stress is dehydration – loss of water from the cell – which triggers osmotic and hormone-related signals (Blum, 2016), in particular the phytohormone abscisic acid (ABA) (Zhu, 2002). Terminology and approaches to drought research vary widely and the issues are often oversimplified (Lawlor, 2013; Blum and Tuberosa, 2018; Kooyers, 2019). Taking our cue from the work of Lawlor (2013) and Blum (2016) and the TNAU Agritech Portal (https://agritech.tnau.ac.in/agriculture/agri_drought_tolerent_mechanism.html), we define drought resistance in terms of the following features: (i) drought survival, ii) drought escape, iii) drought avoidance, and iv) drought tolerance. Drought survival refers to the fact that, under drought conditions, cells, tissues, and organs are able to maintain key cellular functions and can recover, with minimal damage, upon relief of drought stress (Lawlor, 2013). Dehydration avoidance is a response to moderate, temporary drought stress, which involves deposition of cuticular waxes and growth retardation, in addition to the reduction of transpiration *via* ABA-mediated closure of stomata (Gupta et al., 2020). In the drought-escape strategy, which is employed by annual plants like *Arabidopsis thaliana* (Arabidopsis), flowering is accelerated before drought can compromise survival of the plant (Kenney et al., 2014). In drought tolerance, the plant is able to maintain its functions under dehydration – for example, by producing larger amounts of sugars, osmoprotectants, antioxidants, and scavengers of reactive oxygen species (Hu and Xiong, 2014).

Responses to drought and other stresses are accompanied by large-scale changes in gene expression that facilitate the production of compounds needed to counteract the imposed strain (Bashir et al., 2019). Thus, transcriptome-based studies have identified acetate as a compound that helps plants to survive drought stress (Kim et al., 2017), and shown that the transcription factor AGAMOUS-LIKE 22 (also known as SHORT VEGETATIVE PHASE, SVP), which participates in primary metabolism and developmental processes, is activated in drought-stressed Arabidopsis plants (Bechtold et al., 2016). Here it has to be noted that these experiments were performed under short-day conditions. Changes in nuclear gene expression in response to environmental perturbations, including drought stress, are fine-tuned by retrograde signals from the chloroplast (Estavillo et al., 2011; Kleine and Leister, 2016), and chloroplasts act both as a target and as a sensor of environmental changes (Kleine et al., 2021). In a forward genetic screen two chloroplast proteins involved in drought resistance were identified (Hong et al., 2020). Furthermore, the first steps of ABA biosynthesis take place in plastids (Ali et al., 2020), which underlines the importance of the chloroplast in the response to drought stress. Although chloroplasts and mitochondria each harbor only around 100 genes (Kleine et al., 2009), organellar gene expression is complex, and transcripts can undergo post-transcriptional modification events such as splicing and editing (Germain et al., 2013). Therefore, the abundance and functionality of a number of organellar proteins depends not only on the levels of their transcripts, but also on their modification status. The same holds true for nucleus-encoded transcripts: Here, alternative splicing (AS) provides for the synthesis of different transcript isoforms from the same gene, thereby increasing proteome diversity (Laloum et al., 2018; Bashir et al., 2019). It has become clear that AS is of central importance for abiotic stress tolerance in plants (Laloum et al., 2018), and AS itself is dynamically regulated under cold stress (Calixto et al., 2018). Concerning organellar transcriptome changes, it has been demonstrated that heat stress over periods of several hours increases the abundance of chloroplast transcripts, and induces a global reduction in splicing and editing efficiency (Castandet et al., 2016), but to our knowledge, the behavior of the mitochondrial (post) transcriptomic landscape has not been investigated so far.

However, microarray analysis has been the major source of information on transcriptome changes in response to drought (Bechtold et al., 2016; Kim et al., 2017; Bashir et al., 2019), while transcriptome-wide AS analysis in response to cold has been addressed with the aid of mRNA sequencing (mRNA-Seq) (Calixto et al., 2018). Both methods make use of samples enriched for polyadenylated transcripts, and are designed specifically to trace the accumulation of nuclear transcripts. Functional organellar transcripts are not polyadenylated; indeed, unlike nuclear transcripts, they become unstable upon addition of a poly(A) tail (Rorbach et al., 2014).

Therefore, we set out to extend the investigation of changes in nuclear gene expression under drought stress by undertaking an overarching characterization of the post(transcriptome), including alternative splicing of nuclear transcripts, accumulation of organellar (chloroplast and mitochondrion) transcripts, and editing and splicing of organellar transcripts. To this end, an RNA-Seq strategy was applied, which involves library preparation after depletion of ribosomal RNAs instead of enrichment for mRNAs as in mRNA-Seq. For reproducibility, an already published drought kineticsset-up (Kim et al., 2017) was applied. Based on our platform, we describe changes in the various organellar and nuclear (post)transcriptomes under drought and complement this with an analysis of nuclear-encoded transcript isoform switches. We provide a table with the most interesting candidates worth for the investigation of their involvement in drought responses. In particular, we demonstrate increased drought tolerance of the carbonic anhydrase *ca1* and *ca2* mutants, and suggest an FLM (FLOWERING LOCUS M)-dependent early flowering mechanism under long-day drought conditions, which is characterized by massive production of non-functional *FLM* isoforms.

2. Materials and methods

2.1 Plant material and growth conditions

All Arabidopsis (*Arabidopsis thaliana*) lines used in this study share the Columbia genetic background. The carbonic anhydrase

ca1 and *ca2* mutants were described previously (Dabrowska-Bronk et al., 2016). Seeds were sown on 1/2 MS medium containing 1% (w/v) sucrose and 0.8% (w/v) agar, incubated at 4°C for 2 d, and transferred to a climate chamber under a 16-h-light/8-h-dark cycle with a light intensity of 100 *m*E m^{-2} s^{-1} at 22°C. For physiological experiments, the plants were grown on potting soil (A210, Stender, Schermbeck, Germany) for 3 or 4 weeks.

For drought treatments, 7-day-old seedlings were transferred to pots, and grown for a further 2 weeks under normal growth conditions. Three-week-old plants were subjected to drought conditions by withholding water for the indicated times. The drought phenotypes were documented with a camera (Canon 550D, Krefeld, Germany). For strictly controlled drought experiments, seeds were stratified for 3 days, and then sown directly on soil for germination. After 5 days, seedlings were transferred to pots containing 100 g moist soil and sand mixture (150 ± 0.5 g total pot weight) with 5 replicates for each genotype in a randomized design. From this time on, plant growth was in controlled environment on a conveyor-belt organized system allowing programmable watering by pot weight, RGB imaging, and chlorophyll fluorescence analyses (Photon Systems Instruments, Ltd. (PSI), Drasov, Czech Republic); there, plants were grown under short-day conditions (10 h light, 22°C, 45% relative humidity/14h darkness, 20°C, 60% relative humidity; Georgii et al., 2017) with LED (white, blue, red, dark red) illumination at a light intensity of 115 *m*E m^{-2} s^{-1}. The pot weight was increased to 165 g within two days by multiple watering (3 g a time, 2-3 times a day). Drought treatment began for 18-day-old plants. During the drought treatment, the pots lost approximately 3 g/day until pot weight reached 110 g (age of the plants: 39 days). Pots were weighed daily and watered automatically to ensure consistent weight loss for each pot. Drought treatment was terminated when the Fv/Fm value for Col-0 plants were close to zero (44-day-old plants, when pot weight was approximately 110 g). The pots were then gradually re-watered to 130 g over a week for recovery, then survival rates were calculated for each genotype. Throughout the growth period in the PSI system, all parameters were automatically recorded. Surviving plants were monitored by determination of the Fv/Fm value.

2.2 Nucleic acid extraction

Leaf tissue (100 mg) was homogenized in extraction buffer containing 200 mM Tris/HCl (pH 7.5), 25 mM NaCl, 25 mM EDTA and 0.5% (w/v) SDS. After centrifugation, DNA was precipitated from the supernatant by adding isopropyl alcohol. After washing with 70% (v/v) ethanol, the DNA was dissolved in distilled water. For RNA isolation, plant material was harvested, frozen in liquid nitrogen and crushed in a TissueLyser (Retsch, model: MM400). Total RNA was extracted with the Direct-zol RNA Kit (Zymo Research, Irvine, USA) according to the manufacturer's protocol. RNA samples were quantified with a Nanodrop spectrophotometer (ThermoFisher Scientific, Langenselbold, Germany) and RNA integrity and quality were assessed with an Agilent 2100 Bioanalyzer (Agilent, Santa Clara, USA). Isolated RNA was stored at −80°C until further use.

2.3 cDNA synthesis and quantitative reverse transcriptase-polymerase chain reaction analysis

One microgram of RNA was employed to synthesize cDNA using the iScript cDNA Synthesis Kit (Bio-Rad, Munich, Germany). Quantitative real-time PCR analysis was performed on a CFX Connect™ Real-Time PCR Detection System (Bio-Rad) with the SsoAdvanced™ Universal SYBR® Green Supermix (Bio-Rad). The gene-specific primers used for this assay are listed in Supplementary Table 1 in the Supplementary Material file. Each sample was quantified in triplicate and normalized using *AT3G58500* (which codes for protein phosphatase 2A-4 and showed minimal expression changes during drought treatment) as an internal control.

2.4 RNA-sequencing

Total RNA from plants was isolated using TRIzol Reagent™ (Thermo Fisher Scientific, Waltham, MA, USA) and purified using an RNA Clean & Concentrator (Zymo Research, Irvine, USA) according to the manufacturer's instructions. RNA integrity and quality were assessed with an Agilent 2100 Bioanalyzer (Santa Clara, USA). RNA was depleted of ribosomal RNA with the RiboMinus Plant Kit for RNA-seq (Thermo Fisher Scientific), and rRNA-free RNA was cleaned by ethanol precipitation. The directional library was prepared at Novogene Biotech (Beijing, China) with the help of the NGS Stranded RNA Library Prep Set (Novogene Biotech, PT044): The purified RNAs were first fragmented randomly to short fragments of 150-200 bp by addition of fragmentation buffer, followed by cDNA synthesis using random hexamers. After the first strand was synthesized, second-strand synthesis buffer (Illumina), dNTPs (dUTP, dATP, dGTP and dCTP) and DNA polymerase I were added to synthesize the second-strand. This was followed by purification by AMPure XP beads, terminal repair, polyadenylation, sequencing adapter ligation, size selection and degradation of second-strand U-contained cDNA by the USER enzyme. The libraries were checked with Qubit and real-time PCR for quantification and an Agilent 2100 Bioanalyzer (Santa Clara, USA) for size distribution detection. 150-bp paired-end sequencing was conducted on an Illumina HiSeq 2500 system (Illumina, San Diego, USA) at Novogene Biotech with standard Illumina protocols. Three independent biological replicates were used per time point (0, 6, 9, 12 and 15 days). However, sequencing data from one sample (Col-0 subjected to 6 days of drought treatment) were not satisfactory. In this case, two replicates were used. Sequencing data have been deposited to Gene Expression Omnibus (Edgar et al., 2002) under the accession number GSE202931.

2.5 Chloro-Seq analysis

To detect instances of editing and splicing of organellar transcripts in our RNA-Seq data, a modified Chloro-Seq pipeline (Malbert et al., 2018) was used. The RNA-Seq reads were processed on the Galaxy platform (https://usegalaxy.org/) to remove the adaptors by Trimmomatic (Bolger et al., 2014), then sequencing quality was assessed with FastQC (http://www.bioinformatics.babraham.ac.uk/projects/fastqc/). The trimmed reads were mapped using RNA STAR (Dobin et al., 2013) with TAIR10_Chr.all.fasta (https://www.arabidopsis.org/download_files/Genes/TAIR10_genome_release/TAIR10_chromosome_files/TAIR10_chr_all.fas) as referencegenome file, and Araport11_GFF3_genes_transposons.201606.gff (https://www.arabidopsis.org/download_files/Genes/Araport11_genome_release/archived/Araport11_GFF3_genes_transposons.201606.gff.gz) as gene model file for splice junctions. The mapped bam file was later used as the input for Chloro-Seq analysis (https://github.com/BenoitCastandet/chloroseq) to determine editing and splicing efficiency.

2.63D RNA-Seq analysis

To quantify overall transcript accumulation and detect alternative splicing (AS) of nuclear transcripts, the 3D RNA-Seq pipeline (Guo et al., 2021) was used. To this end, RNA-Seq reads were prepared on the Galaxy platform (https://usegalaxy.org/). Adaptors were removed with Trimmomatic (Bolger et al., 2014), and sequencing quality was accessed with FastQC (http://www.bioinformatics.babraham.ac.uk/projects/fastqc/). Transcript abundances were calculated using Salmon (Patro et al., 2017) and AtRTD2-QUASI as reference transcriptome (Zhang et al., 2017). The generated files were uploaded into the 3D RNA-Seq app (https://3drnaseq.hutton.ac.uk/app_direct/3DRNAseq; Calixto et al., 2018; Guo et al., 2021) and transcript per million reads (TPMs) were calculated using the implemented lengthScaledTPM method. Weakly expressed transcripts and genes were filtered out based on the mean-variance trend of the data. The expected decreasing trend between data mean and variance was observed when expressed transcripts were determined as ≥ 1 of the 14 samples with count per million reads (CPM) ≥ 4, which provided an optimal filter of low expression. A gene was declared to be expressed if any of its transcripts met the above criteria. The TMM method was used to normalize the gene and transcript read counts to $\log_2$-CPM, and a principal component analysis (PCA) plot showed that the RNA-seq data did not have distinct batch effects. The $\log_2$ fold change (FC) of gene/transcript abundances was calculated based on contrast groups and the significance of expression changes was determined using t-test. A gene/transcript was significantly differentially expressed (DE) in a contrast group if it had an absolute $\log_2$ FC ≥ 1 and an adjusted *P*-value < 0.01 after applying multiple testing (Benjamini et al., 2001). For comparison with Kim et al. (2017) data an adjusted *P*-value of < 0.05 was used. At the alternative splicing level, DTU (differential transcript usage) transcripts were identified by comparing the $\log_2$ FC of a transcript to the weighted average of $\log_2$ FCs (weights were based on their standard deviation) of all remaining transcripts of the same gene. A transcript was declared to exhibit significant DTU if it had an adjusted *P*-value < 0.01 and a *D* Percent Spliced (*D*PS) ratio ≥ 0.1. For DAS genes, each individual transcript $\log_2$ FC was compared to the gene-level $\log_2$ FC, which was calculated as the weighted average of $\log_2$ FCs of all transcripts of the gene. Then *P*-values of individual transcript comparison were summarized to a single gene-level *P*-value with an F-test. A gene was significantly DAS in a contrast group if it had an adjusted *P*-value < 0.01 and any of its transcripts had a *D*PS ratio ≥ 0.1.

Transcript isoform switches (ISs) were recognized as such if the order of relative expression levels of a pair of alternatively spliced isoforms underwent a reversal. The Pair-Wise Isoform Switch (isokTSP) method was used to detect the isoform switch points between conditions of contrast groups (except for the 6-days samples). The method defined the ISs between any pair of transcripts within genes using mean values of conditions. It described the significant ISs using five different features of metrics: 1) the probability of switching (i.e. the frequency of samples reversing their relative abundances at the switches) was set to > 0.5; (2) the sum of the average differences of the two isoforms in both intervals before and after the switch point was set to *D*TPM > 1; (3) the significance of the differences between the switched isoform abundances before and after the switch was set to a BH-adjusted *P*-value < 0.01; (4) both of the interval lengths before and after switch were set to 1; and (5) the Pearson correlation of two isoforms was set to >0 (see Guo et al. (2021) for more details).

2.7 Visualization of gene expression data

Normalized read depths of transcripts were visualized with the Integrative Genomics Viewer (IGV; Robinson et al., 2011). The heatmaps were generated with the help of ClustVis, a web tool for visualizing clustering of multivariate data (Metsalu and Vilo, 2015).

2.8 Determination of gene ontology enrichments

GO enrichments were obtained from the Database for Annotation, Visualization and Integrated Discovery (DAVID; Huang da et al., 2009), applying a cut-off of 2-fold enrichment compared to the expected frequency in the Arabidopsis genome and an FDR (Benjamini-Hochberg) ≤ 0.05. Non-redundant GO terms were selected in the interface REVIGO using the medium similarity (0.7) parameter (Supek et al., 2011).

3 Results

3.1 Drought-related changes in gene expression are robust across different laboratories

Our goal was to investigate in addition to differential gene expression, the behavior of post-transcriptional processing of

nuclear or organellar transcripts under drought. To this end, RNA sequencing was performed with ribosomal RNA-depleted RNA isolated from 3-week-old Col-0 plants grown under optimal conditions (time-point 0 days; 0d_DS), and after withholding of water for 6, 9, 12 and 15 days (6d_DS, 9d_DS, 12d_DS and 15d_DS, respectively) as described previously (Kim et al., 2017). At 15d_DS, Col-0 accumulated anthocyanins, wilted and displayed lower maximum quantum yield of photosystem (PS) II (Fv/Fm; Figure 1A). Here it is of note, that Kim et al. (2017) used microarrays, which are not suitable for our purpose – monitoring of organellar transcript accumulation and editing events, and the investigation of splicing of transcripts produced in organelles as well as the nucleus. We repeated our experiment separately with different batches of plants, yielding three biological repeats per time point. Principal-component analysis showed that drought was an important driver of gene expression and replicates clustered together (Figure 1B). One replicate of 6d_DS was an outlier and the sequencing quality did not meet our criteria and only two replicates were used for further analysis. The sequencing depth was approximately 25 million 150-bp paired-end reads for each of the samples (Supplementary Table 2).

Investigation of whole-genome wide gene expression changes showed that 16,850 genes were considered as expressed after removal of weakly expressed ones, and most of them (12,523) were differentially expressed in response to drought when compared with the starting condition (Figure 1C; Supplementary Table 3). These findings again show that drought has a substantial impact on the transcriptome. Here, a gene was considered to be differentially expressed (DEG) if it showed an absolute $\log_2$ fold change ≥1 (≥ 2-fold linear change) in expression in at least one contrast group (adjusted $P < 0.05$). 49.2% of these were down- and 50.8% upregulated, respectively (Figure 1C). Our re-analysis of data published by Kim et al. (2017), and comparison with the transcriptome data generated in the present study, showed that drought-related changes in gene expression are robust across different laboratories and transcriptome platforms after prolonged exposure to drought stress (Figure 1D). Accordingly, we provide lists of robust drought-responsive DEGs in Supplementary Table 4. Some of these were exceedingly differentially expressed. For example, levels of *AT1G66100* mRNA were reduced to 0.005% of control levels after 15 days (Supplementary Table 3).

3.2 Gene ontology analysis

The kinetic data were further explored by sorting the DEGs into nine different clusters. Cluster 1 contained the genes that were strongly downregulated at 12d_DS and 15d_DS. Gene Ontology (GO) analysis of this cluster showed enrichments of genes encoding proteins related to the response to low light, protein folding, chlorophyll biosynthesis, cp translation and photosynthesis-related processes in the biological process (BP) category (Figure 1E; Supplementary Table 5). This is in line with the phenotype and Fv/Fm value of Col-0 under drought. Moreover, the GO analysis revealed that, in addition to chloroplast (cp)-encoded genes (see Figure 2), nucleus-encoded chloroplast proteins are also regulated at the transcript level. In the cellular component (CC) category, transcripts coding for components of the PSI, PSII and the cp Ndh complexes, as well as cp and cytosolic ribosomal subunits, were enriched (Figure 1E). The similarities in the behavior of transcripts for both cp and cytosolic ribosomal subunits reflect the importance of coordination between protein synthesis in chloroplasts and the cytosol (Wang R. et al., 2018) during drought stress. The majority of mt transcripts in Col-0 increased or barely changed under drought (see Figure 3). Accordingly, genes encoding mt proteins were found in cluster 6, which encompasses genes whose transcript levels especially increased at 9d_DS and 12d_DS, in particular those encoding proteins of the substrate-carrier family, succinate-dehydrogenase complex II and enzymes of the tricarboxylic acid cycle (TCA). Indeed, TCA cycle metabolites are known to increase after water shortage (Pires et al., 2016). Cluster 6 also includes the categories “peroxisome”, “response to water” and “response to osmotic stress”. The latter two categories both point to a disturbance in water balance, and genes encoding proteins involved in responses to hypoxia, abscisic acid and salt stress are found in cluster 5, which encompasses genes that behave like those of cluster 6. Moreover, genes assigned to the GO categories “cellular water homeostasis”, together with “cell wall thickening” and “fatty acid biosynthesis” in cluster 2 are specifically induced after 6 or 9 days of drought treatment.

In summary, drought treatment induces massive transcriptional reprogramming, and the polarities of changes in gene expression (up or down) are compatible with responses to drought at the phenotypical and metabolic levels. In addition, mRNA expression of the organellar and nuclear genomes are coordinated.

3.3 Drought stress has a negative impact on the chloroplast (post)transcriptome

Heat stress for periods of several hours induces a global reduction in splicing and editing efficiency in chloroplasts (cp), and an overall increase in the abundance of cp transcripts, while short-term drought stress for 3 and 12 hours results in only minor changes in cp transcripts (Castandet et al., 2016).

To investigate cp transcripts under drought stress, reads were mapped and processed with the help of ChloroSeq (Castandet et al., 2016). Overall levels of noncoding cp RNAs are higher after 12 h of heat treatment (Castandet et al., 2016), but inspection of our bamcoverage files, which include reads across all nucleotide (nt) positions of the cp genome, showed that this does not hold for exposure to drought (Supplementary Figure 1). In fact, cp coverage already indicated lower overall cp transcript accumulation in Col-0 after prolonged drought (Supplementary Figure 1). To investigate this for individual transcripts, heatmaps of z-means (Figure 2A) and fold changes of cp transcripts (Supplementary Table 6A) were generated, which revealed substantial reductions in levels of most transcripts under prolonged drought conditions in Col-0 (Figure 2A; Supplementary Table 6A). Here, it should be noted that analysis of tRNAs was excluded (also in the following editing and splice-site analyses) because their small size and many modifications make them difficult to amplify with either our

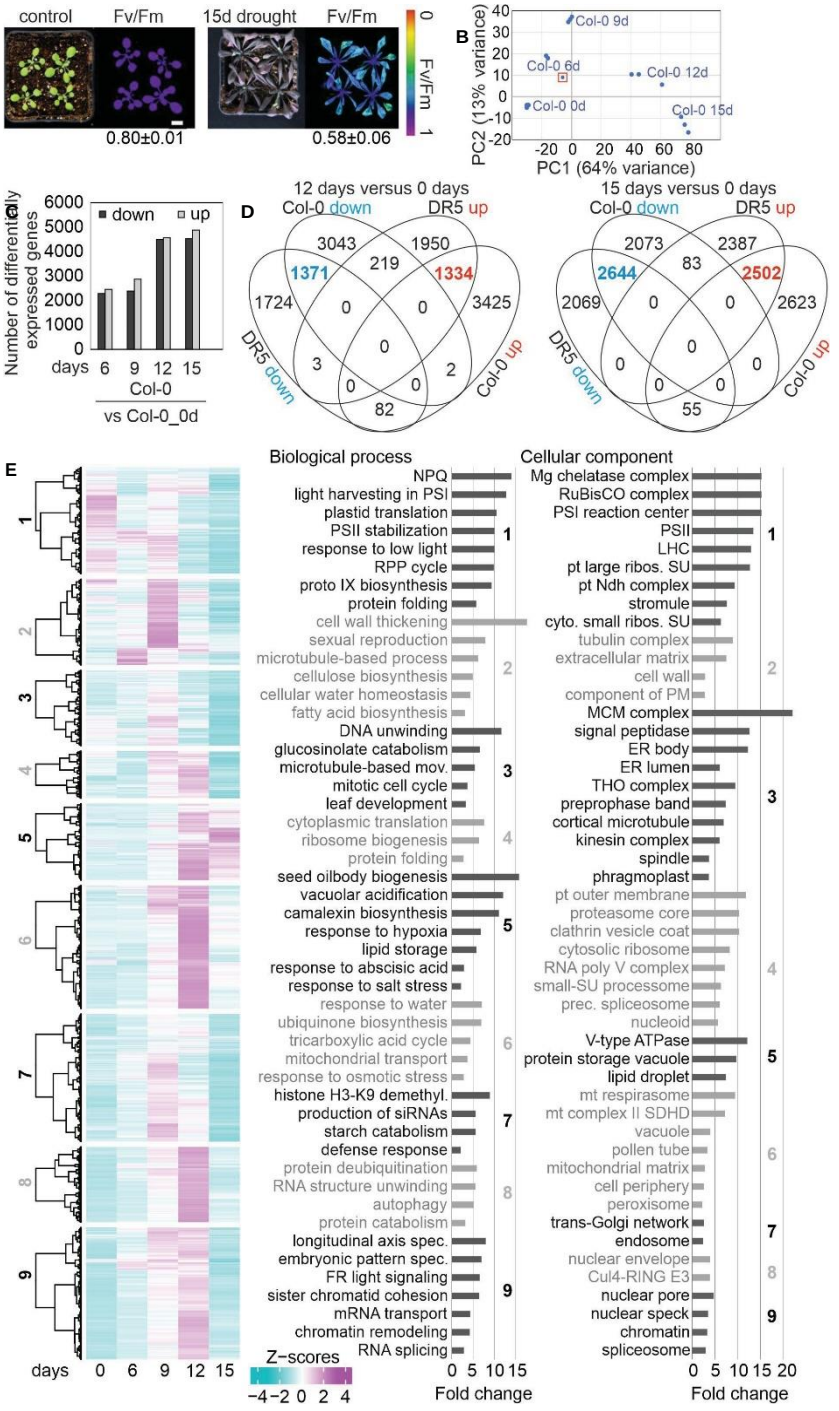

FIGURE 1

Drought-related changes in gene expression are robust across different laboratories. **(A)** Phenotypic characterization of Col-0 plants grown for 3 weeks under normal, well-watered, conditions (control), and then subjected to drought stress by withholding water for 15 days. The maximum quantum efficiency of photosystem II (Fv/Fm) was measured with an imaging Chl fluorometer (Imaging PAM). Bar = 1 cm. **(B)** Principal Component Analysis (PCA) plot visualizing variation between replicates and time-points based on RNA-seq data. The sample marked with a red rectangle was not used for further analysis. **(C)** Numbers of differentially expressed genes (absolute $\log_2$ fold change ≥1; in at least one contrast group with an adjusted $P < 0.01$) subjected to drought exposure compared to the control (0 days) at the indicated time points. **(D)** Comparison of transcript changes evoked by drought stress in Col-0 (this study) or in DR5 [re-analyzed data from Kim et al. (2017)]. Venn diagrams illustrate the total numbers of differentially expressed genes shared between or specific for the different treatments. **(E)** Overview and gene ontology analysis of gene expression changes under drought. Heatmap of differentially expressed (DE) genes under drought stress compared to the control time point (0 days). Hierarchical clustering was used to partition the DE genes into nine clusters with the Euclidean distance and ward. D clustering algorithm. Right side: Graphs illustrating non-redundant Gene Ontology (GO) term enrichment for the biological process and cellular component categories according to DAVID (Huang da et al., 2009) and REVIGO (Supek et al., 2011). GO terms with a >2-fold change and a Benjamini-corrected *P*-value of <0.05 are shown. Cul4-RING E3, Cul4-RING E3 ubiquitin ligase; LHC, light-harvesting complex; mov., movement; NPQ, nonphotochemical quenching; prec., precatalytic; protein catabolism, ubiquitin-dependent protein catabolism; RPP, reductive pentose-phosphate; spec., specification; PS, photosystem; pt, plastid; ribos., ribosomal; SU, subunit.

RNA-Seq method or conventional mRNA-Seq protocols. Of the 69 protein-coding cp genes that were above the detection threshold, 50, 63 and 64 were at least 2-fold reduced (compared to the 0d_DS sample) in Col-0 plants after 9, 12 and 15 days of drought, respectively. The genes most affected (those whose transcripts were reduced to 3% or less of their initial levels) code for the D3, F and K subunits of the NAD(P)H dehydrogenase complex and a protein of the large ribosomal subunit (rpl23, uL23c according to the Nomenclature of Ribosomal Proteins; https://bangroup.ethz.ch/research/nomenclature-of-ribosomal-proteins.html and Scarpin et al., 2023).

To examine post-transcriptional changes in cp transcripts, editing and splicing efficiencies were calculated. Interestingly, unlike transcript accumulation, editing was not generally reduced

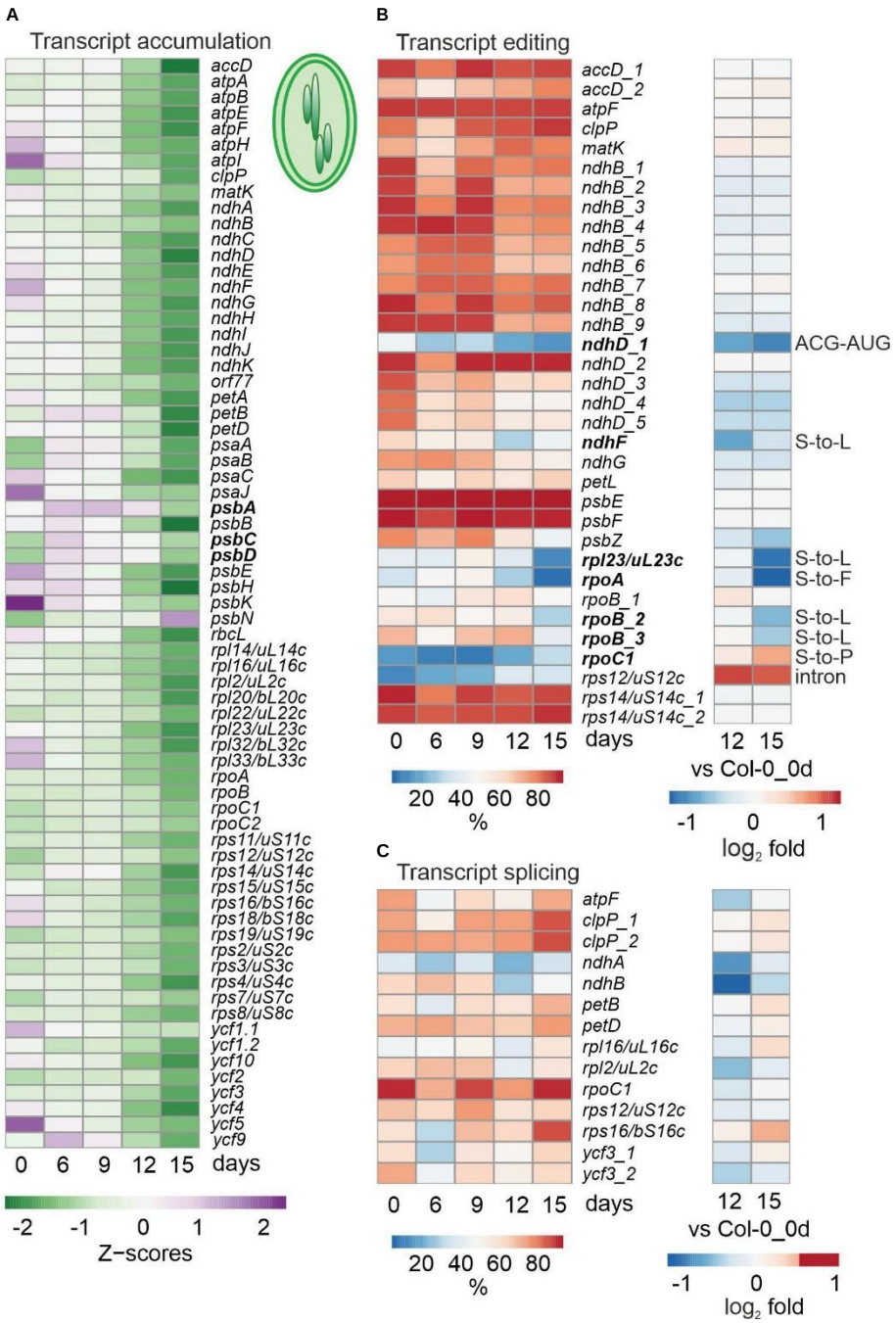

FIGURE 2
Impact of drought treatment on accumulation, editing and splicing of chloroplast transcripts. Water was withheld for 15 days from 3-week-old Col-0 plants grown under standard conditions (0 days), and RNA-Seq was performed as described in Materials and Methods on RNA extracted from plants harvested at the indicated time-points. **(A)** Heatmap illustrating chloroplast transcript accumulation (Z-scores) during the drought time-course. Low to high expression is represented by the green to purple transition. Note that Z-scores are calculated for each individual transcript over the time course. **(B, C)** Percentages of editing **(B)** and splicing **(C)** events during the time-course (left) and log_2 fold changes after 12 and 15 days of drought stress compared to the control time point (right). The effect of editing changes is shown in panel **(B)** on the right.

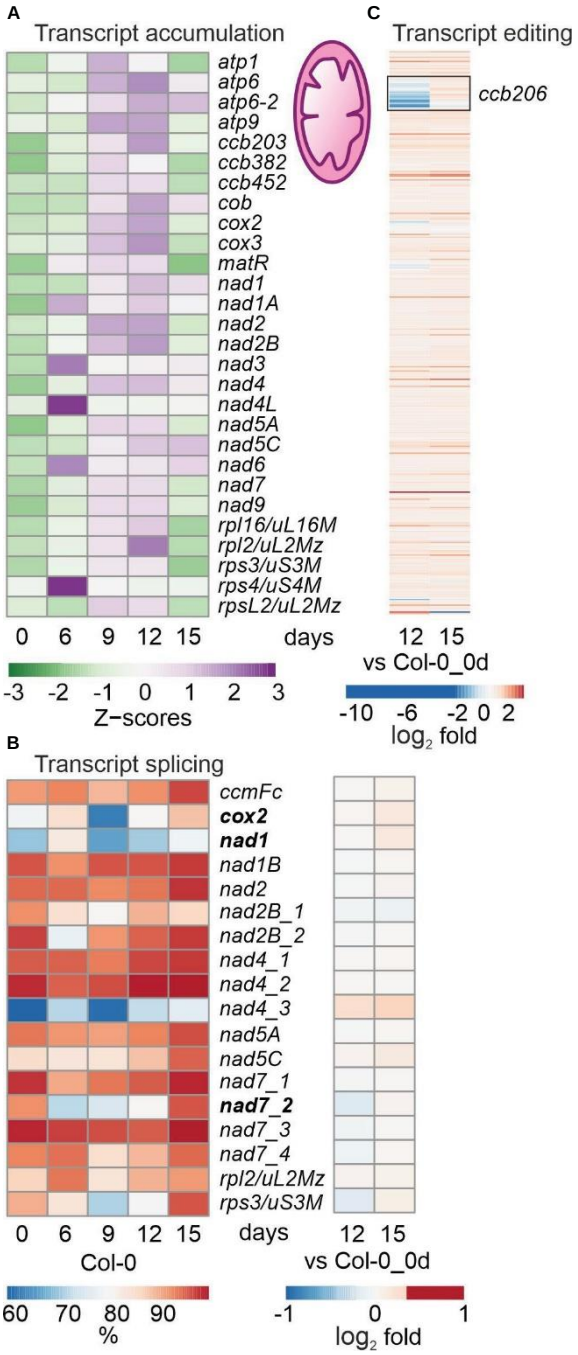

FIGURE 3
Impact of drought treatment on the accumulation, editing and splicing of mitochondrial transcripts. Plants and RNA were treated and analyzed, and data are depicted as described in the legend to Figure 2. **(A)** Heatmap illustrating chloroplast transcript accumulation (Z-scores) during the drought time-course. **(B)** Percentages of transcript splicing during the time course (left) and log_2 fold changes after 12 and 15 days of drought stress compared to the control time point (right side). **(C)** Log_2 fold changes of transcript editing during the time course.

in Col-0 under drought conditions, but was observed especially for *ndhD*, *ndhF*, *rpl23*/*uL23c* and the *rpoA* and *rpoB* genes encoding *a* and *b* subunits of plastid-encoded RNA polymerase (Figure 2B). Although these editing changes do not result in premature stop codons, but rather amino acid changes or an alternative start codon, they may alter the structure of RNA or proteins, or affect the ability of altered proteins to form complexes with other proteins. Moreover, editing of *rps12* and *rpoC1* were enhanced and slightly enhanced, respectively. After 15 days of drought treatment, splicing efficiency was not notably diminished, and in some cases (five out of 14 events) was slightly enhanced (Figure 2C).

To summarize, while overall cp mRNA levels were broadly reduced, impairment of editing events was more marked, and splicing was not compromised at all.

3.4 Mitochondrial transcript accumulation, editing and splicing under drought

Mitochondrial (mt) transcripts were also investigated, and inspection of bamcoverage files of the mt genome suggested even higher mt transcript accumulation under drought (Supplementary Figure 2), in contrast to the fall in levels of cp transcripts (see Supplementary Figure 1). This was confirmed by producing heatmaps of z-means of mt transcripts and their fold changes (Figure 3A; Supplementary Table 6B). Thus, levels of the majority of mt mRNAs increased or were only slightly changed during drought treatment (Figure 3A; Supplementary Table 6B). Of the 49 protein-coding mt genes that were above the detection threshold, 11, 11 and 26 transcripts were at least 2-fold elevated after 9, 12 and 15 days of drought, respectively, compared to 0d_DS. Only a few mRNAs were down-regulated during drought stress, of which the two most strongly reduced transcripts *ATP synthase subunit 1* (*atp1*; 0.3%) and *rpsL2* (*ATMG00980*; 17.8%) were detected at 15d_DS. Interestingly, transcripts coding for mt NADH dehydrogenase subunits increased during prolonged drought treatment – in stark contrast to their counterparts in the cp sister complex.

With regard to post-transcriptional changes of mt transcripts, transient down-regulation of splicing efficiency was observed for *cytochrome oxidase 2* (*cox2*), *nad1* and *nad7-2*, and splicing capacity was slightly enhanced after 15 days (Figure 3B). Editing capacity under drought was not changed relative to 0d_DS, except in the case of *ccb206* (encoding the cytochrome *c* biogenesis protein 206), which was reduced in Col-0 at 12d_DS (Figure 3C).

Overall, mt (post)transcription was not markedly impaired and drought-induced changes tended to show the opposite trend to that seen in the cp transcripts. However, it should be noted that the level of *atp1* transcripts was reduced to 0.3% after 15 days of drought stress.

3.5 Splicing of nuclear transcripts under drought stress

To systematically investigate splicing behavior under drought stress, genome-wide differential alternative splicing (DAS) and differential transcript usage (DTU) during drought stress was examined with the help of the high-quality AtRTD2_QUALI transcriptome and 3D RNA-Seq (Zhang et al., 2017; Guo et al., 2021). By this means, in addition to the expression at the gene level (i.e., the sum of all transcript abundances of a given gene), the individual transcript isoform levels could be determined (Supplementary Table 7). In all, 1,462 DAS genes were identified, of which 847 were also DE genes (regulated by both transcription and AS), while 615 genes were regulated by only AS in at least one contrast group (Figure 4A; Supplementary Table 8). Among the latter are LESION SIMULATING DISEASE 1 (LSD1), which monitors a superoxide-dependent signal and negatively regulates plant cell death (Bernacki et al., 2021), as well as playing an important role in survival of drought stress (Szechynska-Hebda et al., 2016), plastidic acetyl-CoA synthetase (ACS), REGULATORY PARTICLE TRIPLE-A ATPASE 6A (RPT6A) which is a component of the 26S proteasome AAA-ATPase subunit, PROTEASOME REGULATOR1 (PTRE1), and protein synthesis initiation factor eIF2 beta (Supplementary Table 8). Notably, DAS increased after prolonged drought stress (Figure 4B), and was especially pronounced for *GLYCINE RICH PROTEIN 7* (*ATGRP7*). Differential splicing of transcripts of the three phytochrome genes *PHYB*, *PHYC* and *PHYE*, together with *PHYTOCHROME INTERACTING FACTOR 3* (*PIF3*), *PIF3-LIKE 5* and *6*, and *FYPP3* (coding for phy-associated protein phosphatase 3) is particularly striking. PhyB acts in multiple environmental stress pathways (Kim et al., 2021), and PhyB positively mediates drought tolerance (Gonzalez et al., 2012). In summary, 9% of the 16,850 expressed genes were differentially alternatively spliced and 3,283 transcript isoforms were detected whose splicing patterns were altered in at least one contrast group. GO analysis of the corresponding loci revealed enrichments of transcripts for proteins that were localized to the nuclear speck, cytoplasmic vesicle (for example, the AUTOPHAGY group of ubiquitin-like superfamily proteins – ATG8B, E and F, and ATG13) and the spliceosomal complexitself (Figure 4C). Indeed, this is supported by a reduction in the percentage of reads covering the canonical GT-AG splice junction (Figure 4D).

These results suggest the importance of alternative splicing of nuclear genes in the modulation of responses to drought stress.

3.6 Isoform switch analysis – usage of different isoforms during the course of drought stress

We then sought to identify DAS genes that showed isoform switches (ISs), i.e. in which the relative abundance of different isoforms was altered over the course of drought exposure. In total, 927 (covering 404 gene loci; $P < 0.01$) ISs that involved abundant transcript isoforms were detected (Figure 5A; Supplementary Table 9). The majority of ISs (more than 450) were identified after 15 days of drought stress. Among the transcripts undergoing ISs were the above-mentioned *LSD1* and *PHYB*. Other examples include *CARBAMOYL PHOSPHATE SYNTHETASE B* (*CARB*, also named *VENOSA 3*), *ZINC-INDUCED FACILITATOR 2* (*ZIF2*), pre-mRNA processing *PRP39A*, and *FLOWERING LOCUS M* (*FLM*) (Figure 5B; Supplementary Figure 3). The ISs involved different types of AS events, which either generated isoforms that encoded different protein variants, or occurred in the 5′ or 3′UTR, without changing the sequence of the protein (Supplementary Table 9). IS events were also detected in transcripts that did not encode a functional protein, e.g., they contained a premature stop codon or did not contain the start codon (Supplementary Table 9). For example, the s3 isoform of the *CARB* transcript that accumulated under prolonged drought stress is predicted not to be translated, as is the P5 isoform of *PRP39A*, and the predicteds3 isoform is very short (Supplementary Figure 3).

In conclusion, RNA-Seq analysis uncovered numerous DAS and IS events, including the accumulation of putative non-functional transcript isoforms.

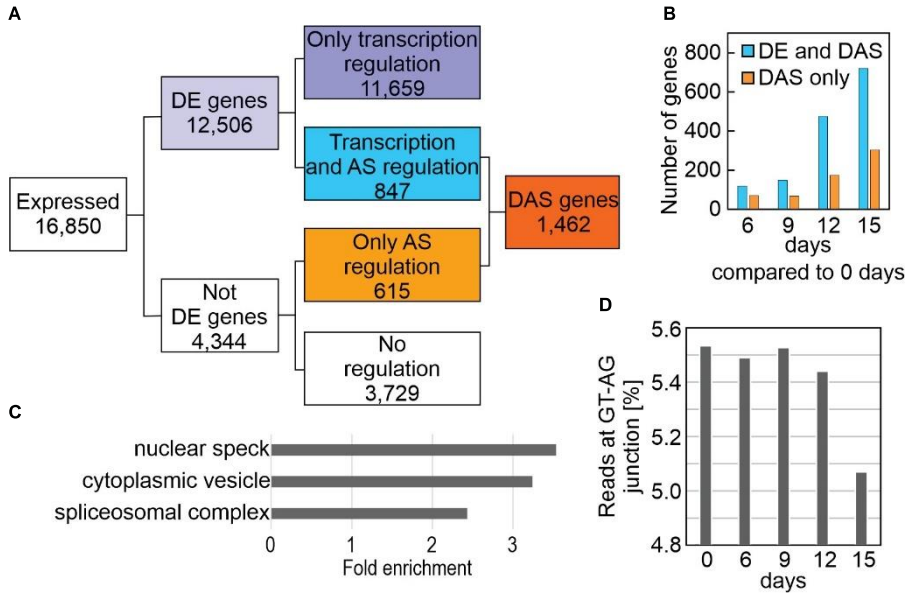

FIGURE 4
Impact of drought treatment on differential alternative splicing (DAS). DAS was calculated as described in Materials and Methods. **(A)** Flow chart showing the distribution of differentially expressed (DE) and DAS genes. **(B)** Number of DE and DAS genes in Col-0 plants exposed to drought stress compared to the control condition (0 days). **(C)** GO enrichment analysis of the cellular component category according to DAVID (Huang da et al., 2009). GO terms with a >2-fold change and a Benjamini corrected value of <0.05 are shown. **(D)** Percentage of reads spanning the canonical GT-AG splice junction in Col-0 under control (0 days) and drought conditions.

3.7 Suggested candidates for further investigation and proof of concepts

We propose in Table 1 several potential candidates from different categories (DE genes, DE transcripts, DAS, IS events, chloroplast and mitochondrial transcripts) for further investigation of responses to drought stress. For example, we include specific genes encoding proteins involved in defense responses; pathogenesis-associated proteins and peptides have already been proposed as promising tools for developing plants with multiple stress tolerance (Ali et al., 2018).

Two of the candidates listed in Table 1 were selected for proof-of-concept studies. First, the expression behavior of the *FLM* transcript isoforms is particularly noteworthy. As shown by analysis of RNA-Seq data (Figures 5B, C) and confirmatory qRT-PCR (Figure 5D), the P10 isoform accumulated to a very high level (15-fold and 60-fold after 12 and 15d_DS, respectively, compared with 0d_DS) during the drought treatment in Col-0 at the expense of *FLM*-β and *FLM*-δ isoforms (Figure 5E), which was confirmed by qRT-PCR (Figure 5E). The P10 form covers the first exon and part of the first intron (Figure 5C), resulting in a premature stop codon (Supplementary Table 9). It has been suggested that *FLM-β* is the functional protein that can prevent early flowering by repressing the expression of the key flowering time regulator FLOWERING LOCUS T (FT, florigen) (summarized in: Zarnack et al. (2020) and Quiroz et al. (2021)). We observed a 40-fold induction of *FT* transcript levels after 12 and 15 days of drought stress compared with 0d_DS (Figure 5F), but after 15 days of drought treatment, *FLM-β* and -δ expression levels were almost undetectable, suggesting that the absence of FLM protein is sufficient to mediate the early flowering phenotype under drought conditions (see Figure 6, Discussion section).

Second, mRNA levels of *CA1* were markedly decreased at both the transcript isoform and gene levels (Figure 7A, Table 1). The expression of *CA1_ID12* and *CA1_P4* was found to be very low under all conditions. Among the isoforms, *CA1_ID11* was the most highly expressed under control conditions, but it was rapidly down-regulated under drought stress (Figure 7A). The *CA1_ID11* isoform encodes a slightly shorter protein than the *CA1.2* isoform (Figures 7B, C). A previous study on the characterization of *CA1* variants identified three of the transcript variants identified in this experiment. The study found that the CA1_ID11 protein was mainly localized in the envelope, while the *CA1.2*-derived protein seemed to be evenly distributed in the chloroplast stroma (Shen et al., 2021), suggesting that particularly the envelope-localized CA1 is of importance for the drought response.

Phosphorylation of CA1 may be important for drought stress adaptation in *Brassica napus* (Wang et al., 2016), and drought experiments with maize *ca1 ca2* plants suggest a role for CAs in water use efficiency (Kolbe et al., 2018). Also, CO_2-induced stomatal closure is altered in an Arabidopsis *ca1 ca4* double mutant. However, single T-DNA mutants in *CA1*, *CA4*, and *CA6* did not show strong phenotypes in CO_2 responses (Hu et al., 2010). Based on the strong reduction in *CA1* transcript isoforms that we observed, we wanted to test whether a single *ca1* mutant of Arabidopsis might also exhibit altered tolerance to drought. To this end, Col-0, *ca1*, and, because *CA2* transcript levels were also greatly reduced under drought (Figure 7A), *ca2* plants were grown for three weeks under normal growth conditions and then not irrigated for 20 days. Interestingly, all *ca1* and *ca2* plants survived,

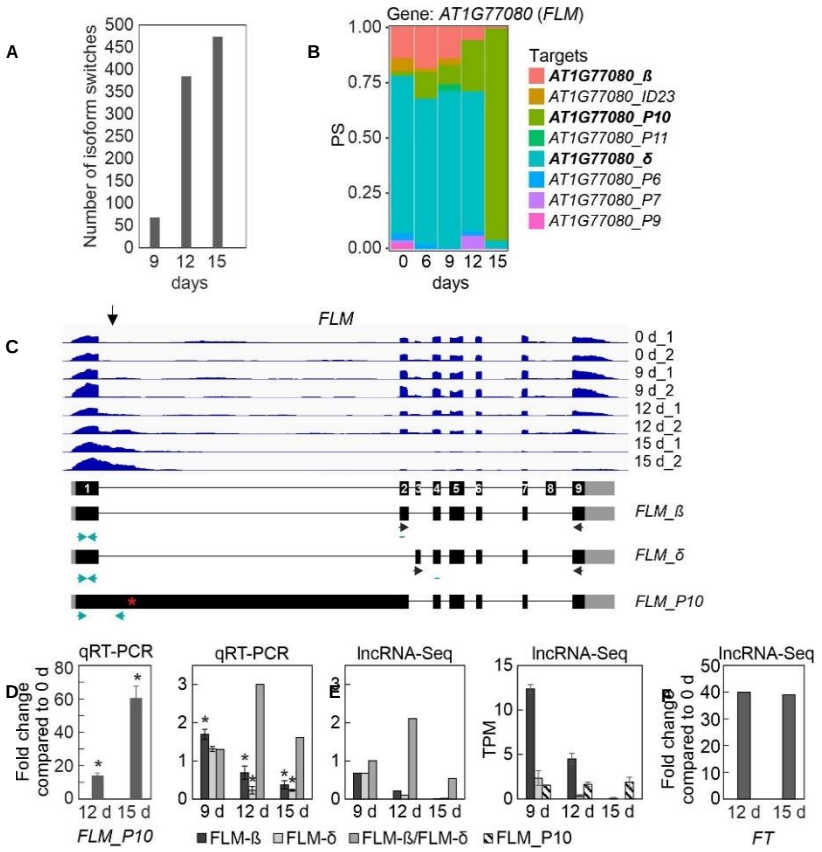

FIGURE 5
Transcript isoform switch (IS) analysis uncovers different *FLOWERING LOCUS M* (*FLM*) isoforms. IS were calculated as described in Materials and Methods. **(A)** Numbers of ISs detected in Col-0 after 9, 12 and 15 days of drought stress. **(B)** Expression profiles of *FLOWERING LOCUS M* (*FLM*) at the whole-gene level (*AT1G77080*) and at the level of detected transcript isoforms are shown. PS, percentage of expressed transcripts spliced. **(C)** Pattern of *FLM* transcript accumulation. The normalized read depths of transcripts detected in Col-0 plants under control and prolonged drought conditions were visualized with the Integrative Genomics Viewer (IGV). The vertical arrow indicates the most differentially spliced region. Exons (black boxes), introns (black lines) and the 5′- and 3′-UTRs (gray boxes) are shown. Black and turquoise horizontal arrows indicate the positions of primers used in RT-PCR reactions done in previous publications (e.g. Pose et al., 2013) and in this publication, respectively. Note that the primers used to amplify *FLM*-β and *FLM*-δ isoforms are exon-exon spanning. Red asterisk, premature stop codon. **(D)** Quantitative reverse transcriptase- polymerase chain reaction (qRT-PCR) analysis of Col-0 control plants (0 d) and plants subjected to drought stress for 12 and 15 days (12 d and 15 d). qRT-PCR was performed with primers specific for the FLM_P10, *FLM*-β and *FLM*-δ isoforms as indicated by the turquoise arrows in panel (C), and for *AT3G58500* [encoding PROTEIN PHOSPHATASE 2A-4 (PP2A-4)] , which served as a control because it did not significantly change its expression level under drought. Expression values are reported relative to the corresponding transcript levels in non-stressed Col-0. The results were normalized with respect to the expression level of *PP2A-4*. Bars indicate standard deviations. Statistically significant differences ($P < 0.05$) between stressed and non-stressed samples are indicated by an asterisk. Note that the *FLM*-β primers probably detect non-canonical splice forms, in addition to *FLM*-β (Sureshkumar et al., 2016). **(E)** Fold changes and TPM (Transcripts Per Million) values of FLM isoforms. **(F)** Fold changes of FT transcripts relative to Col-0 control plants (0 d). Data were extracted from RNA-Seq (lncRNA-Seq) results.

while all Col-0 plants died (Figure 7D). To investigate this further, we conducted a second drought experiment in which we exposed Col-0 and the mutants to the same drought conditions by controlling irrigation through adjustment of pot weights (PSI system described in Materials and Methods; Figure 7E). Remarkably, the Col-0 plants died after drought treatment and re-watering, whereas the *ca1* and *ca2* mutants still exhibited high photosynthetic activity, as shown by measuring the maximum quantum yield of photosystem (PS) II (Fv/Fm; Figures 7E, F).

In summary, the candidates we identified may provide a solid basis for further exploration of responses to drought stress, and we present a summary of the candidates of interest in Table 1. In particular, *FLM* isoform switching offers a possible explanation for the phenotype of early flowering under drought stress. Overall, the results suggest that the identified transcript isoforms may play an important role in the plant response to drought stress, and further studies could provide valuable insights into the mechanisms underlying this response.

4 Discussion

As a drought set-up, we used soil-grown plants from which water was withheld for various periods. Many drought models are available, but there is no “ideal” model that can meet all the requirements for drought studies, and individual methods have their particular limitations (Lawlor, 2013). Aqueous or agar media are more stable and reproducible (Ito et al., 2006; Geissler and

TABLE 1 List of suggested candidates for further investigation of their involvement in drought stress responses.

Differentially expressed genes (see Supplementary Table 3; regulated in both our dataset as well as in Kim et al., 2017)				
Gene ID	Protein Description	Gene Symbol	log2 12d	log2 15d
AT1G66100	Predicted to encode a PR protein. Belongs to the plant thionin (PR-13) family†		-12,5	-11,3
AT5G36910	Predicted to encode a PR protein. Belongs to the plant thionin (PR-13) family†	*THI2.2*	-9,2	-6,6
AT3G05730	Defensin-like (DEFL) family protein		-11,7	-10,4
AT5G65730	Hydrolase activity, acting on glycosyl bonds, involved in response to water deprivation	*XTH6*	-11,4	-9,2
AT4G04840	METHIONINE SULFOXIDE REDUCTASE B6, has peptide-methionine-(S)-S-oxide reductase activity	*MSRB6*	-11,1	-5,6
AT2G18300	HOMOLOG OF BEE2 INTERACTING WITH IBH 1; basic helix-loop-helix (bHLH) DNA-binding superfamily protein	*HBI1*	-10,5	-9,3
AT1G03870	FASCICLIN-LIKE ARABINOOGALACTAN 9	*FLA9*	-10,5	-9,3
AT5G44020	HAD superfamily, subfamily IIIB acid phosphatase		-10,2	-10,8
AT2G21650	MATERNAL EFFECT EMBRYO ARREST 3; member of a small sub-family of single MYB transcription factors	*MEE3; RSM1*	-9,8	-9,1
AT2G29290	NAD(P)-binding Rossmann-fold superfamily protein; functions in oxidoreductase activity		-9,6	-8,4
AT1G72610	GERMIN-LIKE PROTEIN 1	*GER1; GLP1*	-9,5	-8,2
AT5G48490	Protein with similarity to a lipid transfer protein that may contribute to systemic acquired resistance (SAR)	*DIR1-LIKE*	-9,5	-7,0
AT3G01500	CARBONIC ANHYDRASE 1, regulates together with betaCA4 (At1g70410) CO2-controlled stomatal movements in guard cells, see also main text and Figure 6	*CA1*	-8,4	-10,8
AT5G52300	RESPONSIVE TO DESICCATION 29B; induced in expression in response to water deprivation such as cold, high-salt, and desiccation	*RD29B; LTI65*	11,3	10,9
AT4G12960	Gamma interferon responsive lysosomal thiol (GILT) reductase family protein		11,2	9,8
AT1G61800	GLUCOSE-6-PHOSPHATE/PHOSPHATE TRANSLOCATOR 2	*GPT2*	9,7	10,1
AT2G29380	HIGHLY ABA-INDUCED PP2C GENE 3, protein serine/threonine phosphatase activity	*HAI3*	9,3	8,6
Differentially expressed transcript isoforms (see Supplementary Table 7)				
Transcript ID	**Protein Description**	**Gene Symbol**	**log2 12d**	**log2 15d**
AT3G14210_s1	EPITHIOSPECIFIER MODIFIER 1; represses nitrile formation and favors isothiocyanate production; functional allele deters the insect herbivory *T. ni*.	*ESM1*	-6,7	-12,6
AT3G01500_ID11	See above	*CA1*	-8,1	-11,6
AT3G01500.2	See above	*CA1*	-11,8	-11,1
AT4G26530.2	FRUCTOSE-BISPHOSPHATE ALDOLASE 5; involved in glycolysis	*FBA5*	-10,1	-11,2
AT4G26530_P3	FRUCTOSE-BISPHOSPHATE ALDOLASE 5	*FBA5*	-7,4	-9,5
AT5G44020.1	HAD superfamily, subfamily IIIB acid phosphatase		-10,2	-10,8
AT4G14400_P1	ACCELERATED CELL DEATH 6; member of the largest uncharacterized gene families in higher plants; involved in resistance to *Pseudomonas syringae*	*ACD6*	-9,7	-9,9
AT1G75600_P1	Histone superfamily protein; involved in nucleosome assembly	*HTR14*	7,4	11,0
AT3G01420_P1	PLANT ALPHA DIOXYGENASE 1; involved in protection against oxidative stress and cell death	*PADOX-1; DOX1*	9,1	10,0
AT1G32350_P1	ALTERNATIVE OXIDASE 1D; mitochondrion	*AOX1D*	8,0	9,9
AT5G52300_P1	See above	*RD29B*	11,4	10,8

(Continued)

TABLE 1 Continued

Differentially expressed genes (see Supplementary Table 3; regulated in both our dataset as well as in Kim et al., 2017)				
Gene ID	Protein Description	Gene Symbol	log2 12d	log2 15d
AT4G33150_P4	Encodes two proteins. One protein is the monofunctional saccharopine dehydrogenase involved in lysine degradation. The longer protein from the same LKR/SDH locus is bifunctional and also has saccharopine dehydrogenase activity. Gene expression is induced by ABA, jasmonate, and under sucrose starvation		8,3	10,1
AT2G27150.2	ABSCISIC ALDEHYDE OXIDASE 3; aldehyde oxidase delta isoform catalyzing the final step in ABA biosynthesis‡	*AAO3*	9,5	9,1
Differentially alternatively spliced, but not differentially expressed (see Supplementary Table 8)				
Gene ID	Protein description	Gene symbol		
AT4G20380	LESION SIMULATING DISEASE 1; monitors a superoxide-dependent signal and negatively regulates a plant cell death pathway	*LSD1*		
AT5G19990	REGULATORY PARTICLE TRIPLE-A ATPASE 6A; 26S proteasome AAA-ATPase subunit	*RPT6A*		
AT3G53970	PROTEASOME REGULATOR 1; was identified as homologous to human PI31	*PTRE1*		
AT2G18790	PHYTOCHROME B; red/far-red photoreceptor	*PHYB*		
AT1G09530	PHYTOCHROME INTERACTING FACTOR 3	*PIF3*		
AT2G20180	PIF3-LIKE 5; myc-related bHLH transcription factor	*PIL5*		
AT3G59060	PIF3-LIKE 6; myc-related bHLH transcription factor	*PIL6*		
AT3G19980	Phy-associated protein phosphatase 3	*FYPP3*		
AT4G04620, AT2G45170, AT4G16520, AT3G49590	AUTOPHAGY group of ubiquitin-like superfamily proteins	*ATG8B, ATG8E, ATG8 F, ATG13*		
AT1G21980	PHOSPHATIDYLINOSITOL-4-PHOSPHATE 5-KINASE 1; preferentially phosphorylates PtdIns4P. Induced by water stress and ABA	*PIP5K1*		
AT3G44850	Protein kinase superfamily protein			
AT4G15010	Mitochondrial substrate carrier family protein			
AT3G60910	S-adenosyl-L-methionine-dependent methyltransferases superfamily protein			
AT4G32140	EamA-like transporter family protein			
Isoform switch (see Supplementary Table 9)				
Gene ID	Protein description	Gene symbol		
AT4G20380	see above	*LSD1*		
AT2G18790	see above	*PHYB*		
AT1G29900	CARBAMOYL PHOSPHATE SYNTHETASE B	*CARB; VEN3*		
AT2G48020	ZINC-INDUCED FACILITATOR 2	*ZIF2*		
AT1G04080	Pre-mRNA processing protein	*PRP39A*		
AT1G77080	FLOWERING LOCUS M; MADS domain protein; flowering regulator that is closely related to FLC; see also main text	*FLM*		
AT1G09140	SERINE/ARGININE-RICH PROTEIN SPLICING FACTOR 30	*SR30; SRP30*		
Chloroplast-encoded transcripts (Supplementary Table 6A)				
Genes with most down-regulated transcripts encode D3, F and K subunits of the NAD(P)H dehydrogenase complex and a protein of the large ribosomal subunit (rpl23/ *uL23c*)				

(Continued)

TABLE 1 Continued

Differentially expressed genes (see Supplementary Table 3; regulated in both our dataset as well as in Kim et al., 2017)				
Gene ID	Protein Description	Gene Symbol	log2 12d	log2 15d
Edititing altered for *ndhD*, *ndhF*, *rpl23*/*uL23c* and the *rpoA* and *rpoB* genes encoding *α* and *b* subunits of plastid-encoded RNA polymerase				
Mitochondrial-encoded transcripts (Supplementary Table 6B)				
Reduced transcripts for ATP synthase subunit 1 (atp1; 0.3%) and rpsL2 (17.8%) at 15d_DS. Interestingly, transcripts coding for mt NADH dehydrogenase subunits increased during prolonged drought stress – in stark contrast to their counterparts in the cp sister complex				

†Pathogenesis-related proteins and peptides as promising tools for engineering plants with multiple stress tolerance (Ali et al., 2018), ‡involved in drought stress, investigated in rice (Shi et al., 2021).

Wessjohann, 2011; Park et al., 2013) than soil-based models. However, the latter more closely mimic actual drought conditions in the field, which makes it the preferred system in many studies. One typical soil-based model is the "water-withheld-setup", in which plants are deprived of water until symptoms of wilting are observed (Ali et al., 2020). We deliberately chose this system, because it is accessible to all laboratories. Moreover, field conditions do not allow for the strict control of water availability. To test the robustness of this system, we followed the method used by Kim et al. (2017). Despite the usage of different methodologies to analyze transcriptomes (RNA-Seq vs. microarrays), the transcriptome changes (at the gene level) induced by prolonged drought stress detected in the two studies were similar (see Figure 1).

4.1 Organellar (post)transcriptomes under stress

Mitochondria and plastids integrate signals to link metabolic processes with environmental sensing (Dopp et al., 2021). Despite the transfer of most of their genes to the nucleus during evolution, these organelles retain their own gene-expression machinery, thus necessitating tight coordination between organellar and nuclear gene expression (OGE and NGE), which is achieved by retrograde and anterograde signaling (Kleine and Leister, 2016; Dopp et al., 2021). Indeed, under drought, adjustment of organellar and nuclear genomes became apparent at the whole-gene expression level. Drought stress has an overall negative impact on chloroplast transcript accumulation (see Figure 2), which is in line with the down-regulation of nuclear transcripts coding for proteins involved in chloroplast translation and photosynthesis (see Supplementary Table 3). Interestingly, mitochondrial transcripts tended to be slightly upregulated (see Figure 3), e.g., those encoding components of succinate-dehydrogenase complex II and enzymes of the tricarboxylic acid cycle (TCA).

Apart from sensing environmental changes, chloroplasts are also targets of adverse conditions (Kleine et al., 2021), and it has been shown that the accumulation of specific plastid RNAs is regulated in mutants with photosynthetic defects and in plants exposed to stresses (see for instance (Cho et al., 2009). Much effort has been put into the investigation of changes in NGE in response to altered organellar states, at both the whole-gene and more recently post-transcriptome levels (Petrillo et al., 2014; Fang et al., 2019; Tiwari et al., 2020). However, only one study of Arabidopsis organellar post-transcriptomes in chloroplasts has been reported previously (Castandet et al., 2016) and there are none for mitochondria. In the context of the development of a chloroplast RNA-Seq bioinformatics pipeline, an analysis of suitable (i.e., RNA-Seq after ribosomal RNA depletion) published transcriptomes (Di et al., 2014) revealed a global reduction in chloroplast splicing and editing efficiency, and an increased abundance of transcripts in response to heat, while short-term "drought" treatment (3 and 12 h in 300 mM mannitol) had negligible effects on the chloroplast (post) transcriptome (Castandet et al., 2016). It should be noted that the sequencing data used by Castandet et al. (2016) were generated in only one copy, and these data may not be statistically sound. Defects in editing or splicing can have profound effects on plant development, and even result in lethality (Kleine and Leister, 2015), and altered adaptability to environmental stresses (Leister et al., 2017; Zhang et al., 2020). Therefore, we wanted to investigate the reverse case: What impact does drought have on the overall accumulation, splicing and editing of organellar transcripts?

Interestingly, levels of mitochondrial and chloroplast RNAs under drought were inversely regulated. While amounts of mitochondrial RNAs tended to rise (see Figure 3), drought had a profoundly negative impact on the accumulation of chloroplast transcripts (see Figure 2). The most severely affected transcripts – those encoding a component of the large ribosomal subunit (rpl23/uL23c) and the D3, F and K subunits of the NAD(P)H dehydrogenase (NDH) complex – were reduced to 3% of their starting amounts. In contrast, transcripts coding for mitochondrial NADH dehydrogenase subunits increased during prolonged drought stress, and the two most repressed mitochondrial transcripts after 15 days of drought stress were *ATP synthase subunit 1* (*atp1*; 0.3%) and *rpsL2* (17.8%). The function of the NDH complex has been extensively discussed and has yet to be resolved (Labs et al., 2016; Yamori and Shikanai, 2016). In particular, the role of the NDH complex under different stress conditions remains controversial (Yamori and Shikanai, 2016; Lenzen et al., 2020).

Editing capacity in Col-0 mitochondria under drought was not changed (see Figure 3), but a reduced editing capacity was observed especially for the chloroplast *ndhD*, *ndhF*, *rpl23*/*uL23c*transcripts, and *rpoA* and *rpoB* transcripts coding for the *α* and *β* subunits of the plastid-encoded RNA polymerase (PEP) (see Figure 2). Note

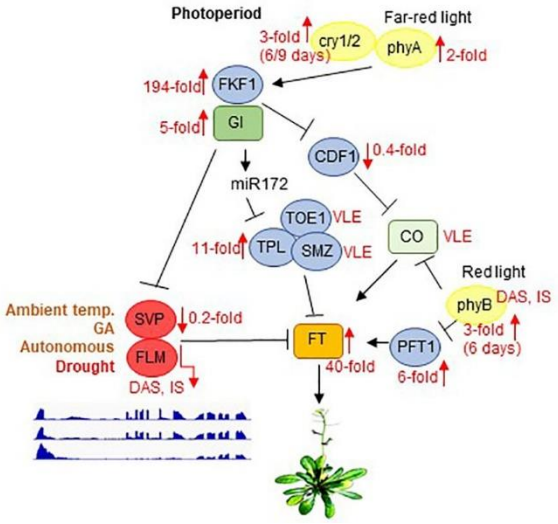

FIGURE 6
Scheme depicting the photoperiod-dependent flowering pathway, together with inputs from light receptors. Note that the components of the flowering pathway are mainly regulated through transcriptional activation or repression. SVP and FLM are components of the ambient-temperature, GA and autonomous pathways. GI acts in both CO-dependent (by suppressing CDF1) and CO-independent branches by either repressing SVP or by promoting *miR172* expression to control flowering. Flowering itself is ultimately mediated by FT, which is an inducer of flowering. phyB acts to suppress CO protein activity, whereas phyA, cry1, and cry2 function to enhance the activity of CO. In parallel, phyB affects *FT* transcription by suppressing *PFT1*, an upstream activator of *FT*. Black arrows and T-ends indicate positive or negative regulation, respectively. Red arrows together with numbers indicate fold changes after drought stress. *FLM* and *PHYB* transcripts are subject to DAS and IS. Only the main regulatory genes are shown here. The complete flowering time network involves several hundred genes, and is available on the WikiPathways website (https://www.wikipathways.org/index.php/Pathway: WP2312). Modified after Kim (2020) and Leijten et al. (2018). DAS, differential alternative splicing; IS, isoform switching; temp., temperature; VLE, very low expressed.

here that *ndhD*, *rpoA* and *rpoB* are not among the most reduced transcripts, implying that editing of these transcripts plays a more prominent role than their accumulation under drought conditions. Furthermore, editing capacity was maintained or even enhanced until the sudden drop occurred after 15 days of drought stress. This explains the maintenance of relatively high levels of *psbA*, *-C* and *-D* transcripts, because non-functional editing of *rpoB* transcripts leads to a significant decrease in PEP activity (Zhou et al., 2009).

In mitochondria, the only detected down-regulation of splicing efficiency was transiently observed for *cytochrome oxidase 2* (*cox2*), *nad1* and *nad7-2*, and this was slightly enhanced after 15 days (see Figure 3). In chloroplasts also, splicing efficiency was not generally reduced, but slightly enhanced after 15 days of drought (see Figure 2). Thus, organelle-specific splicing seems to be of marginal importance for the drought stress response.

4.2 Alternative splicing enhances proteome diversity to counteract stress responses

Differential alternative splicing (DAS), which enables multiple transcripts (and therefore proteins with different properties) to be produced from single genes, turns out to be an important aspect of responses to adverse conditions (Laloum et al., 2018) – and components of the spliceosome (which mediates DAS) are known to be altered during drought stress (Marondedze et al., 2019). Here, we identified nearly 1,500 DAS genes (see Figure 4 and Supplementary Table 8), of which 42% were regulated solely at the level of alternative splicing (AS) rather than by alteration of transcription rates, so that these transcripts would have gone unnoticed in a microarray-based approach. Some of the identified genes have already been shown to encode proteins involved in stress pathways. Thus, phyB, LESION SIMULATING DISEASE 1 (LSD1) and GLYCINE RICH PROTEIN 7 (GRP7) have previously been implicated in survival of Arabidopsis plants under drought stress (Gonzalez et al., 2012; Szechynska-Hebda et al., 2016) or higher grain yields of rice under drought conditions (Yang et al., 2014). However, it was not known until now that these effects are mediated by different transcript isoforms. Interestingly, GRP7 itself regulates AS (Streitner et al., 2012). Moreover, CONSTITUTIVELY STRESSED 1 (COST1) regulates autophagy to enhance plant drought tolerance (Bao et al., 2020). In this respect it is remarkable that *ATG8B*, *-E* and *-F*, and *ATG13* (all of which code for AUTOPHAGY ubiquitin-like superfamily proteins) are subject to DAS under drought.

One known example of DAS under drought is that of the ZINC-INDUCED FACILITATOR-LIKE 1 (ZIFL1) transporter. The full-length isoform is localized in the tonoplast of root cells and regulates transport of auxin, but a truncated variant is targeted to the plasma membrane of leaf stomatal guard cells and mediates drought tolerance (Remy et al., 2013). A homolog, *ZINC-INDUCED FACILITATOR 2* (*ZIF2*), is known to produce two splice variants, *ZIF2.1* and *ZIF2.2*, which encode the same proteins, but an intron retention event in the 5´UTR in *ZIF2.2* enhances translation in a zinc-responsive manner and promotes zinc tolerance (Remy et al., 2013). This makes *ZIF2* an attractive candidate – among the many

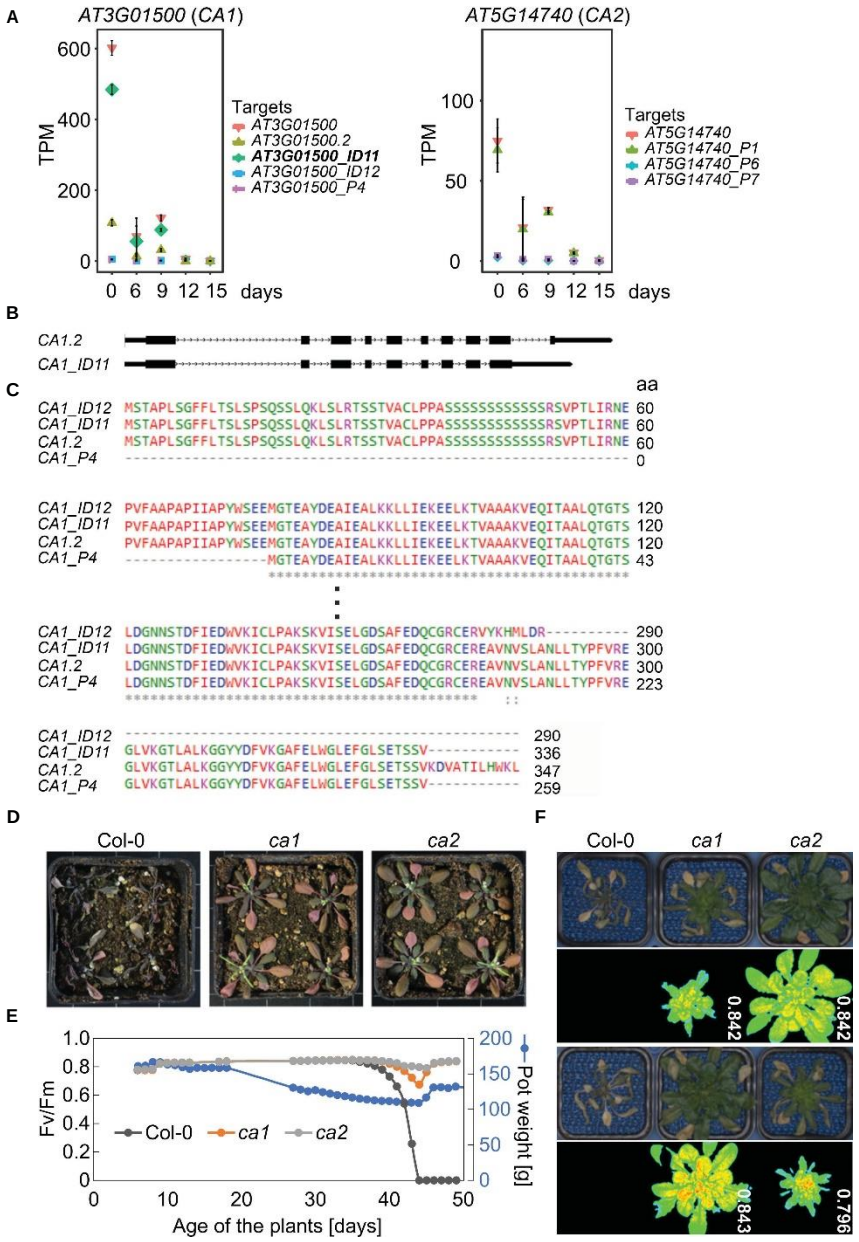

FIGURE 7
Carbonic anhydrases CA1 and CA2 are involved in drought tolerance. **(A)** Expression profiles of *CA1* and *CA2* at the whole-gene level and at the level of detected transcript isoforms. TPM, transcripts per million reads. **(B)** Scheme depicting the UTR-exon-intron structure of *CA1.2* and *CA1_ID11* transcript isoforms. UTRs and exons, lower and higher rectangles, respectively; introns, lines with arrowheads. **(C)** Alignment of the translated proteins encoded by the different isoforms. **(D)** Phenotypic characterization of Col-0 plants grown for 3 weeks under normal, well-watered, conditions, and then subjected to drought stress by withholding water for 20 days. Col-0 and mutant plants were grown in separate pots, but randomized in the same container. **(E)** Characterization of Col-0 and *ca* plants grown under short-day conditions. The water status was controlled by watering pots to the same pot weight (150 g) until the weight was gradually reduced to 110 g. After 44 days, pots were gradually re-watered. The re-watered Col-0 plants died while *ca* plants were still viable as indicated by detectable photosynthetic activity (maximum quantum yield of photosystem II, Fv/Fm). **(F)** Phenotypic characterization and Fv/Fm PAM images of 49-day-old Col-0 and *ca* plants treated as in **D**.

promising DAS genes expressed under drought conditions – for further investigation of the contribution of DAS forms to drought tolerance. Another interesting candidate is *ALDEHYDE DEHYDROGENASE 7B4* (*ALDH7B4*; 3000-fold induced after 12 and 15 days) which also undergoes DAS under drought. Indeed, *aldh7b4* knockout mutants exhibit higher sensitivity to dehydration and salt than do wild-type plants (Kotchoni et al., 2006).

Vascular land plants contain *a*-, *b*-, and *g*-CAs (carbonic anhydrases), and CAs catalyse the interconversion of carbon dioxide and bicarbonate (Hewett-Emmett and Tashian, 1996). *CARBONIC ANHYDRASE1* (*CA1*, *ßCA1*) mRNA levels were reduced to 0.005% of control levels after 15 days of drought stress (see Supplementary Table 3), and the *ca1* mutant is more drought tolerant (see Figure 7). In particular, one isoform, *CA1_ID11*, was

rapidly down-regulated under drought stress, suggesting that the CA1 protein produced by *CA1_ID11* may be important for drought response. The *CA1_ID11* isoform encodes a slightly shorter protein than the *CA1.2* isoform (Figure 7C), and the protein produced by *CA1_ID11* was mainly localized in the envelope, whereas the protein derived from *CA1.2* appeared to be evenly distributed in the chloroplast stroma (Shen et al., 2021). The importance of CA1 localization was demonstrated by Hines et al. (2021): Tobacco stromal CA1 (and CA5) isoforms play no role in photosynthesis but do play a role in plant development, whereas no such function could be ascribed to cytosolic CA1. Arabidopsis contains at least two stromal ßCAs, ßCA1 and ßCA5, while ßCA2 is one of the most abundant isoforms in the cytosol and, together with ßCA4, is required for optimal growth under low CO_2 (DiMario et al., 2016). Remarkably, CA1 has been found to translocate from tobacco chloroplasts to the cytosol under drought stress (Li et al., 2020), and we observed that plants lacking ßCA2 are as drought tolerant as the *ca1* mutant. By studying a *ca1 ca2* mutant of maize, it was suggested that CA1 and CA2 also play a role in water use efficiency in a C4 plant, which is likely mediated by an altered stomatal response (Kolbe et al., 2018). It will be interesting to investigate in the future which CA isoforms at which sites determine drought tolerance and whether this mechanism is conserved in C3 and C4 plants.

4.3 Early flowering under drought stress is most probably caused by a lack of functional *FLM* and/or reduced *SVP* transcripts

The drought escape (DE) strategy involves an earlier switch from vegetative to reproductive development, enabling reproduction before severe water deficit prohibits plant survival (Kenney et al., 2014). Early flowering as a DE mechanism is extremely important and research on the topic has a very long history (Shavrukov et al., 2017). Under a 12 h/12 h light/dark regime, ecotypes with low expression of *FRIGIDA* (*FRI*), or a null *FRI* allele as in Col-0, confer early flowering under drought (Lovell et al., 2013). Also, in our experimental setup in which we used long-day conditions, Col-0 plants began to flower earlier under drought. In Arabidopsis, flowering is ultimately achieved by activating expression of the gene *FLOWERING LOCUS T* (*FT*) (Searle and Coupland, 2004; Figure 6). Accordingly, in our experimental setup, *FT* mRNA levels are strongly elevated under drought treatment (40-fold induction after 12 and 15 days, see Figure 5, Supplementary Table 3). The DE response is dependent on the photoperiod – at least for the Arabidopsis Col-0 and L*er* ecotypes – because short-day-grown plants do not flower earlier under drought stress (Riboni et al., 2013). In addition to FT, the photoperiodic pathway is characterized by two other key components, GIGANTEA (GI) and CONSTANS (CO) (Putterill et al., 1995; Fowler et al., 1999). Complete absence of the DE response was observed in *gi* mutants in both the Col-0 and L*er* backgrounds, but this response does not appear to require the activity of CO (Riboni et al., 2013), which is a transcriptional regulator of *FT* that acts downstream of GI. Correspondingly, *GI* mRNA levels are 5-fold induced and those of *CO* barely detectable under our drought conditions (Figure 6). GI also acts in CO-independent branches by either directly binding to the FT promoter and competing with some repressors of *FT* such as SHORT VEGETATIVE PHASE (SVP), or promoting *miR172* expression which inhibits the expression of AP2-like transcription factors, such as *TOE1*, *TPL*, *SMZ*, thus repressing *FT* transcription [summarized in Kim (2020)]. Under our drought conditions, *TOE1* and *SMZ* mRNAs are barely detectable, while levels of *TPL* are elevated 11-fold (Figure 6). Amounts of *SVP* mRNAs are reduced to 20% of their starting levels in accordance with the elevated *GI* and *FT* levels and this mechanism might contribute to the earlier flowering phenotype under long-day drought conditions. However, the alternative splicing and isoform switching (IS) of *FLOWERING LOCUS M* (*FLM*) (see Figure 5), another repressor of *FT* transcription which also acts independently of CO (Balasubramanian et al., 2006), is particularly noteworthy. FLM and SVP also participate in the autonomous (Scortecci et al., 2001) and the thermosensory (Balasubramanian et al., 2006) flowering pathways. *FLM* undergoes temperature-dependent alternative splicing, and the roles of the different isoforms have been extensively and controversially discussed in the literature. It was proposed that the major isoforms, *FLM-β* and *FLM*-δ, which result from the alternative usage of exons 2 (*FLM-β*) and 3 (*FLM*-δ) (Lee et al., 2013; Pose et al., 2013) might compete for interaction with SVP, and the SVP-FLM-β complex is predominantly formed at low temperatures and prevents precocious flowering (Pose et al., 2013). One model for flowering at high temperatures suggests that degradation of SVP reduces the abundance of the SVP-FLM-β repressor complex (Lee et al., 2013), the other model is based on the idea that a higher *FLM*-δ/*FLM-β* ratio favors the formation of an SVP–FLM-*δ* complex that is impaired in DNA binding and acts as a dominant-negative activator of flowering at higher temperatures (Pose et al., 2013). We assume that under (our) drought conditions a higher FLM-β/FLM-δ ratio is unlikely to be the trigger for the flowering DE response. Our qRT-PCR data suggest that amounts of the *FLM*-β isoform increase after 9 days of drought stress, while RNA-Seq analysis indicates that levels of FLM-β are slightly reduced relative to the onset of drought treatment (see Figure 5). This discrepancy can be explained by accumulation of other non-functional isoforms containing exon 2 or exon 3, respectively (see also Sureshkumar et al., 2016), which are amplified by qRT-PCR owing to the frequent use of primer designs in which the reverse primer is situated in exon 2 (*FLM-ß*) or 3 (*FLM*-δ), respectively (for example also used in Pose et al., 2013). Although the *FLM*-β/*FLM*-δ ratio rises especially after 12 days of drought stress, the accumulation of these forms is very low in comparison to that prior to drought stress, and both are nearly undetectable anymore after 15 days. Moreover, the *FLM_P10* form, which is predominantly produced under prolonged drought stress, contains a premature stop codon that would encode a protein of only 62 amino acids (see Supplementary Table 9). Indeed, under high temperatures too, *FLM* expression is downregulated by AS coupled with nonsense-

mediated mRNA decay (AS-NMD), and the majority of non-canonical *FLM* transcripts contained premature termination codons that would result in truncated proteins of less than 100 amino acids (Sureshkumar et al., 2016). Moreover, allelic variation at *FLM* modulates plant growth strategy observable across thousands of plant species. The authors found that functional differences at *FLM* rely on a single intronic substitution, disturbing transcript splicing and leading also to the accumulation of non-functional *FLM* transcripts (Hanemian et al., 2020). All in all, we suggest that drought-mediated early flowering under long-day conditions is caused by the absence of functional FLM protein and not by the ratio of isoforms.

The decision whether to investigate under long- or short-day conditions is a very important one, since it may result in contrasting outcomes. In relation to drought research, SVP was shown to be up-regulated at the mRNA level and to confer drought tolerance in short-day-grown plants (Bechtold et al., 2016; Wang Z. et al., 2018). However, in our long-day kinetic experiment, SVP is downregulated at all times, and would not have been discovered as a positive factor in drought stress.

Moreover, our transcriptomic data sets provide a rich resource (see also Table 1) for the elucidation of the many facets of drought stress mechanisms. In particular, evaluation of the relative contributions of different splicing isoforms to drought tolerance will increase our understanding of the modulation of abiotic stress responses, thus enabling the development of new strategies to improve plant performance under adverse environmental conditions.

Data availability statement

The datasets presented in this study can be found in online repositories. The names of the repository/repositories and accession number(s) can be found in the article/Supplementary Material.

Author contributions

Conceptualization, TK and DX; Methodology, DX, QT, PX, and TK; Validation, DX and QT; Formal Analysis, TK; Investigation, DX, QT, and TK; Resources, DL, AS and TK; Writing – Original Draft, TK; Writing – Review & Editing, QT, DX, DL, AS and TK; Funding Acquisition, DL and TK Supervision, TK. All authors contributed to the article and approved the submitted version.

Funding

This work was supported by the Deutsche Forschungsgemeinschaft (TRR175, Project C01 to TK and Project C05 to DL). PX is supported by a fellowship of China Scholarship Council.

Acknowledgments

We thank Stanislaw Karpinski and Joanna Dabrowska-Bronk for providing us with the *ßca1* and *ßca2* mutants, and Paul Hardy for critical reading of the manuscript.

Conflict of interest

The authors declare that the research was conducted in the absence of any commercial or financial relationships that could be construed as a potential conflict of interest.

Publisher's note

Supplementary material

The Supplementary Material for this article can be found online at: https://www.frontiersin.org/articles/10.3389/fpls.2023.1220928/full#supplementary-material

References

Ali, S., Ganai, B. A., Kamili, A. N., Bhat, A. A., Mir, Z. A., Bhat, J. A., et al. (2018). Pathogenesis-related proteins and peptides as promising tools for engineering plants with multiple stress tolerance. *Microbiol. Res.*, 212–213, 29-37. doi: 10.1016/j.micres.2018.04.008

Ali, S., Hayat, K., Iqbal, A., and Xie, L. (2020). Implications of abscisic acid in the drought stress tolerance of plants. *Agronomy* 10 (9), 1323. doi: 10.3390/agronomy10091323

Armenteros, J. J. A., Salvatore, M., Emanuelsson, O., Winther, O., Heijne, G. V., Elofsson, A., et al. (2019). Detecting sequence signals in targeting peptides using deep learning. *Life Sci. Alliance* 2 (5), e201900429. doi: 10.26508/lsa.201900429

Balasubramanian, S., Sureshkumar, S., Lempe, J., and Weigel, D. (2006). Potent induction of Arabidopsis thaliana flowering by elevated growth temperature. *PloS Genet.* 2 (7), e106. doi: 10.1371/journal.pgen.0020106

Bao, Y., Song, W. M., Wang, P., Yu, X., Li, B., Jiang, C., et al. (2020). COST1 regulates autophagy to control plant drought tolerance. *Proc. Natl. Acad. Sci. U.S.A.* 117 (13), 7482–7493. doi: 10.1073/pnas.1918539117

Bashir, K., Matsui, A., Rasheed, S., and Seki, M. (2019). Recent advances in the characterization of plant transcriptomes in response to drought, salinity, heat, and cold stress. *F1000Res* 8. doi: 10.12688/f1000research.18424.1

Bechtold, U., Penfold, C. A., Jenkins, D. J., Legaie, R., Moore, J. D., Lawson, T., et al. (2016). Time-series transcriptomics reveals that AGAMOUS-LIKE22 affects primary metabolism and developmental processes in drought-stressed Arabidopsis. *Plant Cell* 28 (2), 345–366. doi: 10.1105/tpc.15.00910

Benjamini, Y., Drai, D., Elmer, G., Kafkafi, N., and Golani, I. (2001). Controlling the false discovery rate in behavior genetics research. *Behav. Brain Res.* 125 (1-2), 279–284. doi: 10.1016/s0166-4328(01)00297-2

Bernacki, M. J., Rusaczonek, A., Czarnocka, W., and Karpinski, S. (2021). Salicylic acid accumulation controlled by LSD1 is essential in triggering cell death in response to abiotic stress. *Cells* 10 (4), 962. doi: 10.3390/cells10040962

Blum, A. (2016). Stress, strain, signaling, and adaptation–not just a matter of definition. *J. Exp. Bot.* 67 (3), 562–565. doi: 10.1093/jxb/erv497

Blum, A., and Tuberosa, R. (2018). Dehydration survival of crop plants and its measurement. *J. Exp. Bot.* 69 (5), 975–981. doi: 10.1093/jxb/erx445

Bolger, A. M., Lohse, M., and Usadel, B. (2014). Trimmomatic: a flexible trimmer for illumina sequence data. *Bioinformatics* 30 (15), 2114–2120. doi: 10.1093/bioinformatics/btu170

Calixto, C. P. G., Guo, W., James, A. B., Tzioutziou, N. A., Entizne, J. C., Panter, P. E., et al. (2018). Rapid and dynamic alternative splicing impacts the Arabidopsis cold response transcriptome. *Plant Cell* 30 (7), 1424–1444. doi: 10.1105/tpc.18.00177

Castandet, B., Hotto, A. M., Strickler, S. R., and Stern, D. B. (2016). ChloroSeq, an optimized chloroplast RNA-seq bioinformatic pipeline, reveals remodeling of the organellar transcriptome under heat stress. *G3 (Bethesda) 6* (9), 2817–2827. doi: 10.1534/g3.116.030783

Cho, W. K., Geimer, S., and Meurer, J. (2009). Cluster analysis and comparison of various chloroplast transcriptomes and genes in Arabidopsis thaliana. *DNA Res.* 16 (1), 31–44. doi: 10.1093/dnares/dsn031

Dabrowska-Bronk, J., Komar, D. N., Rusaczonek, A., Kozlowska-Makulska, A., Szechynska-Hebda, M., and Karpinski, S. (2016). Beta-carbonic anhydrases and carbonic ions uptake positively influence Arabidopsis photosynthesis, oxidative stress tolerance and growth in light dependent manner. *J. Plant Physiol.* 203, 44–54. doi: 10.1016/j.jplph.2016.05.013

Di, C., Yuan, J., Wu, Y., Li, J., Lin, H., Hu, L., et al. (2014). Characterization of stress-responsive lncRNAs in Arabidopsis thaliana by integrating expression, epigenetic and structural features. *Plant J.* 80 (5), 848–861. doi: 10.1111/tpj.12679

DiMario, R. J., Quebedeaux, J. C., Longstreth, D. J., Dassanayake, M., Hartman, M. M., and Moroney, J. V. (2016). The cytoplasmic carbonic anhydrases betaCA2 and betaCA4 are required for optimal plant growth at low CO2. *Plant Physiol.* 171 (1), 280– 293. doi: 10.1104/pp.15.01990

Dobin, A., Davis, C. A., Schlesinger, F., Drenkow, J., Zaleski, C., Jha, S., et al. (2013). STAR: ultrafast universal RNA-seq aligner. *Bioinformatics* 29 (1), 15–21. doi: 10.1093/bioinformatics/bts635

Dopp, I. J., Yang, X., and Mackenzie, S. A. (2021). A new take on organelle-mediated stress sensing in plants. *New Phytol.* 230 (6), 2148–2153. doi: 10.1111/nph.17333

Edgar, R., Domrachev, M., and Lash, A. E. (2002). Gene expression omnibus: NCBI gene expression and hybridization array data repository. *Nucleic Acids Res.* 30 (1), 207– 210. doi: 10.1093/nar/30.1.207

Estavillo, G. M., Crisp, P. A., Pornsiriwong, W., Wirtz, M., Collinge, D., Carrie, C., et al. (2011). Evidence for a SAL1-PAP chloroplast retrograde pathway that functions in drought and high light signaling in Arabidopsis. *Plant Cell* 23 (11), 3992–4012. doi: 10.1105/tpc.111.091033

Fang, X., Zhao, G., Zhang, S., Li, Y., Gu, H., Li, Y., et al. (2019). Chloroplast-to-Nucleus signaling regulates MicroRNA biogenesis in Arabidopsis. *Dev. Cell* 48 (3), 371–382 e374. doi: 10.1016/j.devcel.2018.11.046

Fowler, S., Lee, K., Onouchi, H., Samach, A., Richardson, K., Morris, B., et al. (1999). GIGANTEA: a circadian clock-controlled gene that regulates photoperiodic flowering in Arabidopsis and encodes a protein with several possible membrane-spanning domains. *EMBO J.* 18 (17), 4679–4688. doi: 10.1093/emboj/18.17.4679

Geissler, T., and Wessjohann, L. A. (2011). A whole-plant microtiter plate assay for drought stress tolerance-inducing effects. *J. Plant Growth Regul.* 30, 504–511. doi: 10.1007/s00344-011-9212-1

Georgii, E., Jin, M., Zhao, J., Kanawati, B., Schmitt-Kopplin, P., Albert, A., et al. (2017). Relationships between drought, heat and air humidity responses revealed by transcriptome-metabolome co-analysis. *BMC Plant Biol.* 17 (1), 120. doi: 10.1186/s12870-017-1062-y

Germain, A., Hotto, A. M., Barkan, A., and Stern, D. B. (2013). RNA Processing and decay in plastids. *Wiley Interdiscip. Rev. RNA* 4 (3), 295–316. doi: 10.1002/wrna.1161

Gonzalez, C. V., Ibarra, S. E., Piccoli, P. N., Botto, J. F., and Boccalandro, H. E. (2012). Phytochrome b increases drought tolerance by enhancing ABA sensitivity in Arabidopsis thaliana. *Plant Cell Environ.* 35 (11), 1958–1968. doi: 10.1111/j.1365-3040.2012.02529.x

Guo, W., Tzioutziou, N. A., Stephen, G., Milne, I., Calixto, C. P., Waugh, R., et al. (2021). 3D RNA-seq: a powerful and flexible tool for rapid and accurate differential expression and alternative splicing analysis of RNA-seq data for biologists. *RNA Biol.* 18 (11), 1574–1587. doi: 10.1080/15476286.2020.1858253

Gupta, A., Rico-Medina, A., and Cano-Delgado, A. I. (2020). The physiology of plant responses to drought. *Science* 368 (6488), 266–269. doi: 10.1126/science. aaz7614

Hanemian, M., Vasseur, F., Marchadier, E., Gilbault, E., Bresson, J., Gy, I., et al. (2020). Natural variation at FLM splicing has pleiotropic effects modulating ecological strategies in Arabidopsis thaliana. *Nat. Commun.* 11 (1), 4140. doi: 10.1038/s41467- 020-17896-w

Hewett-Emmett, D., and Tashian, R. E. (1996). Functional diversity, conservation, and convergence in the evolution of the alpha-, beta-, and gamma-carbonic anhydrase gene families. *Mol. Phylogenet. Evol.* 5 (1), 50–77. doi: 10.1006/mpev.1996.0006

Hines, K. M., Chaudhari, V., Edgeworth, K. N., Owens, T. G., and Hanson, M. R. (2021). Absence of carbonic anhydrase in chloroplasts affects C(3) plant development but not photosynthesis. *Proc. Natl. Acad. Sci. U.S.A.* 118 (33), e2107425118. doi: 10.1073/pnas.2107425118

Hong, Y., Wang, Z., Liu, X., Yao, J., Kong, X., Shi, H., et al. (2020). Two chloroplast proteins negatively regulate plant drought resistance through separate pathways. *Plant Physiol.* 182 (2), 1007–1021. doi: 10.1104/pp.19.01106

Hu, H., Boisson-Dernier, A., Israelsson-Nordstrom, M., Bohmer, M., Xue, S., Ries, A., et al. (2010). Carbonic anhydrases are upstream regulators of CO2-controlled stomatal movements in guard cells. *Nat. Cell Biol.* 12 (1), 87–93; sup pp 81-18. doi: 10.1038/ncb2009

Hu, H., and Xiong, L. (2014). Genetic engineering and breeding of drought-resistant crops. *Annu. Rev. Plant Biol.* 65, 715–741. doi: 10.1146/annurev-arplant-050213- 040000

Huang da, W., Sherman, B. T., and Lempicki, R. A. (2009). Bioinformatics enrichment tools: paths toward the comprehensive functional analysis of large gene lists. *Nucleic Acids Res.* 37 (1), 1–13. doi: 10.1093/nar/gkn923

Ito, K., Matsukawa, K., and Kato, Y. (2006). Functional analysis of skunk cabbage SfUCPB, a unique uncoupling protein lacking the fifth transmembrane domain, in yeast cells. *Biochem. Biophys. Res. Commun.* 349 (1), 383–390. doi: 10.1016/j.bbrc.2006.08.058

Kenney, A. M., McKay, J. K., Richards, J. H., and Juenger, T. E. (2014). Direct and indirect selection on flowering time, water-use efficiency (WUE, delta (13)C), and WUE plasticity to drought in Arabidopsis thaliana. *Ecol. Evol.* 4 (23), 4505–4521. doi: 10.1002/ece3.1270

Kim, D. H. (2020). Current understanding of flowering pathways in plants: focusing on the vernalization pathway in Arabidopsis and several vegetable crop plants. *Horticult. Environ. Biotechnol.* 61 (2), 209–227. doi: 10.1007/s13580-019-00218-5

Kim, J. Y., Lee, J. H., and Park, C. M. (2021). A multifaceted action of phytochrome b in plant environmental adaptation. *Front. Plant Sci.* 12. doi: 10.3389/fpls.2021.659712

Kim, J. M., To, T. K., Matsui, A., Tanoi, K., Kobayashi, N. I., Matsuda, F., et al. (2017). Acetate-mediated novel survival strategy against drought in plants. *Nat. Plants* 3, 17097. doi: 10.1038/nplants.2017.97

Kleine, T., and Leister, D. (2015). Emerging functions of mammalian and plant mTERFs. *Biochim. Biophys. Acta* 1847 (9), 786–797. doi: 10.1016/j.bbabio.2014.12.009

Kleine, T., and Leister, D. (2016). Retrograde signaling: organelles go networking. *Biochim. Biophys. Acta* 1857 (8), 1313–1325. doi: 10.1016/j.bbabio.2016.03.017

Kleine, T., Maier, U. G., and Leister, D. (2009). DNA Transfer from organelles to the nucleus: the idiosyncratic genetics of endosymbiosis. *Annu. Rev. Plant Biol.* 60, 115–138. doi: 10.1146/annurev.arplant.043008.092119

Kleine, T., Nagele, T., Neuhaus, H. E., Schmitz-Linneweber, C., Fernie, A. R., Geigenberger, P., et al. (2021). Acclimation in plants - the green hub consortium. *Plant J.* 106 (1), 23–40. doi: 10.1111/tpj.15144

Kolbe, A. R., Brutnell, T. P., Cousins, A. B., and Studer, A. J. (2018). Carbonic anhydrase mutants in zea mays have altered stomatal responses to environmental signals. *Plant Physiol.* 177 (3), 980–989. doi: 10.1104/pp.18.00176

Kooyers, N. (2019). Are drought resistance strategies associated with life history strategy? a commentary on: 'Arabidopsis species deploy distinct strategies to cope with drought stress'. *Ann. Bot.* 124 (1), vi–viii. doi: 10.1093/aob/mcz096

Kotchoni, S. O., Kuhns, C., Ditzer, A., Kirch, H. H., and Bartels, D. (2006). Over-expression of different aldehyde dehydrogenase genes in Arabidopsis thaliana confers tolerance to abiotic stress and protects plants against lipid peroxidation and oxidative stress. *Plant Cell Environ.* 29 (6), 1033–1048. doi: 10.1111/j.1365-3040.2005. 01458.x

Labs, M., Ruhle, T., and Leister, D. (2016). The antimycin a-sensitive pathway of cyclic electron flow: from 1963 to 2015. *Photosynth. Res.* 129 (3), 231–238. doi: 10.1007/ s11120-016-0217-2

Laloum, T., Martin, G., and Duque, P. (2018). Alternative splicing control of abiotic stress responses. *Trends Plant Sci.* 23 (2), 140–150. doi: 10.1016/j.tplants.2017.09.019

Lawlor, D. W. (2013). Genetic engineering to improve plant performance under drought: physiological evaluation of achievements, limitations, and possibilities. *J. Exp. Bot.* 64 (1), 83–108. doi: 10.1093/jxb/ers326

Lee, J. H., Ryu, H. S., Chung, K. S., Pose, D., Kim, S., Schmid, M., et al. (2013). Regulation of temperature-responsive flowering by MADS-box transcription factor repressors. *Science* 342 (6158), 628–632. doi: 10.1126/science.1241097

Leijten, W., Koes, R., Roobeek, I., and Frugis, G. (2018). Translating flowering time from Arabidopsis thaliana to Brassicaceae and asteraceae crop species. *Plants (Basel)* 7(4), 111. doi: 10.3390/plants7040111

Leister, D., Wang, L., and Kleine, T. (2017). Organellar gene expression and acclimation of plants to environmental stress. *Front. Plant Sci.* 8. doi: 10.3389/ fpls.2017.00387

Lenzen, B., Ruhle, T., Lehniger, M. K., Okuzaki, A., Labs, M., Muino, J. M., et al. (2020). The chloroplast RNA binding protein CP31A has a preference for mRNAs encoding the subunits of the chloroplast NAD(P)H dehydrogenase complex and is required for their accumulation. *Int. J. Mol. Sci.* 21 (16), 5633. doi: 10.3390/ ijms21165633

Li, P., Liu, H., Yang, H., Pu, X., Li, C., Huo, H., et al. (2020). Translocation of drought-responsive proteins from the chloroplasts. *Cells* 9 (1), 259. doi: 10.3390/ cells9010259

Lovell, J. T., Juenger, T. E., Michaels, S. D., Lasky, J. R., Platt, A., Richards, J. H., et al. (2013). Pleiotropy of FRIGIDA enhances the potential for multivariate adaptation. *Proc. Biol. Sci.* 280 (1763), 20131043. doi: 10.1098/rspb.2013.1043

Malbert, B., Rigaill, G., Brunaud, V., Lurin, C., and Delannoy, E. (2018). Bioinformatic analysis of chloroplast gene expression and RNA posttranscriptional maturations using RNA sequencing. *Methods Mol. Biol.* 1829, 279–294. doi: 10.1007/ 978-1-4939-8654-5_19

Marondedze, C., Thomas, L., Lilley, K. S., and Gehring, C. (2019). Drought stress causes specific changes to the spliceosome and stress granule components. *Front. Mol. Biosci.* 6. doi: 10.3389/fmolb.2019.00163

Metsalu, T., and Vilo, J. (2015). ClustVis: a web tool for visualizing clustering of multivariate data using principal component analysis and heatmap. *Nucleic Acids Res.* 43 (W1), W566–W570. doi: 10.1093/nar/gkv468

Park, H. J., Lee, S. S., You, Y. N., Yoon, D. H., Kim, B. G., Ahn, J. C., et al. (2013). A rice immunophilin gene, OsFKBP16-3, confers tolerance to environmental stress in Arabidopsis and rice. *Int. J. Mol. Sci.* 14 (3), 5899–5919. doi: 10.3390/ijms14035899

Patro, R., Duggal, G., Love, M. I., Irizarry, R. A., and Kingsford, C. (2017). Salmon provides fast and bias-aware quantification of transcript expression. *Nat. Methods* 14 (4), 417–419. doi: 10.1038/nmeth.4197

Petrillo, E., Godoy Herz, M. A., Fuchs, A., Reifer, D., Fuller, J., Yanovsky, M. J., et al. (2014). A chloroplast retrograde signal regulates nuclear alternative splicing. *Science* 344 (6182), 427–430. doi: 10.1126/science.1250322

Pires, M. V., Pereira Junior, A. A., Medeiros, D. B., Daloso, D. M., Pham, P. A., Barros, K. A., et al. (2016). The influence of alternative pathways of respiration that utilize branched-chain amino acids following water shortage in Arabidopsis. *Plant Cell Environ.* 39 (6), 1304–1319. doi: 10.1111/pce.12682

Pose, D., Verhage, L., Ott, F., Yant, L., Mathieu, J., Angenent, G. C., et al. (2013). Temperature-dependent regulation of flowering by antagonistic FLM variants. *Nature* 503 (7476), 414–417. doi: 10.1038/nature12633

Putterill, J., Robson, F., Lee, K., Simon, R., and Coupland, G. (1995). The CONSTANS gene of Arabidopsis promotes flowering and encodes a protein showing similarities to zinc finger transcription factors. *Cell* 80 (6), 847–857. doi: 10.1016/0092- 8674(95)90288-0

Quiroz, S., Yustis, J. C., Chavez-Hernandez, E. C., Martinez, T., Sanchez, M. P., Garay-Arroyo, A., et al. (2021). Beyond the genetic pathways, flowering regulation complexity in Arabidopsis thaliana. *Int. J. Mol. Sci.* 22 (11), 5716. doi: 10.3390/ ijms22115716

Remy, E., Cabrito, T. R., Baster, P., Batista, R. A., Teixeira, M. C., Friml, J., et al. (2013). A major facilitator superfamily transporter plays a dual role in polar auxin transport and drought stress tolerance in Arabidopsis. *Plant Cell* 25 (3), 901–926. doi: 10.1105/tpc.113.110353

Riboni, M., Galbiati, M., Tonelli, C., and Conti, L. (2013). GIGANTEA enables drought escape response *via* abscisic acid-dependent activation of the florigens and SUPPRESSOR OF OVEREXPRESSION OF CONSTANS. *Plant Physiol.* 162 (3), 1706– 1719. doi: 10.1104/pp.113.217729

Robinson, J. T., Thorvaldsdottir, H., Winckler, W., Guttman, M., Lander, E. S., Getz, G., et al. (2011). Integrative genomics viewer. *Nat. Biotechnol.* 29 (1), 24–26. doi: 10.1038/nbt.1754

Rorbach, J., Bobrowicz, A., Pearce, S., and Minczuk, M. (2014). Polyadenylation in bacteria and organelles. *Methods Mol. Biol.* 1125, 211–227. doi: 10.1007/978-1-62703-971-0_18

Scarpin, M. R., Busche, M., Martinez, R. E., Harper, L. C., Reiser, L., Szakonyi, D., et al. (2023). An updated nomenclature for plant ribosomal protein genes. *Plant Cell* 35 (2), 640–643. doi: 10.1093/plcell/koac333

Scortecci, K. C., Michaels, S. D., and Amasino, R. M. (2001). Identification of a MADS-box gene, FLOWERING LOCUS m, that represses flowering. *Plant J.* 26 (2), 229–236. doi: 10.1046/j.1365-313x.2001. 01024.x

Searle, I., and Coupland, G. (2004). Induction of flowering by seasonal changes in photoperiod. *EMBO J.* 23 (6), 1217–1222. doi: 10.1038/sj.emboj.7600117

Shavrukov, Y., Kurishbayev, A., Jatayev, S., Shvidchenko, V., Zotova, L., Koekemoer, F., et al. (2017). Early flowering as a drought escape mechanism in plants: how can it aid wheat production? *Front. Plant Sci.* 8. doi: 10.3389/fpls.2017.01950

Shen, J., Li, Z., Fu, Y., and Liang, J. (2021). Identification and molecular characterization of the alternative spliced variants of beta carbonic anhydrase 1 (betaCA1) from Arabidopsis thaliana. *PeerJ* 9, e12673. doi: 10.7717/peerj.12673

Shi, X., Tian, Q., Deng, P., Zhang, W., and Jing, W. (2021). The rice aldehyde oxidase OsAO3 gene regulates plant growth, grain yield, and drought tolerance by participating in ABA biosynthesis. *Biochem. Biophys. Res. Commun.* 548, 189–195. doi: 10.1016/ j.bbrc.2021.02.047

Singh, B., Kukreja, S., and Goutam, U. (2018). Milestones achieved in response to drought stress through reverse genetic approaches. *F1000Res* 7, 1311. doi: 10.12688/ f1000research.15606.1

Streitner, C., Koster, T., Simpson, C. G., Shaw, P., Danisman, S., Brown, J. W., et al. (2012). An hnRNP-like RNA-binding protein affects alternative splicing by *in vivo* interaction with transcripts in Arabidopsis thaliana. *Nucleic Acids Res.* 40 (22), 11240–11255. doi: 10.1093/nar/gks873

Supek, F., Bosnjak, M., Skunca, N., and Smuc, T. (2011). REVIGO summarizes and visualizes long lists of gene ontology terms. *PloS One* 6 (7), e21800. doi: 10.1371/ journal.pone.0021800

Sureshkumar, S., Dent, C., Seleznev, A., Tasset, C., and Balasubramanian, S. (2016). Nonsense-mediated mRNA decay modulates FLM-dependent thermosensory flowering response in Arabidopsis. *Nat. Plants* 2 (5), 16055. doi: 10.1038/ nplants.2016.55

Szechynska-Hebda, M., Czarnocka, W., Hebda, M., Bernacki, M. J., and Karpinski, S. (2016). PAD4, LSD1 and EDS1 regulate drought tolerance, plant biomass production, and cell wall properties. *Plant Cell Rep.* 35 (3), 527–539. doi: 10.1007/s00299-015-1901- y

Tiwari, B., Habermann, K., Arif, M. A., Weil, H. L., Garcia-Molina, A., Kleine, T., et al. (2020). Identification of small RNAs during cold acclimation in Arabidopsis thaliana. *BMC Plant Biol.* 20 (1), 298. doi: 10.1186/s12870-020-02511-3

Wang, L., Jin, X., Li, Q., Wang, X., Li, Z., and Wu, X. (2016). Comparative proteomics reveals that phosphorylation of beta carbonic anhydrase 1 might be important for adaptation to drought stress in brassica napus. *Sci. Rep.* 6, 39024. doi: 10.1038/srep39024

Wang, Z., Wang, F. X., Hong, Y. C., Yao, J. J., Ren, Z. Z., Shi, H. Z., et al. (2018b). The flowering repressor SVP confers drought resistance in Arabidopsis by regulating abscisic acid catabolism. *Mol. Plant* 11 (9), 1184–1197. doi: 10.1016/j.molp.2018.06.009

Wang, R., Zhao, J., Jia, M., Xu, N., Liang, S., Shao, J., et al. (2018a). Balance between cytosolic and chloroplast translation affects leaf variegation. *Plant Physiol.* 176 (1), 804–818. doi: 10.1104/pp.17.00673

Yamori, W., and Shikanai, T. (2016). Physiological functions of cyclic electron transport around photosystem I in sustaining photosynthesis and plant growth. *Annu. Rev. Plant Biol.* 67, 81–106. doi: 10.1146/annurev-arplant-043015-112002

Yang, D. H., Kwak, K. J., Kim, M. K., Park, S. J., Yang, K. Y., and Kang, H. (2014). Expression of Arabidopsis glycine-rich RNA-binding protein AtGRP2 or AtGRP7 improves grain yield of rice (Oryza sativa) under drought stress conditions. *Plant Sci.* 214, 106–112. doi: 10.1016/j.plantsci.2013.10.006

Zarnack, K., Balasubramanian, S., Gantier, M. P., Kunetsky, V., Kracht, M., Schmitz, M. L., et al. (2020). Dynamic mRNP remodeling in response to internal and external stimuli. *Biomolecules* 10 (9), 1310. doi: 10.3390/biom10091310

Zhang, R., Calixto, C. P. G., Marquez, Y., Venhuizen, P., Tzioutziou, N. A., Guo, W., et al. (2017). A high-quality Arabidopsis transcriptome for accurate transcript-level analysis of alternative splicing. *Nucleic Acids Res.* 45 (9), 5061–5073. doi: 10.1093/nar/ gkx267

Zhang, Y., Zhang, A., Li, X., and Lu, C. (2020). The role of chloroplast gene expression in plant responses to environmental stress. *Int. J. Mol. Sci.* 21 (17), 6082. doi: 10.3390/ijms21176082

Zhao, C., Liu, B., Piao, S., Wang, X., Lobell, D. B., Huang, Y., et al. (2017). Temperature increase reduces global yields of major crops in four independent estimates. *Proc. Natl. Acad. Sci. U.S.A.* 114 (35), 9326–9331. doi: 10.1073/ pnas.1701762114

Zhou, W., Cheng, Y., Yap, A., Chateigner-Boutin, A. L., Delannoy, E., Hammani, K., et al. (2009). The Arabidopsis gene YS1 encoding a DYW protein is required for editing of rpoB transcripts and the rapid development of chloroplasts during early growth. *Plant J.* 58 (1), 82–96. doi: 10.1111/j.1365-313X.2008. 03766.x

Zhu, J. K. (2002). Salt and drought stress signal transduction in plants. *Annu. Rev. Plant Biol.* 53, 247–273. doi: 10.1146/annurev.arplant.53.091401.143329

4. Discussion

4.1 GUN1 binds to plastid RNAs and promotes their maturation

GUN1, a well-known protein in retrograde signaling, has long been enigmatic in terms of its molecular function (Richter et al., 2023). Despite its critical role in chloroplast-to-nucleus communication, the *gun1* mutant typically exhibits a wild-type-like phenotype, with the exception of occasional seedlings displaying chlorophyll-deficient cotyledons (Ruckle et al., 2008; Wu et al., 2018). This observation is puzzling, as one would expect that mutants of such an important integrator would present with severe phenotypes. However, *gun1* mutants only manifest the "*gun*" phenotype at the molecular level after treatments that trigger retrograde signaling. This raises a particularly intriguing and challenging question: How does GUN1 fulfill its role in retrograde signaling in *Arabidopsis*?

4.1.1 Cotyledon chlorophyll deficiency phenotype in *gun1* mutants

Aside from the wild-type-like phenotype, the low abundance of GUN1 protein further complicates the study of its function, as GUN1 protein levels are barely detectable through proteomic methods (Liu et al., 2013). However, the observation of marble and white cotyledons, alongside normal true leaves, suggests a specific role for GUN1 in the early development of cotyledons. This finding aligns with previous studies showing that GUN1 protein levels accumulate during the early stages of cotyledon development (Wu et al., 2018), highlighting its specialized role during this critical developmental phase.

Interestingly, the variegated cotyledon phenotype is observed among progeny from the same mother plant, suggesting incomplete penetrance and variable expressivity. While these genetic traits are not widely documented in plant biology, they are well-established in animal genetics. For example, diseases such as *BRCA1*/*BRCA2*-associated hereditary breast and ovarian cancer display these characteristics (Petrucelli et al., 1993). In animal studies, such variability is often attributed to a combination of genetic, environmental, and lifestyle factors (Coll et al., 2017). Regarding GUN1 function in chloroplast development within cotyledons, a possible hypothesis is that GUN1 expression must reach a critical threshold to trigger proper chloroplast

development. Below this threshold, chloroplast formation might be incomplete or aberrant, potentially explaining the observed variation in cotyledon phenotypes across genetically similar progeny. This hypothesis also explains previous study of *gun1* sensitivity to inhibitors like LIN and NF (Zhao, Huang, and Chory, 2018) as well as ABA treatments (Cottage et al., 2010).

In the absence of *GUN1*, compensatory mechanisms may be triggered during seedling development. The inability of these mechanisms to fully compensate in some individuals likely depends on the severity or specific type of environmental stresses experienced by the parent plants. This suggests that environmental factors may need to surpass certain critical thresholds before the compensatory mechanisms fail, resulting in variability in phenotypes within the population. Supporting this scenario, a recent study found that *gun1* mutants exhibited higher levels of superoxide anions and lipid peroxidation (Fortunato et al., 2022), indicating increased oxidative stress. This suggests that, even under non-stress conditions, additional protective mechanisms are activated to protect *gun1* mutants from internal oxidative stress, which arises due to the absence of GUN1 protein. The significantly reduced levels of plastid rRNA in *gun1W* and *gun1M* mutants could result from partial or failed compensation once the GUN1 protein threshold is surpassed, which may explain the phenotype, though this is likely a secondary effect.

4.1.2 GUN1 as an RNA binding protein

Like described before in the introduction part, GUN1 is one of the 5 PPR-SMR chloroplast proteins and they are all responsible for normal chloroplast development (Zhang and Lu, 2019). As a P-type PPR protein, GUN1 was also thought to have RNA binding capacity when comes to its molecular function and its SMR domain was shown to bind DNA (Koussevitzky et al., 2007). Zhao et al. (2019) recently proposed that GUN1 plays a role in RNA regulation under NF treatment, particularly in RNA editing. GUN1modulates RNA by interacting with MORF2, without directly binding to RNA. It is a rational explanation since no *in vivo* binding of GUN1 was reported. Although previous NIP-chip analysis (Tadini et al., 2016) on adult plant failed to detect any significant GUN1-nucleic acid interaction, we realized it is necessary to perform RIP

again given the fact that GUN1 is important in early development of chloroplast in seedling stage. *In silico* decoding of PPR motifs of GUN1 and *in vivo* RIP-Seq analysis suggest *ycf1.2*, *ycf2*, *rps2*, *rps12C* and *rpl20*, *rpoC1* and *rpoC2*, *ndhB*, *ndhA* and *ndhG*, *matK*, and tRNAs such as *trnK*, *trnG.1*, and *trnI.2* as putative targets.

Additional EMSAs confirmed *ndhG* and *trnG.1* as *in vitro* targets of GUN1. *ndhG*, a component of the plastid NADH dehydrogenase-like (NDH) complex, is involved in cyclic electron flow and maintaining energy balance within the chloroplast (Strand et al., 2017). The NDH complex dissipates excess reducing power, preventing the over-reduction of the photosynthetic electron transport chain and limiting the generation of ROS. In addition, even without a visible phenotype, *gun1* mutants exhibit reduced activity of antioxidant enzymes such as superoxide dismutase (SOD) and ascorbate peroxidase (APX), along with increased superoxide (O^{2-}) accumulation and lipid peroxidation (Fortunato et al., 2022). This suggests that GUN1 indirectly safeguards chloroplasts from oxidative damage and *gun1* mutant is more sensitive under oxidative stress. Since *ndhG* is a direct binding target of GUN1, it likely contributes to GUN1's role in maintaining chloroplast function, especially under oxidative stress conditions, by stabilizing the NDH complex's activity and ensuring effective management of reducing power to ensure proper expression of plastid genome.

trnG.1 encodes tRNA-Gly (UCC) in *Arabidopsis* and recognizes GGA and GGG codons, while another glycine precursor tRNA, tRNA-Gly (GCC), is encoded by *trnG.2* and recognizes GGC and GGU codons (Tiller and Bock, 2014). In tobacco, it has been reported that *trnG.1* is essential for plant survival, whereas knocking out *trnG.2* only moderately compromises translation (Rogalski et al., 2008). In addition, tRNA-derived RNA fragments (tRFs) from tRNA-Gly (UCC) have been shown to accumulate in *Arabidopsis* plants under stress conditions such as phosphate starvation and UV stress (Hsieh et al., 2009). In *Arabidopsis*, these tRNA-Gly-derived fragments associate with Argonaute proteins (Cognat et al., 2017), indicating their potential role in RNA silencing pathways or other regulatory functions. Notably, northern blot experiments with highly purified chloroplast and mitochondrial fractions confirmed that organellar tRFs accumulate outside the organelles, predominantly in the cytosol. This observation

provides an attractive hypothesis that tRFs may have the potential to serve as signaling particles during retrograde signaling. In a study by Habermann et al. (2020), all the tRNAs identified among differentially expressed genes in Col-0 (3 tRNAs down regulated) and *gun1* mutants (4 tRNA down regulated) treated with norflurazon, compared to untreated conditions, were of chloroplast origin. Notably, *trnG.1*, encoding tRNA-Gly, was exclusively present in the *gun1*-NF vs. *gun1* comparison (Habermann et al., 2020), this evidence suggests that *tRNG.1* is likely responsive to treatments like NF or abiotic stress in the absence of functional GUN1, and may have a potential molecular function as a retrograde signaling element.

Interestingly, GUN1 is predicted to bind to multiple sites within *ycf1.2*, and no specific maturation factors for *ycf1.2* have been identified to date. The data from this study provide strong evidence that GUN1 binds to RNA and suggest specific target sites. These findings lay the groundwork for future studies aimed at exploring the role of GUN1 in plastid RNA metabolism and its broader involvement in retrograde signaling.

4.2 Response of the organellar and nuclear (post)transcriptomes of *Arabidopsis* to drought

Chloroplasts and mitochondria not only sense environmental changes but also serve as primary targets of stress factors (Kleine et al., 2021). The intricate drought response mechanisms in *Arabidopsis thaliana* provide valuable insights into the plant's adaptive strategies at both organellar and nuclear levels. While nuclear gene changes in response to drought have been extensively studied, only one study has examined the organellar post-transcriptomes in *Arabidopsis* chloroplasts (Castandet et al., 2016), and no equivalent studies have been conducted for mitochondria. Castandet et al. (2016) developed a chloroplast RNA-Seq bioinformatics pipeline using RNA-Seq following ribosomal RNA depletion. Their analysis revealed a global reduction in chloroplast splicing and editing efficiency, along with an increase in transcript abundance in response to heat. In contrast, short-term drought treatments (3 and 12 hours in 300 mM mannitol) had minimal impact on the chloroplast post-transcriptome. Although only one copy of the sequencing data was used by Castandet et al. (2016) which is not statistically meaningful, leveraging this pipeline, we now have a broader understanding of how

transcriptome-wide changes and post-transcriptional modifications dynamically modulate energy production, stress responses, and developmental pathways in plants under drought conditions, as demonstrated in the 'water-withheld setup' (Ali et al., 2020).

4.2.1 Organellar transcriptomic changes: chloroplast and mitochondrial interplay during drought stress

Chloroplast transcript levels, particularly those linked to photosynthesis, exhibit a notable reduction under drought stress. This is consistent with earlier studies on *Arabidopsis* and other plant species, where drought-induced downregulation of the photosynthetic machinery is a common energy-saving response (Thatcher et al., 2016). Reduced chloroplast activity during stress may reflect a strategic shift in energy management, minimizing high-energy processes like photosynthesis to conserve resources (Goltsev et al., 2012; Thatcher et al., 2016) . This decline in chloroplast activity has also been associated with impaired stomatal conductance and overall reduced photosynthetic efficiency (Haworth et al., 2016), further suggesting that the plant prioritizes essential survival processes over growth under adverse conditions.

In contrast, mitochondrial transcripts show a slight increase, particularly those involved in the tricarboxylic acid (TCA) cycle and the components of succinate-dehydrogenase complex II. This indicates a compensatory mechanism where mitochondrial respiration becomes more critical for maintaining energy production under drought. Juszczuk and Rychter (2003) previously noted that during stress or low oxygen conditions, mitochondrial pathways play a pivotal role in sustaining ATP levels. This shift in organellar activity, where chloroplast function declines while mitochondrial activity increases, reflects a broader strategy of energy reallocation, enhancing metabolic flexibility to ensure survival during drought. Similar observations were made in other studies of abiotic stress, where increased mitochondrial respiration helps meet the metabolic demands when photosynthesis is downregulated (Atkin et al., 2000).

The interplay between chloroplasts and mitochondria in *Arabidopsis* under drought stress underscores a highly adaptive energy management system, balancing photosynthetic downregulation with heightened respiratory activity (Igamberdiev and

Bykova, 2023). The ability of plants to modulate energy production across different organelles suggests an intricate coordination of nuclear and organellar genomes, ensuring that metabolic demands are met despite fluctuating environmental conditions. Understanding how these mechanisms function in crops could provide insights for improving drought tolerance through targeted breeding or genetic modifications.

4.2.2 Alternative splicing as a dynamic response mechanism

Alternative splicing emerges as a crucial mechanism through which plants adjust their proteome in response to environmental stress (Liu et al., 2022). AS enhances proteome diversity, allowing for fine-tuning of gene expression and expanding the plant's adaptive capacity (Laloum et al., 2018). AS greatly enhances the coding capacity of a genome and expands the proteome, regulating up to 95% of human and 70% of plant multi-exon genes (Liu et al., 2022). The differential splicing of over 1,400 genes observed during drought stress in this study aligns with previous reports in various species, including *Oryza sativa*, where AS of key stress-response genes enables enhanced drought resilience (Ganie and Reddy, 2021). The widespread nature of AS in stress responses suggests it is a highly conserved and fundamental process in higher plants.

Particularly striking is the isoform switching observed in *FLOWERING LOCUS M* (*FLM*), suggesting that AS acts as a molecular switch to promote early flowering, a well-documented drought escape strategy (Shavrukov, 2024; Shavrukov et al., 2017). Similar AS-mediated early flowering mechanisms have been identified in cereal crops, further demonstrating the conserved role of splicing in developmental timing under drought conditions (Shavrukov et al., 2017). Furthermore, the role of AS in drought responses extends beyond the regulation of flowering time. Data demonstrate that nearly 9% of expressed nuclear genes undergo AS under drought stress, affecting approximately 1,500 genes. Of these, 42% are regulated solely at the level of AS, a finding that would have been missed in previous microarray-based approaches. For example, the AS of *CARBONIC ANHYDRASE* (*CA*) genes has been linked to enhanced drought tolerance. The *ca1* and *ca2* mutants exhibit increased drought resistance, suggesting that modulation of isoform contributions can improve stress adaptation by altering metabolic and physiological processes critical for drought response.

Beyond developmental regulation, AS also impacts metabolic and signaling pathways, as shown in *Zea mays*, where stress-induced splicing affects both developmental and metabolic genes (Thatcher et al., 2016). This ability to modify multiple layers (developmental, metabolic and signaling pathways) of gene expression enables plants to orchestrate a more comprehensive response to drought stress. In *Arabidopsis*, AS-mediated reprogramming impacts both nuclear-encoded and organellar transcripts, highlighting the interconnected nature of post-transcriptional regulation in response to abiotic stress.

The extensive use of AS during drought reflects a dynamic regulatory system that enhances the plant's ability to cope with environmental challenges (Staiger and Brown, 2013). By modifying both developmental and metabolic processes, plants can respond to stress in a highly coordinated manner. The conservation of these mechanisms across species (Cai et al., 1998; McKibbin et al., 2002) highlights potential targets for crop improvement strategies aimed at enhancing drought tolerance. Understanding how these transcriptomic shifts occur across different plant systems could provide valuable insights into improving resilience in agricultural settings.

In summary, these transcriptomic datasets provide a valuable resource for uncovering the various mechanisms involved in drought stress responses. In particular, investigating the role of different splicing isoforms in drought tolerance will deepen our understanding of how plants modulate their responses to abiotic stress. This knowledge can drive the development of innovative strategies to enhance plant resilience and performance under unfavorable environmental conditions.

References

Abdallah, F., Salamini, F., & Leister, D. (2000). A prediction of the size and evolutionary origin of the proteome of chloroplasts of Arabidopsis. *Trends in Plant Science*, *5*(4), 141–142. https://doi.org/10.1016/S1360-1385(00)01574-0

Adhikari, N. D., Froehlich, J. E., Strand, D. D., Buck, S. M., Kramer, D. M., & Larkin, R. M. (2011). GUN4-Porphyrin Complexes Bind the ChlH/GUN5 Subunit of Mg-Chelatase and Promote Chlorophyll Biosynthesis in *Arabidopsis*. *The Plant Cell*, *23*(4), 1449–1467. https://doi.org/10.1105/tpc.110.082503

Ali, S., Hayat, K., Iqbal, A., & Xie, L. (2020). Implications of Abscisic Acid in the Drought Stress Tolerance of Plants. *Agronomy*, *10*(9), 1323. https://doi.org/10.3390/agronomy10091323

Archibald, J. M. (2015). Endosymbiosis and Eukaryotic Cell Evolution. *Current Biology*, *25*(19), R911–R921. https://doi.org/10.1016/j.cub.2015.07.055

Atkin, O. K., Millar, A. H., Gardeström, P., & Day, D. A. (2000). *Photosynthesis, Carbohydrate Metabolism and Respiration in Leaves of Higher Plants* (pp. 153–175). https://doi.org/10.1007/0-306-48137-5_7

Ball, S. G., Bhattacharya, D., & Weber, A. P. M. (2016). Pathogen to powerhouse. *Science*, *351*(6274), 659–660. https://doi.org/10.1126/science.aad8864

Ban, T., Ke, J., Chen, R., Gu, X., Tan, M. H. E., Zhou, X. E., Kang, Y., Melcher, K., Zhu, J.-K., & Xu, H. E. (2013). Structure of a PLS-class Pentatricopeptide Repeat Protein Provides Insights into Mechanism of RNA Recognition. *Journal of Biological Chemistry*, *288*(44), 31540–31548. https://doi.org/10.1074/jbc.M113.496828

Barkan, A. (2011). *Studying the Structure and Processing of Chloroplast Transcripts* (pp. 183–197). https://doi.org/10.1007/978-1-61779-234-2_12

Barkan, A., & Small, I. (2014). Pentatricopeptide Repeat Proteins in Plants. *Annual Review of Plant Biology*, *65*(1), 415–442. https://doi.org/10.1146/annurev-arplant-050213-040159

Baruah, A., Šimková, K., Apel, K., & Laloi, C. (2009). Arabidopsis mutants reveal multiple singlet oxygen signaling pathways involved in stress response and development. *Plant Molecular Biology*, *70*(5), 547–563. https://doi.org/10.1007/s11103-009-9491-0

Bédard, J., & Jarvis, P. (2005). Recognition and envelope translocation of chloroplast preproteins. *Journal of Experimental Botany*, *56*(419), 2287–2320. https://doi.org/10.1093/jxb/eri243

References

Bock, R. (2007). *Structure, function, and inheritance of plastid genomes* (pp. 29–63). https://doi.org/10.1007/4735_2007_0223

Boussardon, C., Salone, V., Avon, A., Berthomé, R., Hammani, K., Okuda, K., Shikanai, T., Small, I., & Lurin, C. (2012). Two Interacting Proteins Are Necessary for the Editing of the NdhD-1 Site in *Arabidopsis* Plastids. *The Plant Cell*, *24*(9), 3684–3694. https://doi.org/10.1105/tpc.112.099507

Brunkard, J. O., & Burch-Smith, T. M. (2018). Ties that bind: the integration of plastid signaling pathways in plant cell metabolism. *Essays in Biochemistry*, *62*(1), 95–107. https://doi.org/10.1042/EBC20170011

Cai, X., Wang, Z., Xing, Y., Zhang, J., & Hong, M. (1998). Aberrant splicing of intron 1 leads to the heterogeneous 5′ UTR and decreased expression of *waxy* gene in rice cultivars of intermediate amylose content. *The Plant Journal*, *14*(4), 459–465. https://doi.org/10.1046/j.1365-313X.1998.00126.x

Castandet, B., Hotto, A. M., Strickler, S. R., & Stern, D. B. (2016). ChloroSeq, an Optimized Chloroplast RNA-Seq Bioinformatic Pipeline, Reveals Remodeling of the Organellar Transcriptome Under Heat Stress. *G3 Genes |Genomes | Genetics*, *6*(9), 2817–2827. https://doi.org/10.1534/g3.116.030783

Chan, K. X., Phua, S. Y., Crisp, P., McQuinn, R., & Pogson, B. J. (2016). Learning the Languages of the Chloroplast: Retrograde Signaling and Beyond. *Annual Review of Plant Biology*, *67*(1), 25–53. https://doi.org/10.1146/annurev-arplant-043015-111854

Cheng, S., Gutmann, B., Zhong, X., Ye, Y., Fisher, M. F., Bai, F., Castleden, I., Song, Y., Song, B., Huang, J., Liu, X., Xu, X., Lim, B. L., Bond, C. S., Yiu, S., & Small, I. (2016). Redefining the structural motifs that determine RNA binding and RNA editing by pentatricopeptide repeat proteins in land plants. *The Plant Journal*, *85*(4), 532–547. https://doi.org/10.1111/tpj.13121

Cline, K., & Henry, R. (1996). Import and routing of nucleus-encoded chloroplast proteins. *Annual Review of Cell and Developmental Biology*, *12*(1), 1–26. https://doi.org/10.1146/annurev.cellbio.12.1.1

Cognat, V., Morelle, G., Megel, C., Lalande, S., Molinier, J., Vincent, T., Small, I., Duchêne, A.-M., & Maréchal-Drouard, L. (2017). The nuclear and organellar tRNA-derived RNA fragment population in Arabidopsis thaliana is highly dynamic. *Nucleic Acids Research*, *45*(6), 3460–3472. https://doi.org/10.1093/nar/gkw1122

Coll, M., Pérez-Serra, A., Mates, J., Del Olmo, B., Puigmulé, M., Fernandez-Falgueras, A., Iglesias, A., Picó, F., Lopez, L., Brugada, R., & Campuzano, O. (2017). Incomplete Penetrance and Variable Expressivity: Hallmarks in Channelopathies Associated with Sudden Cardiac Death. *Biology*, *7*(1), 3. https://doi.org/10.3390/biology7010003

References

Corti, F., Festa, M., Stein, F., Stevanato, P., Siroka, J., Navazio, L., Vothknecht, U. C., Alboresi, A., Novák, O., Formentin, E., & Szabò, I. (2023). Comparative analysis of wild-type and chloroplast MCU-deficient plants reveals multiple consequences of chloroplast calcium handling under drought stress. *Frontiers in Plant Science*, *14*. https://doi.org/10.3389/fpls.2023.1228060

Cottage, A., Mott, E. K., Kempster, J. A., & Gray, J. C. (2010). The Arabidopsis plastid-signaling mutant gun1 (genomes uncoupled1) shows altered sensitivity to sucrose and abscisic acid and alterations in early seedling development. *Journal of Experimental Botany*, *61*(13), 3773–3786. https://doi.org/10.1093/jxb/erq186

Cruz de Carvalho, M. H. (2008). Drought stress and reactive oxygen species. *Plant Signaling & Behavior*, *3*(3), 156–165. https://doi.org/10.4161/psb.3.3.5536

Davis, S. J., Kurepa, J., & Vierstra, R. D. (1999). The Arabidopsis thaliana HY1 locus, required for phytochrome-chromophore biosynthesis, encodes a protein related to heme oxygenases. *Proceedings of the National Academy of Sciences*, *96*(11), 6541–6546. https://doi.org/10.1073/pnas.96.11.6541

de Longevialle, A. F., Small, I. D., & Lurin, C. (2010). Nuclearly Encoded Splicing Factors Implicated in RNA Splicing in Higher Plant Organelles. *Molecular Plant*, *3*(4), 691–705. https://doi.org/10.1093/mp/ssq025

Fang, Y., & Xiong, L. (2015). General mechanisms of drought response and their application in drought resistance improvement in plants. *Cellular and Molecular Life Sciences*, *72*(4), 673–689. https://doi.org/10.1007/s00018-014-1767-0

Fortunato, S., Lasorella, C., Tadini, L., Jeran, N., Vita, F., Pesaresi, P., & de Pinto, M. C. (2022). GUN1 involvement in the redox changes occurring during biogenic retrograde signaling. *Plant Science*, *320*, 111265. https://doi.org/10.1016/j.plantsci.2022.111265

Ganie, S. A., & Reddy, A. S. N. (2021). Stress-Induced Changes in Alternative Splicing Landscape in Rice: Functional Significance of Splice Isoforms in Stress Tolerance. *Biology*, *10*(4), 309. https://doi.org/10.3390/biology10040309

Gläßer, C., Haberer, G., Finkemeier, I., Pfannschmidt, T., Kleine, T., Leister, D., Dietz, K.-J., Häusler, R. E., Grimm, B., & Mayer, K. F. X. (2014). Meta-Analysis of Retrograde Signaling in Arabidopsis thaliana Reveals a Core Module of Genes Embedded in Complex Cellular Signaling Networks. *Molecular Plant*, *7*(7), 1167–1190. https://doi.org/10.1093/mp/ssu042

Goltsev, V., Zaharieva, I., Chernev, P., Kouzmanova, M., Kalaji, H. M., Yordanov, I., Krasteva, V., Alexandrov, V., Stefanov, D., Allakhverdiev, S. I., & Strasser, R. J. (2012). Drought-induced modifications of photosynthetic electron transport in intact leaves: Analysis and use of neural networks as a tool for a rapid non-invasive estimation. *Biochimica et Biophysica Acta (BBA) - Bioenergetics*, *1817*(8), 1490–1498. https://doi.org/10.1016/j.bbabio.2012.04.018

References

Green, B. R. (2011). Chloroplast genomes of photosynthetic eukaryotes. *The Plant Journal*, *66*(1), 34–44. https://doi.org/10.1111/j.1365-313X.2011.04541.x

Guo, P., Baum, M., Varshney, R. K., Graner, A., Grando, S., & Ceccarelli, S. (2008). QTLs for chlorophyll and chlorophyll fluorescence parameters in barley under post-flowering drought. *Euphytica*, *163*(2), 203–214. https://doi.org/10.1007/s10681-007-9629-6

Habermann, K., Tiwari, B., Krantz, M., Adler, S. O., Klipp, E., Arif, M. A., & Frank, W. (2020). Identification of small non-coding RNAs responsive to *GUN1* and *GUN5* related retrograde signals in *Arabidopsis thaliana*. *The Plant Journal*, *104*(1), 138–155. https://doi.org/10.1111/tpj.14912

Hajdukiewicz, P. T. J., Allison, L. A., & Maliga, P. (1997). The two RNA polymerases encoded by the nuclear and the plastid compartments transcribe distinct groups of genes in tobacco plastids. *The EMBO Journal*, *16*(13), 4041–4048. https://doi.org/10.1093/emboj/16.13.4041

Haworth, M., Killi, D., Materassi, A., Raschi, A., & Centritto, M. (2016). Impaired Stomatal Control Is Associated with Reduced Photosynthetic Physiology in Crop Species Grown at Elevated [CO2]. *Frontiers in Plant Science*, *7*. https://doi.org/10.3389/fpls.2016.01568

Hernández-Verdeja, T., & Strand, Å. (2018). Retrograde Signals Navigate the Path to Chloroplast Development. *Plant Physiology*, *176*(2), 967–976. https://doi.org/10.1104/pp.17.01299

Hirose, T. (2001). Involvement of a site-specific trans-acting factor and a common RNA-binding protein in the editing of chloroplast mRNAs: development of a chloroplast in vitro RNA editing system. *The EMBO Journal*, *20*(5), 1144–1152. https://doi.org/10.1093/emboj/20.5.1144

Hong, W., Zeng, J., & Xie, J. (2014). Antibiotic drugs targeting bacterial RNAs. *Acta Pharmaceutica Sinica B*, *4*(4), 258–265. https://doi.org/10.1016/j.apsb.2014.06.012

Honkanen, S., & Small, I. (2022). The GENOMES UNCOUPLED1 protein has an ancient, highly conserved role but not in retrograde signaling. *New Phytologist*, *236*(1), 99–113. https://doi.org/10.1111/nph.18318

Hsieh, L.-C., Lin, S.-I., Shih, A. C.-C., Chen, J.-W., Lin, W.-Y., Tseng, C.-Y., Li, W.-H., & Chiou, T.-J. (2009). Uncovering Small RNA-Mediated Responses to Phosphate Deficiency in Arabidopsis by Deep Sequencing. *Plant Physiology*, *151*(4), 2120–2132. https://doi.org/10.1104/pp.109.147280

Hu, C., Elias, E., Nawrocki, W. J., & Croce, R. (2023). Drought affects both photosystems in *Arabidopsis thaliana*. *New Phytologist*, *240*(2), 663–675. https://doi.org/10.1111/nph.19171

References

Hwang, Y., Han, S., Yoo, C. Y., Hong, L., You, C., Le, B. H., Shi, H., Zhong, S., Hoecker, U., Chen, X., & Chen, M. (2022). Anterograde signaling controls plastid transcription via sigma factors separately from nuclear photosynthesis genes. *Nature Communications*, *13*, 7440. https://doi.org/10.1038/s41467-022-35080-0

Igamberdiev, A. U., & Bykova, N. V. (2023). Mitochondria in photosynthetic cells: Coordinating redox control and energy balance. *Plant Physiology*, *191*(4), 2104–2119. https://doi.org/10.1093/plphys/kiac541

Jan, M., Liu, Z., Rochaix, J.-D., & Sun, X. (2022). Retrograde and anterograde signaling in the crosstalk between chloroplast and nucleus. *Frontiers in Plant Science*, *13*. https://doi.org/10.3389/fpls.2022.980237

Jarvis, P. (2008). Targeting of nucleus-encoded proteins to chloroplasts in plants. *New Phytologist*, *179*(2), 257–285. https://doi.org/10.1111/j.1469-8137.2008.02452.x

Jenkins, B. D., Kulhanek, D. J., & Barkan, A. (1997). Nuclear mutations that block group II RNA splicing in maize chloroplasts reveal several intron classes with distinct requirements for splicing factors. *The Plant Cell*, *9*(3), 283–296. https://doi.org/10.1105/tpc.9.3.283

Ji, Y., Lehotai, N., Zan, Y., Dubreuil, C., Díaz, M. G., & Strand, Å. (2021). A fully assembled plastid-encoded RNA polymerase complex detected in etioplasts and proplastids in Arabidopsis. *Physiologia Plantarum*, *171*(3), 435–446. https://doi.org/10.1111/ppl.13256

Juszczuk, I. M., & Rychter, A. M. (2003). Alternative oxidase in higher plants. *Acta Biochimica Polonica*, *50*(4), 1257–1271.

Kacprzak, S. M., Mochizuki, N., Naranjo, B., Xu, D., Leister, D., Kleine, T., Okamoto, H., & Terry, M. J. (2019). Plastid-to-Nucleus Retrograde Signalling during Chloroplast Biogenesis Does Not Require ABI4. *Plant Physiology*, *179*(1), 18–23. https://doi.org/10.1104/pp.18.01047

Kleine, T., Nägele, T., Neuhaus, H. E., Schmitz-Linneweber, C., Fernie, A. R., Geigenberger, P., Grimm, B., Kaufmann, K., Klipp, E., Meurer, J., Möhlmann, T., Mühlhaus, T., Naranjo, B., Nickelsen, J., Richter, A., Ruwe, H., Schroda, M., Schwenkert, S., Trentmann, O., … Leister, D. (2021). Acclimation in plants – the Green Hub consortium. *The Plant Journal*, *106*(1), 23–40. https://doi.org/10.1111/tpj.15144

Kocheva, K., Lambrev, P., Georgiev, G., Goltsev, V., & Karabaliev, M. (2004). Evaluation of chlorophyll fluorescence and membrane injury in the leaves of barley cultivars under osmotic stress. *Bioelectrochemistry*, *63*(1–2), 121–124. https://doi.org/10.1016/j.bioelechem.2003.09.020

Kohchi, T., Mukougawa, K., Frankenberg, N., Masuda, M., Yokota, A., & Lagarias, J. C. (2001). The Arabidopsis HY2 Gene Encodes Phytochromobilin Synthase, a

Ferredoxin-Dependent Biliverdin Reductase. *The Plant Cell*, *13*(2), 425–436. https://doi.org/10.1105/tpc.13.2.425

Koussevitzky, S., Nott, A., Mockler, T. C., Hong, F., Sachetto-Martins, G., Surpin, M., Lim, J., Mittler, R., & Chory, J. (2007). Signals from chloroplasts converge to regulate nuclear gene expression. *Science (New York, N.Y.)*, *316*(5825), 715–719.

Kupsch, C., Ruwe, H., Gusewski, S., Tillich, M., Small, I., & Schmitz-Linneweber, C. (2012). Arabidopsis Chloroplast RNA Binding Proteins CP31A and CP29A Associate with Large Transcript Pools and Confer Cold Stress Tolerance by Influencing Multiple Chloroplast RNA Processing Steps. *The Plant Cell*, *24*(10), 4266–4280. https://doi.org/10.1105/tpc.112.103002

Kuromori, T., Fujita, M., Takahashi, F., Yamaguchi-Shinozaki, K., & Shinozaki, K. (2022). Inter-tissue and inter-organ signaling in drought stress response and phenotyping of drought tolerance. *The Plant Journal*, *109*(2), 342–358. https://doi.org/10.1111/tpj.15619

Laloum, T., Martín, G., & Duque, P. (2018). Alternative Splicing Control of Abiotic Stress Responses. *Trends in Plant Science*, *23*(2), 140–150. https://doi.org/10.1016/j.tplants.2017.09.019

Li, H., & Chiu, C.-C. (2010). Protein Transport into Chloroplasts. *Annual Review of Plant Biology*, *61*(1), 157–180. https://doi.org/10.1146/annurev-arplant-042809-112222

Liu, S., Melonek, J., Boykin, L. M., Small, I., & Howell, K. A. (2013). PPR-SMRs: ancient proteins with enigmatic functions. *RNA Biology*, *10*(9), 1501–1510. https://doi.org/10.4161/rna.26172

Liu, X.-X., Guo, Q.-H., Xu, W.-B., Liu, P., & Yan, K. (2022). Rapid Regulation of Alternative Splicing in Response to Environmental Stresses. *Frontiers in Plant Science*, *13*. https://doi.org/10.3389/fpls.2022.832177

Manna, S. (2015). An overview of pentatricopeptide repeat proteins and their applications. *Biochimie*, *113*, 93–99. https://doi.org/10.1016/j.biochi.2015.04.004

Martin, W., Rujan, T., Richly, E., Hansen, A., Cornelsen, S., Lins, T., Leister, D., Stoebe, B., Hasegawa, M., & Penny, D. (2002). Evolutionary analysis of Arabidopsis, cyanobacterial, and chloroplast genomes reveals plastid phylogeny and thousands of cyanobacterial genes in the nucleus. *Proceedings of the National Academy of Sciences*, *99*(19), 12246–12251. https://doi.org/10.1073/pnas.182432999

McKibbin, R. S., Wilkinson, M. D., Bailey, P. C., Flintham, J. E., Andrew, L. M., Lazzeri, P. A., Gale, M. D., Lenton, J. R., & Holdsworth, M. J. (2002). Transcripts of Vp-1 homeologues are misspliced in modern wheat and ancestral species. *Proceedings of the National Academy of Sciences*, *99*(15), 10203–10208. https://doi.org/10.1073/pnas.152318599

References

Meierhoff, K., Felder, S., Nakamura, T., Bechtold, N., & Schuster, G. (2003). HCF152, an Arabidopsis RNA Binding Pentatricopeptide Repeat Protein Involved in the Processing of Chloroplast *psbB-psbT-psbH-petB-petD* RNAs. *The Plant Cell*, *15*(6), 1480–1495. https://doi.org/10.1105/tpc.010397

Mochizuki, N., Brusslan, J. A., Larkin, R., Nagatani, A., & Chory, J. (2001). Arabidopsis genomes uncoupled 5 (GUN5) mutant reveals the involvement of Mg-chelatase H subunit in plastid-to-nucleus signal transduction. *Proceedings of the National Academy of Sciences*, *98*(4), 2053–2058. https://doi.org/10.1073/pnas.98.4.2053

Mochizuki, N., Susek, R., & Chory, J. (1996). An Intracellular Signal Transduction Pathway between the Chloroplast and Nucleus Is Involved in De-Etiolation. *Plant Physiology*, *112*(4), 1465–1469. https://doi.org/10.1104/pp.112.4.1465

Mochizuki, N., Tanaka, R., Tanaka, A., Masuda, T., & Nagatani, A. (2008). The steady-state level of Mg-protoporphyrin IX is not a determinant of plastid-to-nucleus signaling in *Arabidopsis*. *Proceedings of the National Academy of Sciences*, *105*(39), 15184–15189. https://doi.org/10.1073/pnas.0803245105

Muhammad Aslam, M., Waseem, M., Jakada, B. H., Okal, E. J., Lei, Z., Saqib, H. S. A., Yuan, W., Xu, W., & Zhang, Q. (2022). Mechanisms of Abscisic Acid-Mediated Drought Stress Responses in Plants. *International Journal of Molecular Sciences*, *23*(3), 1084. https://doi.org/10.3390/ijms23031084

Mulo, P., Pursiheimo, S., Hou, C.-X., Tyystjärvi, T., & Aro, E.-M. (2003). Multiple effects of antibiotics on chloroplast and nuclear gene expression. *Functional Plant Biology*, *30*(11), 1097. https://doi.org/10.1071/FP03149

Nosalewicz, A., Okoń, K., & Skorupka, M. (2022). Non-Photochemical Quenching under Drought and Fluctuating Light. *International Journal of Molecular Sciences*, *23*(9), 5182. https://doi.org/10.3390/ijms23095182

Oldenburg, D. J., & Bendich, A. J. (2015). DNA maintenance in plastids and mitochondria of plants. *Frontiers in Plant Science*, *6*. https://doi.org/10.3389/fpls.2015.00883

Ostersetzer, O., Cooke, A. M., Watkins, K. P., & Barkan, A. (2005). CRS1, a Chloroplast Group II Intron Splicing Factor, Promotes Intron Folding through Specific Interactions with Two Intron Domains. *The Plant Cell*, *17*(1), 241–255. https://doi.org/10.1105/tpc.104.027516

O'Toole, N., Hattori, M., Andres, C., Iida, K., Lurin, C., Schmitz-Linneweber, C., Sugita, M., & Small, I. (2008). On the Expansion of the Pentatricopeptide Repeat Gene Family in Plants. *Molecular Biology and Evolution*, *25*(6), 1120–1128. https://doi.org/10.1093/molbev/msn057

Petrucelli, N., Daly, M. B., & Pal, T. (1993). *BRCA1- and BRCA2-Associated Hereditary Breast and Ovarian Cancer*.

References

Pogson, B. J., Woo, N. S., Förster, B., & Small, I. D. (2008). Plastid signalling to the nucleus and beyond. *Trends in Plant Science*, *13*(11), 602–609. https://doi.org/10.1016/j.tplants.2008.08.008

Qin, T., Zhao, P., Sun, J., Zhao, Y., Zhang, Y., Yang, Q., Wang, W., Chen, Z., Mai, T., Zou, Y., Liu, G., & Hao, W. (2021). Research Progress of PPR Proteins in RNA Editing, Stress Response, Plant Growth and Development. *Frontiers in Genetics*, *12*. https://doi.org/10.3389/fgene.2021.765580

Richter, A. S., Nägele, T., Grimm, B., Kaufmann, K., Schroda, M., Leister, D., & Kleine, T. (2023). Retrograde signaling in plants: A critical review focusing on the GUN pathway and beyond. *Plant Communications*, *4*(1), 100511. https://doi.org/10.1016/j.xplc.2022.100511

Richter, S., & Lamppa, G. K. (1998). A chloroplast processing enzyme functions as the general stromal processing peptidase. *Proceedings of the National Academy of Sciences*, *95*(13), 7463–7468. https://doi.org/10.1073/pnas.95.13.7463

Rogalski, M., Karcher, D., & Bock, R. (2008). Superwobbling facilitates translation with reduced tRNA sets. *Nature Structural & Molecular Biology*, *15*(2), 192–198. https://doi.org/10.1038/nsmb.1370

Ruckle, M. E., DeMarco, S. M., & Larkin, R. M. (2008). Plastid Signals Remodel Light Signaling Networks and Are Essential for Efficient Chloroplast Biogenesis in *Arabidopsis*. *The Plant Cell*, *19*(12), 3944–3960. https://doi.org/10.1105/tpc.107.054312

Saha, D., Prasad, A. M., & Srinivasan, R. (2007). Pentatricopeptide repeat proteins and their emerging roles in plants. *Plant Physiology and Biochemistry*, *45*(8), 521–534. https://doi.org/10.1016/j.plaphy.2007.03.026

Sato, S. (1999). Complete Structure of the Chloroplast Genome of Arabidopsis thaliana. *DNA Research*, *6*(5), 283–290. https://doi.org/10.1093/dnares/6.5.283

Schmitz-Linneweber, C., & Small, I. (2008). Pentatricopeptide repeat proteins: a socket set for organelle gene expression. *Trends in Plant Science*, *13*(12), 663–670. https://doi.org/10.1016/j.tplants.2008.10.001

Shavrukov, Y. (2024). Pathway to the Molecular Origins of Drought Escape and Early Flowering Illuminated via the Phosphorylation of SnRK2-Substrate 1 in *Arabidopsis*. *Plant And Cell Physiology*, *65*(2), 179–180. https://doi.org/10.1093/pcp/pcae004

Shavrukov, Y., Kurishbayev, A., Jatayev, S., Shvidchenko, V., Zotova, L., Koekemoer, F., de Groot, S., Soole, K., & Langridge, P. (2017). Early Flowering as a Drought Escape Mechanism in Plants: How Can It Aid Wheat Production? *Frontiers in Plant Science*, *8*. https://doi.org/10.3389/fpls.2017.01950

Shields, D. C., & Wolfe, K. H. (1997). Accelerated evolution of sites undergoing mRNA editing in plant mitochondria and chloroplasts. *Molecular Biology and Evolution*, *14*(3), 344–349. https://doi.org/10.1093/oxfordjournals.molbev.a025768

Small, I., Melonek, J., Bohne, A.-V., Nickelsen, J., & Schmitz-Linneweber, C. (2023). Plant organellar RNA maturation. *The Plant Cell*, *35*(6), 1727–1751. https://doi.org/10.1093/plcell/koad049

Staiger, D., & Brown, J. W. S. (2013). Alternative Splicing at the Intersection of Biological Timing, Development, and Stress Responses. *The Plant Cell*, *25*(10), 3640–3656. https://doi.org/10.1105/tpc.113.113803

Stegemann, S., Keuthe, M., Greiner, S., & Bock, R. (2012). Horizontal transfer of chloroplast genomes between plant species. *Proceedings of the National Academy of Sciences*, *109*(7), 2434–2438. https://doi.org/10.1073/pnas.1114076109

Strand, D. D., Fisher, N., & Kramer, D. M. (2017). The higher plant plastid NAD(P)H dehydrogenase-like complex (NDH) is a high efficiency proton pump that increases ATP production by cyclic electron flow. *Journal of Biological Chemistry*, *292*(28), 11850–11860. https://doi.org/10.1074/jbc.M116.770792

Sugiura, M. (1992). The chloroplast genome. *Plant Molecular Biology*, *19*(1), 149–168. https://doi.org/10.1007/BF00015612

Sun, X., Feng, P., Xu, X., Guo, H., Ma, J., Chi, W., Lin, R., Lu, C., & Zhang, L. (2011). A chloroplast envelope-bound PHD transcription factor mediates chloroplast signals to the nucleus. *Nature Communications*, *2*(1), 477. https://doi.org/10.1038/ncomms1486

Sun, Y., Li, J., Zhang, L., & Lin, R. (2023). Regulation of chloroplast protein degradation. *Journal of Genetics and Genomics*, *50*(6), 375–384. https://doi.org/10.1016/j.jgg.2023.02.010

Susek, R. E., Ausubel, F. M., & Chory, J. (1993). Signal transduction mutants of Arabidopsis uncouple nuclear CAB and RBCS gene expression from chloroplast development. *Cell*, *74*(5), 787–799. https://doi.org/10.1016/0092-8674(93)90459-4

Tadini, L., Pesaresi, P., Kleine, T., Rossi, F., Guljamow, A., Sommer, F., Mühlhaus, T., Schroda, M., Masiero, S., Pribil, M., Rothbart, M., Hedtke, B., Grimm, B., & Leister, D. (2016). GUN1 Controls Accumulation of the Plastid Ribosomal Protein S1 at the Protein Level and Interacts with Proteins Involved in Plastid Protein Homeostasis. *Plant Physiology*, *170*(3), 1817–1830. https://doi.org/10.1104/pp.15.02033

Takahashi, F., Kuromori, T., Urano, K., Yamaguchi-Shinozaki, K., & Shinozaki, K. (2020a). Drought Stress Responses and Resistance in Plants: From Cellular Responses to Long-Distance Intercellular Communication. *Frontiers in Plant Science*, *11*. https://doi.org/10.3389/fpls.2020.556972

References

Takahashi, F., Kuromori, T., Urano, K., Yamaguchi-Shinozaki, K., & Shinozaki, K. (2020b). Drought Stress Responses and Resistance in Plants: From Cellular Responses to Long-Distance Intercellular Communication. *Frontiers in Plant Science*, *11*. https://doi.org/10.3389/fpls.2020.556972

Terry, M. J., & Smith, A. G. (2013). A model for tetrapyrrole synthesis as the primary mechanism for plastid-to-nucleus signaling during chloroplast biogenesis. *Frontiers in Plant Science*, *4*. https://doi.org/10.3389/fpls.2013.00014

Thatcher, S. R., Danilevskaya, O. N., Meng, X., Beatty, M., Zastrow-Hayes, G., Harris, C., Van Allen, B., Habben, J., & Li, B. (2016). Genome-Wide Analysis of Alternative Splicing during Development and Drought Stress in Maize. *Plant Physiology*, *170*(1), 586–599. https://doi.org/10.1104/pp.15.01267

Tiller, N., & Bock, R. (2014). The Translational Apparatus of Plastids and Its Role in Plant Development. *Molecular Plant*, *7*(7), 1105–1120. https://doi.org/10.1093/mp/ssu022

Van den Broeck, G., Timko, M. P., Kausch, A. P., Cashmore, A. R., Van Montagu, M., & Herrera-Estrella, L. (1985). Targeting of a foreign protein to chloroplasts by fusion to the transit peptide from the small subunit of ribulose 1,5-bisphosphate carboxylase. *Nature*, *313*(6001), 358–363. https://doi.org/10.1038/313358a0

Vasileuskaya, Z., Oster, U., & Beck, C. F. (2005). Mg-Protoporphyrin IX and Heme Control HEMA, the Gene Encoding the First Specific Step of Tetrapyrrole Biosynthesis, in Chlamydomonas reinhardtii. *Eukaryotic Cell*, *4*(10), 1620–1628. https://doi.org/10.1128/EC.4.10.1620-1628.2005

Wang, X., An, Y., Xu, P., & Xiao, J. (2021). Functioning of PPR Proteins in Organelle RNA Metabolism and Chloroplast Biogenesis. *Frontiers in Plant Science*, *12*. https://doi.org/10.3389/fpls.2021.627501

Woodson, J. D., Perez-Ruiz, J. M., & Chory, J. (2011). Heme Synthesis by Plastid Ferrochelatase I Regulates Nuclear Gene Expression in Plants. *Current Biology*, *21*(10), 897–903. https://doi.org/10.1016/j.cub.2011.04.004

Wu, G.-Z., & Bock, R. (2021). GUN control in retrograde signaling: How GENOMES UNCOUPLED proteins adjust nuclear gene expression to plastid biogenesis. *The Plant Cell*, *33*(3), 457–474. https://doi.org/10.1093/plcell/koaa048

Wu, G.-Z., Chalvin, C., Hoelscher, M., Meyer, E. H., Wu, X. N., & Bock, R. (2018). Control of Retrograde Signaling by Rapid Turnover of GENOMES UNCOUPLED1. *Plant Physiology*, *176*(3), 2472–2495. https://doi.org/10.1104/pp.18.00009

Xing, H., Fu, X., Yang, C., Tang, X., Guo, L., Li, C., Xu, C., & Luo, K. (2018). Genome-wide investigation of pentatricopeptide repeat gene family in poplar and their expression analysis in response to biotic and abiotic stresses. *Scientific Reports*, *8*(1), 2817. https://doi.org/10.1038/s41598-018-21269-1

Yagi, Y., & Shiina, T. (2014). Recent advances in the study of chloroplast gene expression and its evolution. *Frontiers in Plant Science*, *5*. https://doi.org/10.3389/fpls.2014.00061

References

Yamaguchi, K., & Subramanian, A. R. (2000). The Plastid Ribosomal Proteins. *Journal of Biological Chemistry*, *275*(37), 28466–28482. https://doi.org/10.1074/jbc.M005012200

Zeng, C., Jiao, Q., Jia, T., & Hu, X. (2022). Updated Progress on Group II Intron Splicing Factors in Plant Chloroplasts. *Current Issues in Molecular Biology*, *44*(9), 4229–4239. https://doi.org/10.3390/cimb44090290

Zhang, Y., & Lu, C. (2019). The Enigmatic Roles of PPR-SMR Proteins in Plants. *Advanced Science*, *6*(13). https://doi.org/10.1002/advs.201900361

Zhao, X., Huang, J., & Chory, J. (2018). genome uncoupled1 Mutants Are Hypersensitive to Norflurazon and Lincomycin. *Plant Physiology*, *178*(3), 960–964. https://doi.org/10.1104/pp.18.00772

Zhao, X., Huang, J., & Chory, J. (2019). GUN1 interacts with MORF2 to regulate plastid RNA editing during retrograde signaling. *Proceedings of the National Academy of Sciences*, *116*(20), 10162–10167. https://doi.org/10.1073/pnas.1820426116

Zoschke, R., & Bock, R. (2018). Chloroplast Translation: Structural and Functional Organization, Operational Control, and Regulation. *The Plant Cell*, *30*(4), 745–770. https://doi.org/10.1105/tpc.18.00016

Zou, W., Yu, Q., Ma, Y., Sun, G., Feng, X., & Ge, L. (2024). Pivotal role of heterotrimeric G protein in the cstalk between sugar signaling and abiotic stress response in plants. *Plant Physiology and Biochemistry*, *210*, 108567. https://doi.org/10.1016/j.plaphy.2024.108567

Supplemental information

Supplemental information – Chapter 1

Plant Communications, Volume *5*

GENOMES UNCOUPLED PROTEIN1 binds to plastid RNAs and promotes their maturation

Qian Tang, Duorong Xu, Benjamin Lenzen, Andreas Brachmann, Madhura M. Yapa, Paymon Doroodian, Christian Schmitz-Linneweber, Tatsuru Masuda, Zhihua Hua, Dario Leister, and Tatjana Kleine

GENOMES UNCOUPLED PROTEIN1 binds to plastid RNAs and promotes their maturation

Qian Tang[a], Duorong Xu[a], Benjamin Lenzen[b], Andreas Brachmann[c], Madhura M Yapa[d], Paymon Doroodian[d], Christian Schmitz-Linneweber[b], Tatsuru Masuda[e], Zhihua Hua[d], Dario Leister[a], Tatjana Kleine[a,*]

[a]Plant Molecular Biology (Botany), Faculty of Biology, Ludwig-Maximilians-University München, 82152 Martinsried, Germany
[b]Molecular Genetics, Humboldt-University Berlin, Philippstr. 13, 10115 Berlin, Germany
[c]Biocenter of the LMU Munich, Genetics Section, Grosshaderner Str. 2-4, 82152 Planegg-Martinsried, Germany
[d]Department of Environmental and Plant Biology, Ohio University, Athens, Ohio 45701, United States
[e]Graduate School of Arts and Sciences, The University of Tokyo, Komaba, Meguro-ku, 153-8902 Tokyo, Japan

[*]Corresponding author:
Tatjana Kleine
e-mail: tatjana.kleine@lmu.de

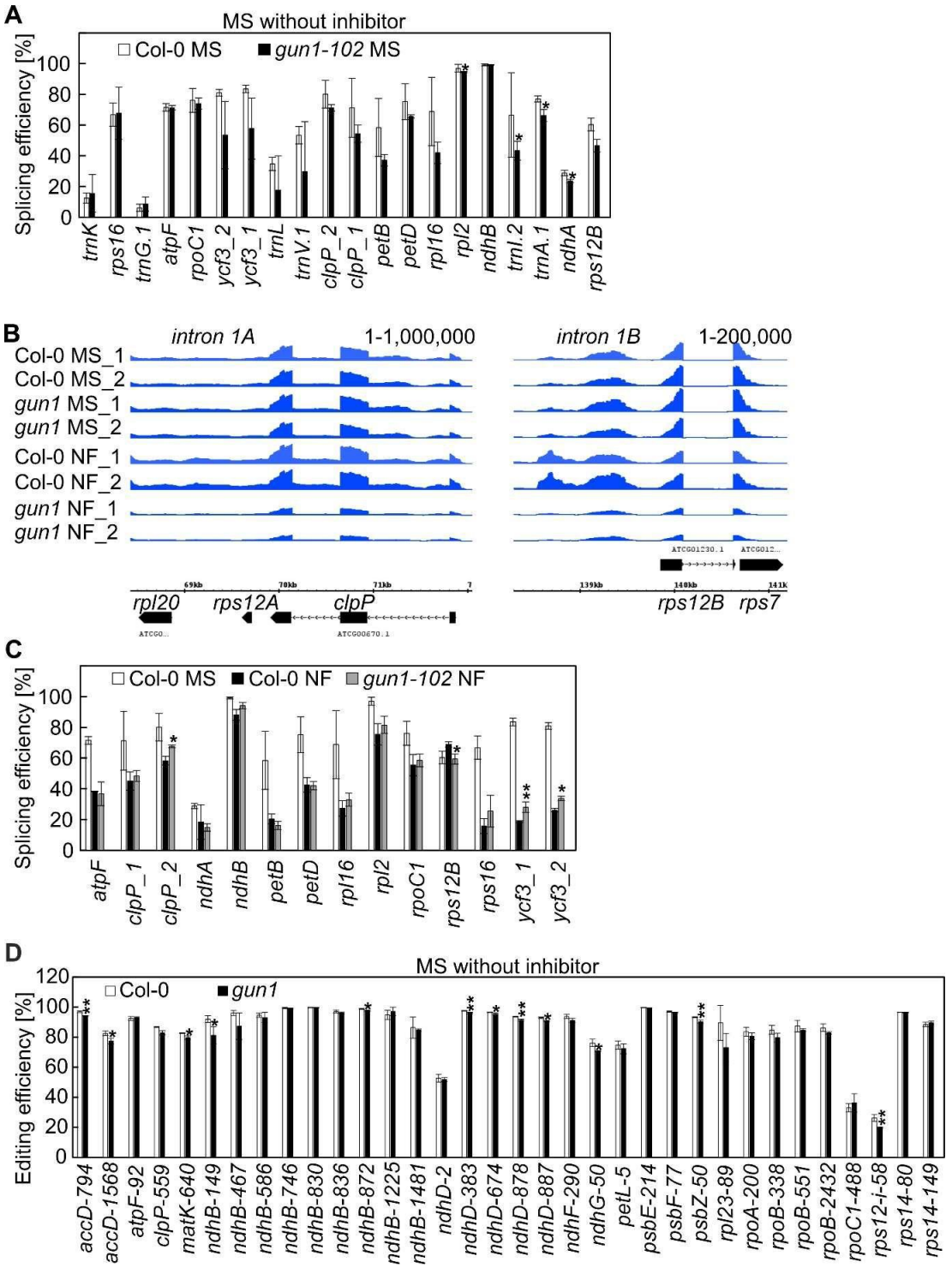
A
MS without inhibitor
Col-0 MS
gun1-102 MS
Splicing efficiency [%]
trnK
rps16
trnG.1
atpF
rpoC1
ycf3_2
ycf3_1
trnL
trnV.1
clpP_2
clpP_1
petB
petD
rpl16
rpl2
ndhB
trnI.2
trnA.1
ndhA
rps12B
B
intron 1A
1-1,000,000
intron 1B
1-200,000
Col-0 MS_1
Col-0 MS_2
gun1 MS_1
gun1 MS_2
Col-0 NF_1
Col-0 NF_2
gun1 NF_1
gun1 NF_2
rpl20
rps12A
clpP
rps12B
rps7
C
Col-0 MS
Col-0 NF
gun1-102 NF
Splicing efficiency [%]
atpF
clpP_1
clpP_2
ndhA
ndhB
petB
petD
rpl16
rpl2
rpoC1
rps12B
rps16
ycf3_1
ycf3_2
D
MS without inhibitor
Col-0
gun1
Editing efficiency [%]
accD-794
accD-1568
atpF-92
clpP-559
matK-640
ndhB-149
ndhB-467
ndhB-586
ndhB-746
ndhB-830
ndhB-836
ndhB-872
ndhB-1225
ndhB-1481
ndhD-2
ndhD-383
ndhD-674
ndhD-878
ndhD-887
ndhF-290
ndhG-50
petL-5
psbE-214
psbF-77
psbZ-50
rpl23-89
rpoA-200
rpoB-338
rpoB-551
rpoB-2432
rpoC1-488
rps12-i-58
rps14-80
rps14-149

Supplemental Figure 1. GUN1 does not play a significant role in plastid RNA editing or splicing under normal growth conditions.

(A) RNA splicing efficiencies of 4-day-old Col-0 and *gun1-102* seedlings grown on MS were determined using previously published RNA-Seq data (Habermann et al., 2020). These sequencing data were generated to allow for detection of organellar transcripts. Mean values ± SD were obtained from three independent experiments. Statistically significant differences between Col-0 MS and *gun1-102* MS are indicated (post-hoc Tukey HSD test; **P* < 0.05).
(B) Snapshots across the *clpP* gene and intron 1B of *rps12B.* The read depths were visualized with the Integrated Genome Browser. Intron 1 of *rps12* is transcribed from two separate chromosomal regions: one downstream of *rps12A* and the other upstream of *rps12B.* They are then spliced together in trans. Therefore, we conducted a manual investigation of this intron using coverage files from the sequencing data.
(C) RNA splicing efficiencies of 4-day-old Col-0 and *gun1-102* seedlings grown on MS and norflurazon (NF) were determined using previously published RNA-Seq data (Habermann et al., 2020). These sequencing data were generated to allow for detection of organellar transcripts. Mean values ± SD were obtained from three independent experiments. Statistically significant differences between Col-0 NF and *gun1-102* NF are indicated (post-hoc Tukey HSD test; **P* < 0.05, ***P* < 0.01). Due to the numerous modifications, structure and small size of tRNAs, the lncRNA-Seq library preparation method is not reliable for their detection. Hence, the splicing efficiency data for the six tRNA introns have to be viewed with caution and were excluded from further analysis.
(D) RNA editing efficiencies were calculated from data described in **(A)**.

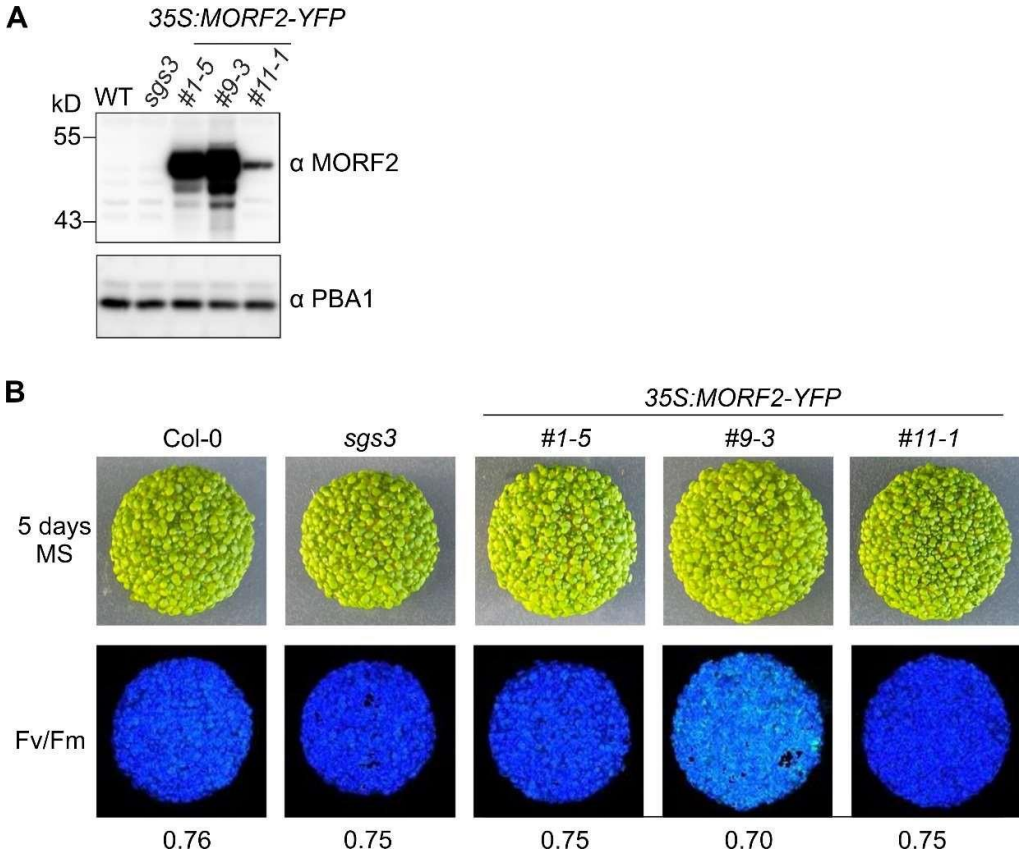

Supplemental Figure 2. Characterization of *35S:MORF2-YFP* lines.
(A) Immunoblot analysis showing protein levels of MORF2-YFP in three overexpression transgenic lines (*35S:MORF2-YFP*). Total proteins from 7-d-old seedlings were directly extracted in 2 x SDS sample buffer and denatured at 95°C for 6 min before being resolved on a 10% SDS-PAGE gel. MORF2-YFP was detected with an anti-MORF2 polyclonal antibody as described in (Yapa et al., 2023). The 20S proteasome subunit PBA1 was used to verify nearly equal loading of total protein. The three lines, *35S-MORF2-YFP #1-5*, *#9-3* and *#11-1*, were selected for further analysis as they exhibit *MORF2* overexpression to varying degrees.
(B) Phenotypes and Fv/Fm Imaging PAM pictures of 5-day-old Col-0, *sgs3-1* and *35S:MORF2-YFP* lines grown on MS medium without inhibitor supplementation.

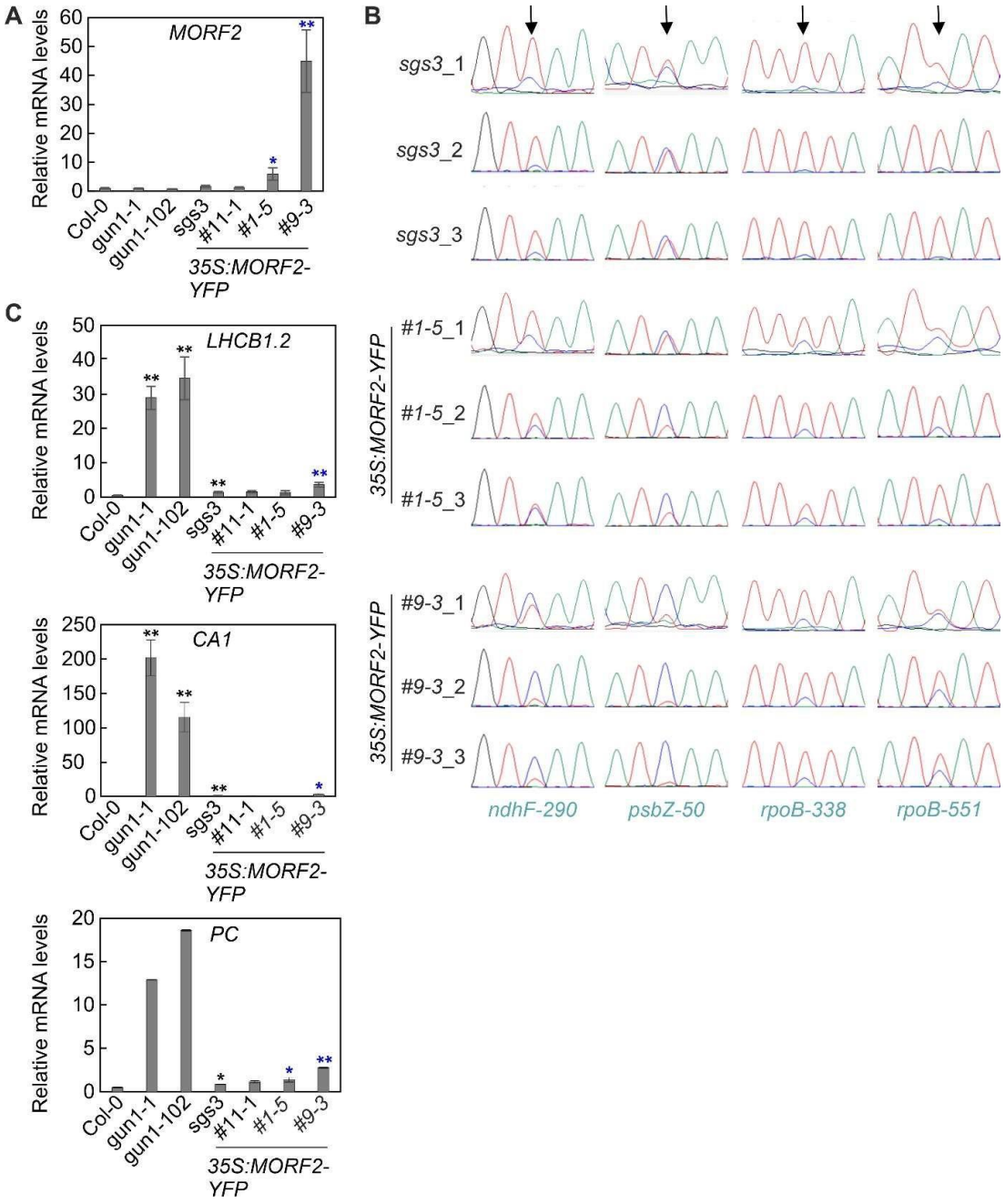

Supplemental Figure 3. Overexpression of MORF2 does not result in a significant *gun* phenotype.

(A) RT-qPCR of *MORF2* expression in 5-day-old seedlings grown under norflurazon (NF) conditions. The results were normalized to *AT4G36800*, which encodes a RUB1-conjugating enzyme (RCE1). Expression values are reported relative to the corresponding transcript levels in Col-0, which were set to 1. Mean values ± SE were derived from three independent experiments, each performed with three technical replicates per sample. Statistically significant differences (post-hoc Tukey HSD test; **P* < 0.05; ***P* < 0.01) between Col-0, *gun1* and *sgs3-1* mutants are indicated by black asterisks, and those between *sgs3-1* and the *35S:MORF2-YFP* lines are indicated by blue asterisks.

(B) Seedlings were grown as in (A). Editing efficiency of selected sites was visualized by Sanger sequencing for three biological replicates.
(C) RT-qPCR of *LHCB1.2*, *CARBONIC ANHYDRASE 1* (*CA1*), and *PLASTOCYANIN* (*PC*) was performed using the identical cDNAs as in (A).

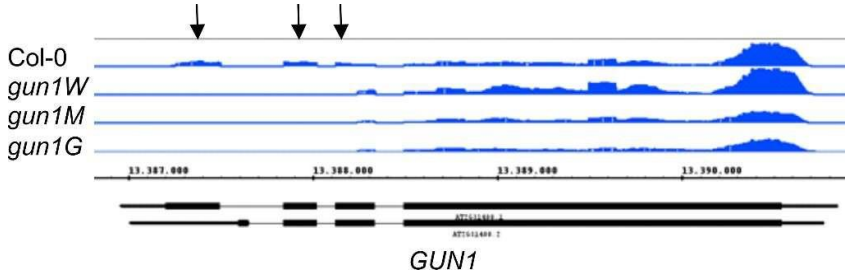

Supplemental Figure 4. Validation of RNA-Seq data and the *gun1-102* allele.
A snapshot across the *GUN1* gene is shown. The read depths were visualized with the Integrated Genome Browser. Arrows point to the absence of reads in a portion of exon 2 and the subsequent exons in *gun1W*, *gun1M*, and *gun1G*. The absence of transcription in a portion of exon 2 and subsequent exons of the *GUN1* gene was verified in all *gun1* mutant seedlings, confirming the T-DNA insertion in all *gun1* seedlings and validating the RNA-Seq data.

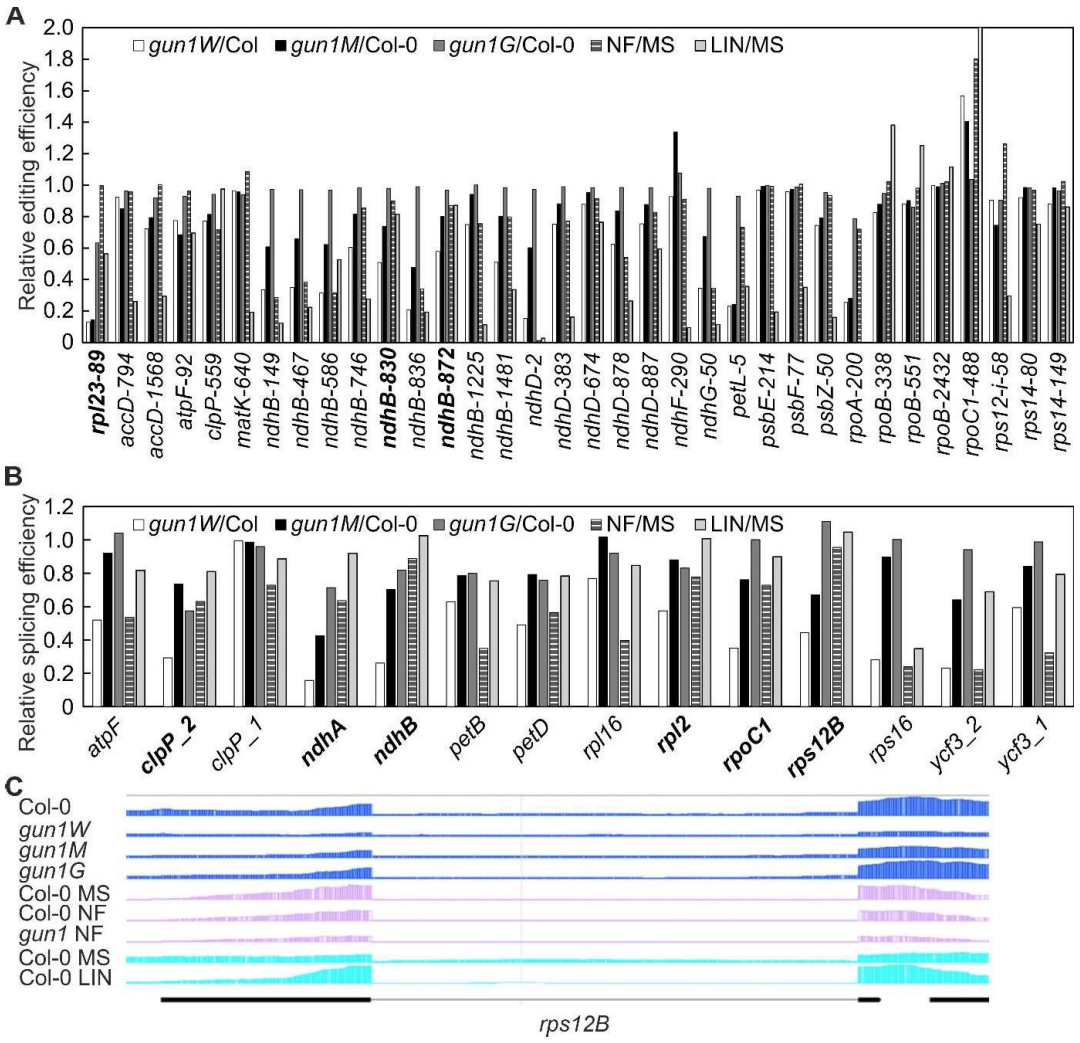

Supplemental Figure 5. Analysis of editing and splicing efficiencies of *gun1W*, *gun1M* and *gun1G* seedlings in comparison to seedlings grown on norflurazon (NF) and lincomycin (LIN).

A, B) RNA editing **(A)** and splicing **(B)** ratios of 4-day-old white (*gun1W*), marble (*gun1M*), and green (*gun1G*) *gun1-102* seedlings compared to Col-0 (Col), and ratios of seedlings grown on norflurazon (NF) or lincomycin (LIN) compared to seedlings grown on MS. The NF, LIN, and MS data were extracted from previously published RNA-Seq data (Habermann et al., 2020). We identified loci in which the relative ratio of editing or splicing was lower in *gun1W*/Col-0, progressively rescued in *gun1M*/Col-0 and *gun1G*/Col-0, and absent in NF/MS or LIN/MS. Concerning editing changes, the *ndhB-830* and *ndhB-872* editing sites were weak candidates, while *rpl23-89* was a stronger candidate. However, the editing efficiency of *rpl23* is reduced under stresses (Xu et al., 2023), speaking for a pleiotropic effect. Additionally, editing of *rpl23* was not progressively restored in *gun1M* seedlings. Regarding splicing alterations, potential affected loci included *ndhA*, *ndhB*, *rpoC1*, *rps12B*, *clpP_1* (no progressive rescue observed for *clpP_1*), and *rpl2* (weak; see fig. S7).

(C) Snapshots across the *rps12B* gene. The read depths were visualized with the Integrated Genome Browser. Splicing for *rps12B* was still observed, and notably, *rps12B* transcripts were largely decreased.

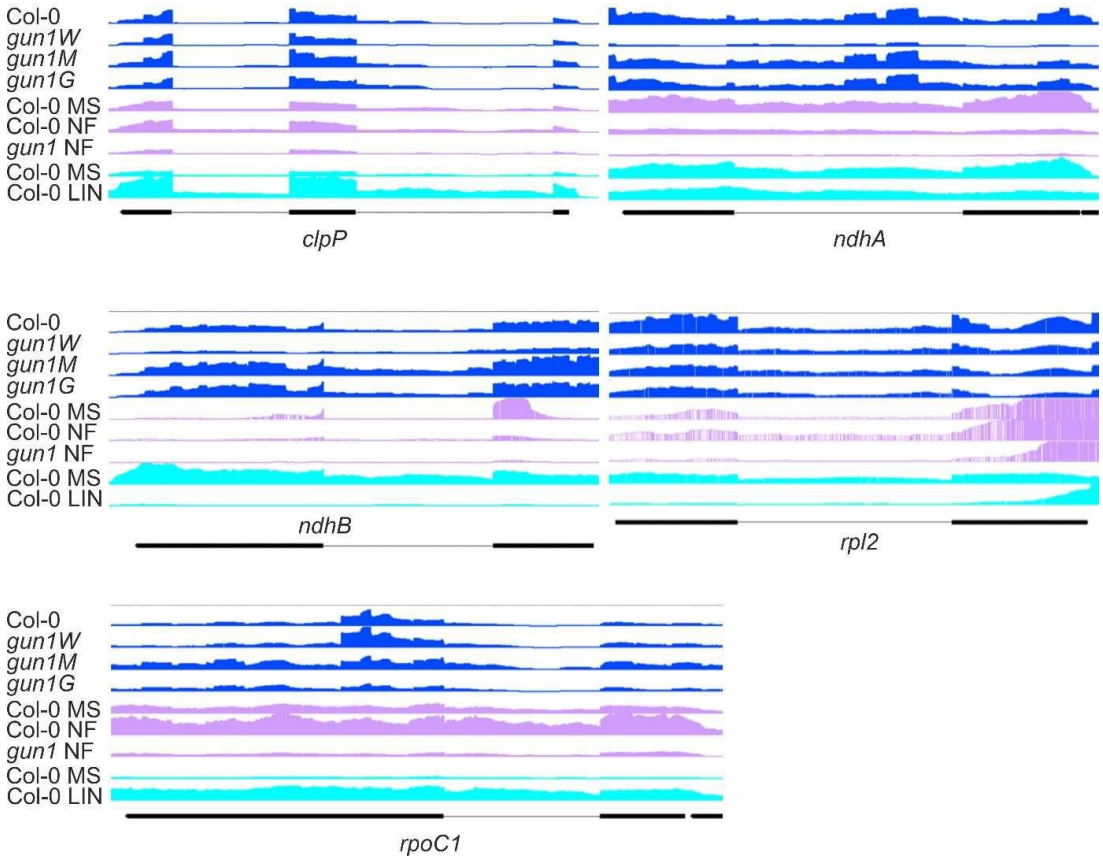

Supplemental Figure 6. Illustration of splicing behavior of selected transcripts.
Snapshots across the *clpP*, *ndhA*, *ndhB*, rpl2, and *rpoC1* genes are shown. The read depths were visualized with the Integrated Genome Browser.

A

ID	Gene	*gun1W*	*gun1M*	*gun1G*	NF	LIN	Pred. target of GUN1
ATCG00360	*ycf3*	0.42	1.30	1.10	0.66	0.99	no
ATCG00380	*rps4*	0.48	1.05	0.96	0.83	0.79	no
ATCG00500	*accD*	0.46	0.85	0.80	0.65	0.71	no
ATCG00520	*ycf4*	0.31	0.94	1.04	0.50	0.79	yes
ATCG00640	*rpl33*	0.38	0.85	0.97	0.55	0.87	no
ATCG00660	*rpl20*	0.45	0.68	0.77	0.76	2.42	yes
ATCG00740	*rpoA*	0.28	0.74	1.03	0.99	1.85	no
ATCG00750	*rps11*	0.24	0.72	1.14	1.13	2.02	no
ATCG00760	*rpl36*	0.22	0.78	1.30	1.11	2.30	no
ATCG00770	*rps8*	0.17	0.50	0.99	1.21	2.37	no
ATCG00780	*rpl14*	0.15	0.43	0.99	0.74	1.79	no
ATCG00790	*rpl16*	0.13	0.32	0.77	0.73	1.70	no
ATCG00800	*rps3*	0.19	0.63	1.29	0.98	1.44	no
ATCG00810	*rpl22*	0.17	0.43	0.93	1.07	1.41	no
ATCG00820	*rps19*	0.25	0.42	0.58	1.12	1.53	no
ATCG01120	*rps15*	0.42	0.96	0.97	0.68	1.96	no

B

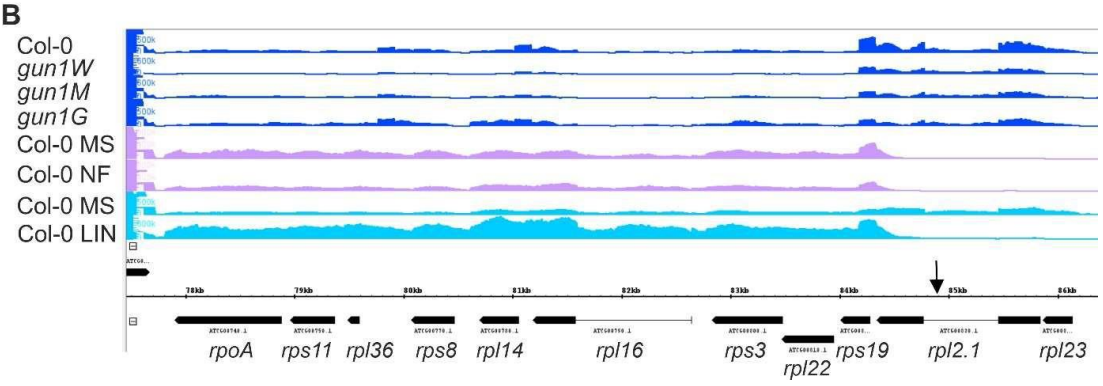

Supplemental Figure 7. GUN1 deficiency has a significant impact on the entire chloroplast transcriptome.

(A) Fold changes of transcripts that are exclusively reduced in *gun1W* are shown. n.d. denotes that these transcripts were not detected in the RNA-Seq analysis; red., reduced

(B) Coverage plots depict the accumulation of reads across the indicated gene cluster.

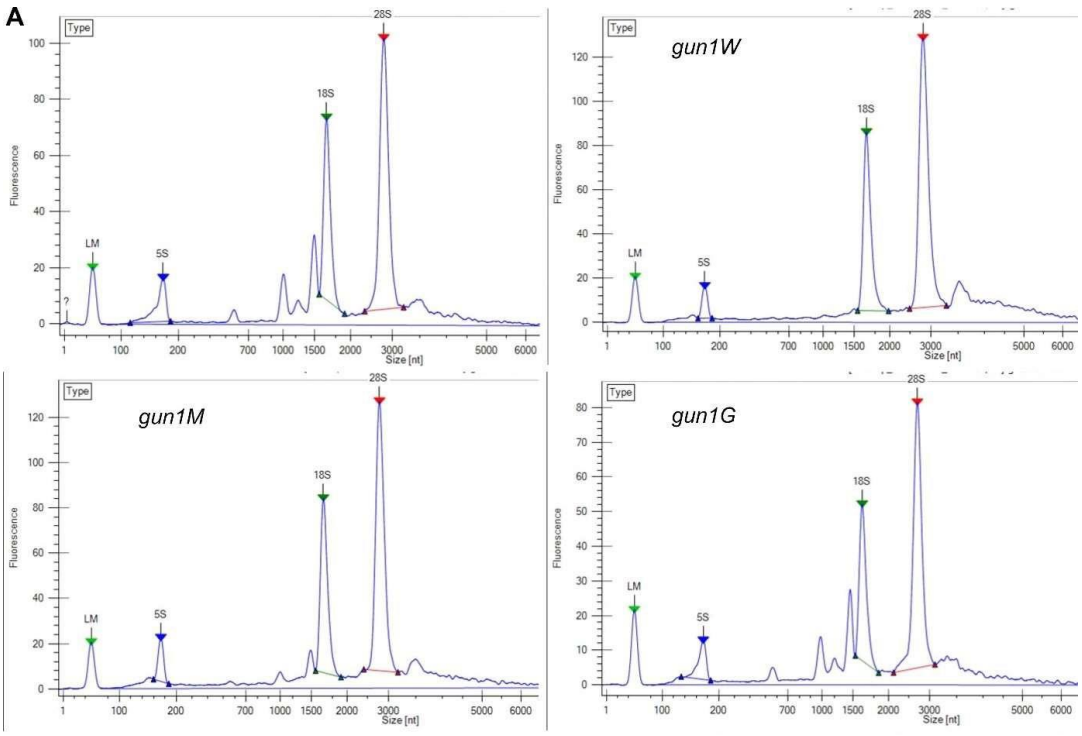

Supplemental Figure 8. Bioanalyzer profiles of total RNAs prepared with the RNA 6000 Nano Kit (Agilent).

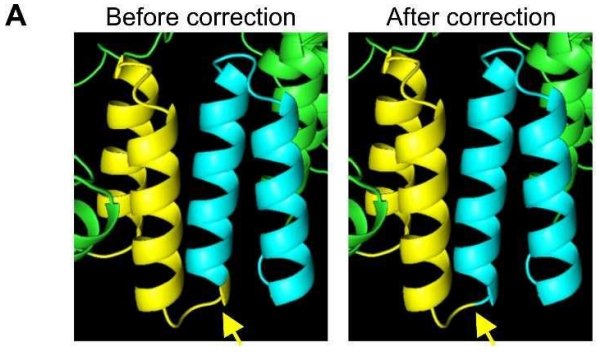

Supplemental Figure 9. PPR domain modeling of the GUN1 protein.
Section of PPR domain modeling of the GUN1 protein. The 12 predicted PPR domains of GUN1 by ScanProsite and the PPR CODE PREDICTION WEB SERVER (http://yinlab.hzau.edu.cn/pprcode; Yan et al., 2019) differ by a shift of one amino acid. Since the correct PPR code is crucial for determining the binding sequence, we investigated the structural configuration of the GUN1 protein by modeling with PyMOL. Each PPR domain was marked with a unique color for easy differentiation and visualization. Notably, within this color- coded scheme, helix b (yellow) of the initial PPR domain is observed to extend beyond (marked with an arrow) helix a (turquoise) of the subsequent PPR domain.

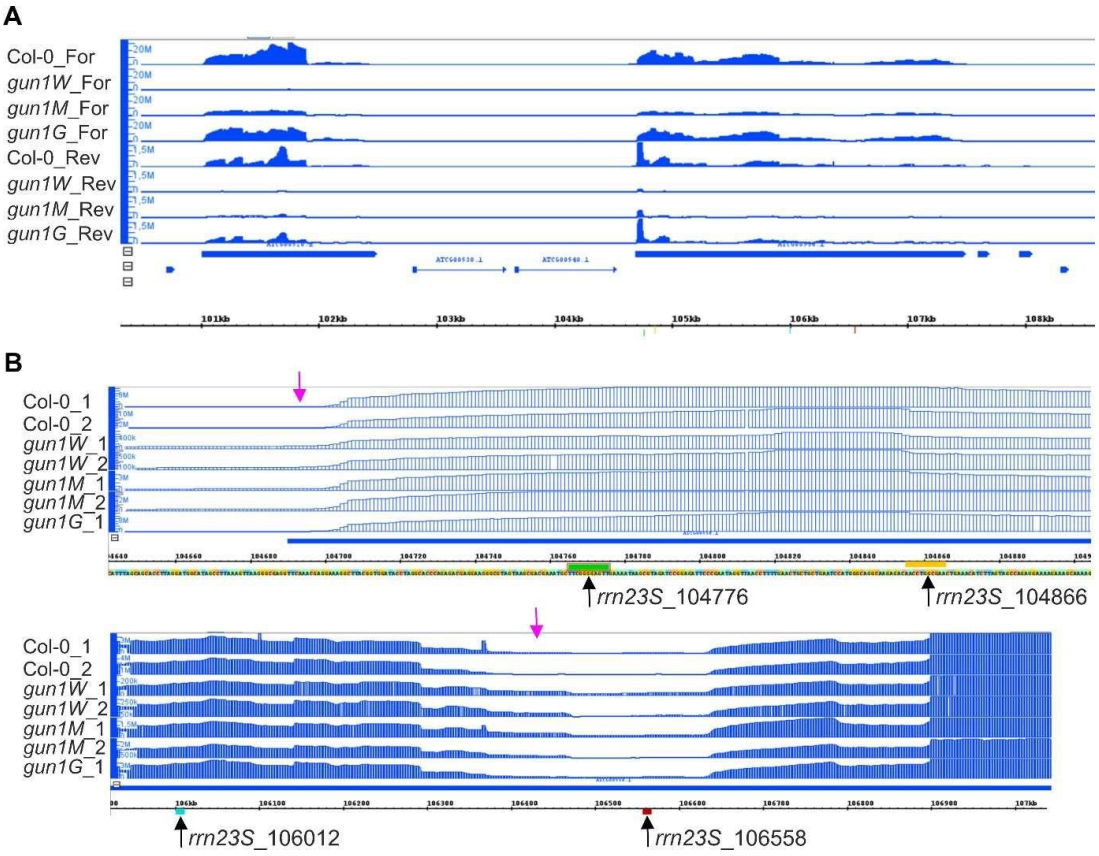

Supplemental Figure 10. Plastid ribosomal RNAs are significantly reduced in *gun1W* and *gun1M* seedlings.

(A) Read depths across the ribosomal operon were visualized using the Integrated Genome Browser. Note that this sequencing technique does not reliably capture tRNAs.

(B) Plots of RNA-Seq data produced without rRNA depletion depict a proportional increase in reads in *gun1W* and *gun1M* that map to 23S ribosomal RNA regions (magenta arrows) close to the four predicted GUN1 binding sites (marked with black arrows).

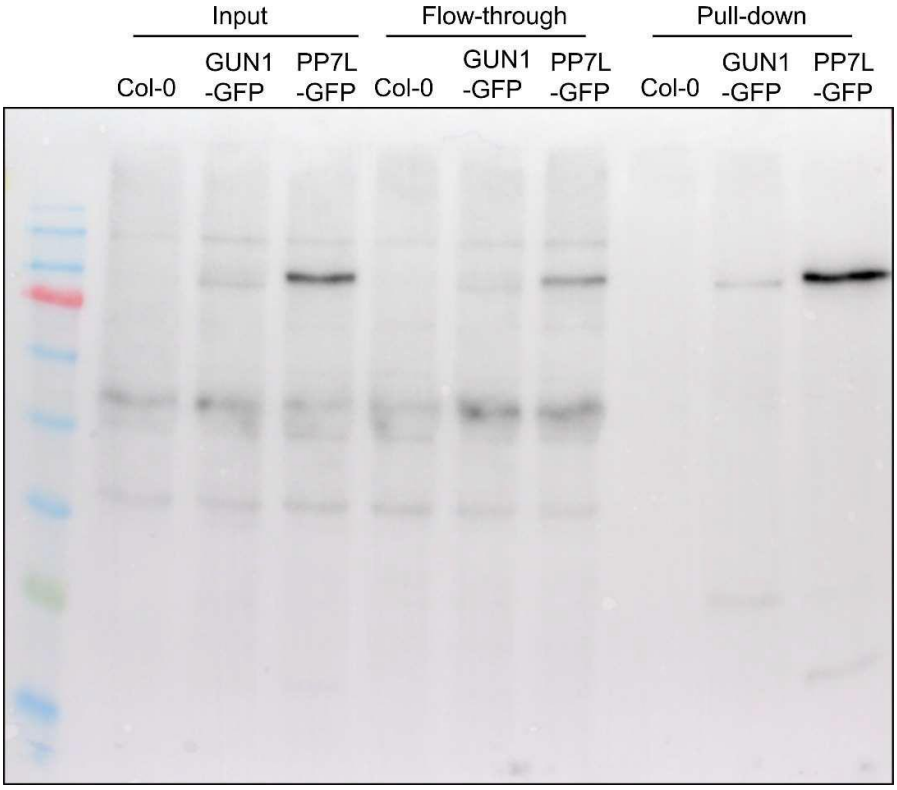

Supplemental Figure 11. Immunoblot analysis for the validation of the GUN1 RIP experiment.
Immunoblot analysis of proteins isolated from the input, flow-through and pellet (pull-down) fractions of the RIP experiment performed with proteins isolated from 4-day-old Col-0, *35S:GUN1-GFP*, and *35S:PP7L-GFP* seedlings. Proteins were fractionated by SDS-PAGE, and blots were probed with an antibody detecting GFP.

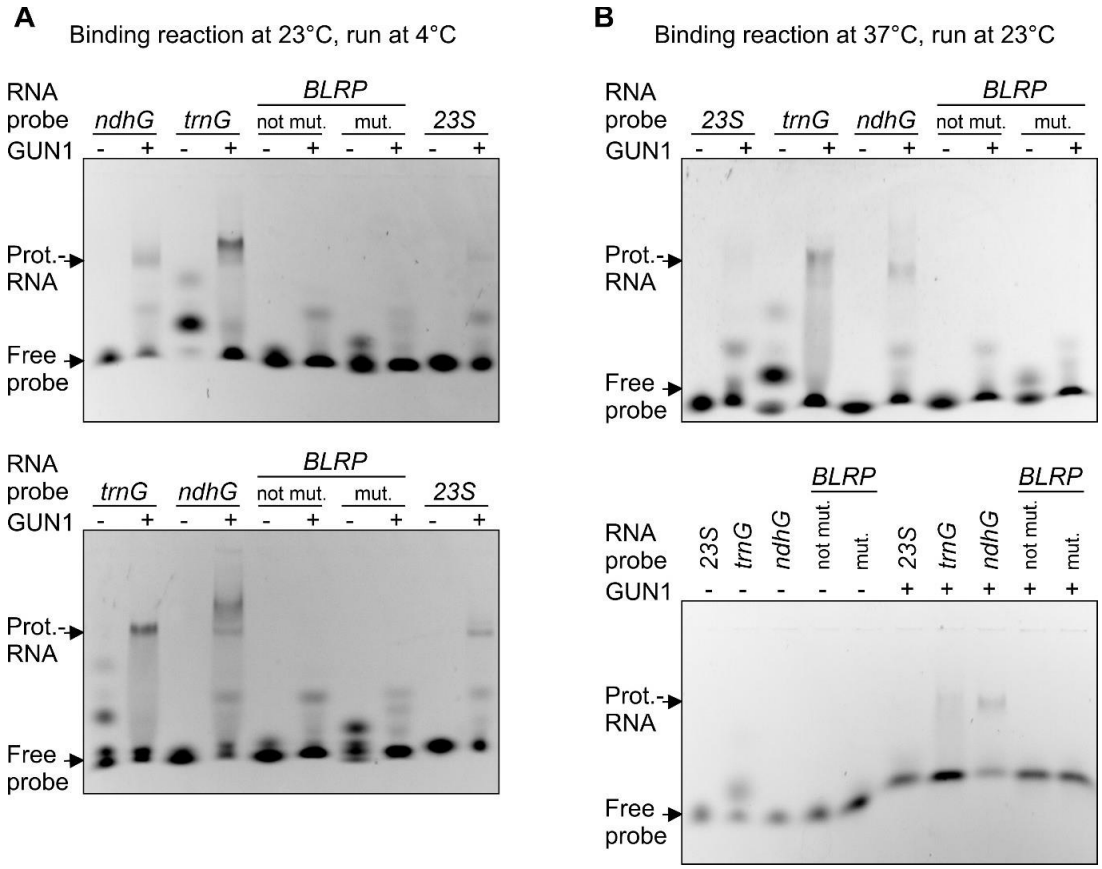

Supplemental Figure 12. EMSA experiments to test for GUN1 binding at the *BLRP*.
(A) EMSAs were performed with purified His-tagged GUN1 protein that was produced in *E. coli*. Aliquots (0, and 800 nM) of purified GUN1 protein were incubated with Cy5-labeled ssRNA probes representing the putative target sequences and a *BLRP* probe containing 10 mutated sites (mut.). Binding reactions were performed at 23°C, followed by electrophoresis on nondenaturing TBE polyacrylamide gels at 4°C.
(B) EMSAs were performed as in panel (A), but binding reactions were performed at 37°C, followed by electrophoresis on nondenaturing TBE polyacrylamide gels at 23°C.

Supplemental Table 7. Primers used in this study.

AGI number	Description	Primer sequence (from 5' to 3')
RT-qPCR		
AT4G36800	"Housekeeping" gene RCE1	CTGTTCACGGAACCCAATTC
		GGAAAAAGGTCTGACCGACA
AT2G33430	MORF2	ATGGCTTTGCCTTTGTCTG
		AACCTGACCGGTTAGCTC
AT1G29910	LHCB1.2	CCGTGAGCTAGAAGTTATCC
		GTTTCCCAAGTAATCGAGTCC
AT3G01500	CA1	GAGAAATACGAAACCAACCCT
		ACATAAGCCCTTTGATCCCA
AT1G67100	PC1	CAACGCAGGGTTCCCACAT

	(Primer combination used by Zhao et al. (2019))	CGCACAATAGAAACCGTAAGAGC
ATCG00730	petD	TCAAATACTTCGTACAGTGCCT
		TTGCTCCAATACCTAACCACAG
ATCG00790	rpl16	GACAAACCAGTTACAGTAAGACCT
		ACACCACCCATTTCATAAAGGA
ATCG00660	rpl20	CTTACACGAACTATGACTCAACAG
		TACGGCATTTATTCGAGTGATCC
ATCG00650	rps18	TTATCTAGACGGGTGAATAGAGTG
		TAAGACTAGTAGTTCTAGGAGTCG
ATCG00830	rpl2	CAGCATCATTGTGGTAAAGGT
		GCATATCGGTCAAAGGTAGG
AT2G31400	GUN1	GTCTTGAGTATATTGACTGGCTG
		GAGGCTGTAAAGCAAACGAC
ATCG00270	BLRP	ACCCATCGAATCATGACTATATCC
		AGAGATATCGACGGATTTCCT
Editing detection by Sanger sequencing		
ATCG00670	clpP_559	AATGATCCATCAACCCGC
		ATTGAACCGCTACAAGATC
ATCG00300	psbZ_50	GGGATTCGAACCCTCGATAG
		TCAAGTTCCATAAGTTCGACCC
ATCG00180	rpoC1_448 (same like Zhao et al. (2019))	TTTTCTTTTGCTAGGCCCATAA
		TTCGCAAATCTAAATCGGCT
ATCG00190	rpoB_338_and_551	TATCGGTTTATTGATCAGGG
		GCAGCTGCTAACACATCTC
ATCG00890	ndhB_467	TGCTTCTCTTCGATGGAAG
		TCCTTCGTATACGTCAGG
ATCG01010	ndhF_290	ACTGCCAGTTATCCAATAAAGAC
		TCATCCCTTTCATTCCACTTC
ATCG00065	rps12_-58	TGATTAGGTCATTTACCCTG
		AAATACAAGACAGCCAATCC
Editing detection by amplicon sequencing		
ATCG00670	clpP_559	TCTTGGAAGCGGAAGAATTACT
		TGAACCGCTACAAGATCAAC
ATCG00300	psbZ_50	CCACCAAGAAGACTAATCCAATCC
		GCTTTCCAATTGGCAGTTTTTG
ATCG00180	rpoC1_448	AGAAGGCCTAGTATACTGCGA
		TAATAATTCGCAAATCTAAATCG
ATCG00190	rpoB_551	GAAAACCAGTAGGAATATGC
		TCCCCACCTACACAAGAAAATTG

ATCG00890	ndhB_467	CCGATGGAGAGAAGAACCTATG
		TATCCAGATAATAGGTAGGAGC
ATCG01010	ndhF_290	AAAACCTTCGCCGCATGTGG
		ATCAGAACCAAAATCCCAACAG
Northern blotting		
AT1G29910	LHCB1.2	GACTTTCAGCTGATCCCGAG
		CGGTCCCTTACCAGTGACAA
ATCG01080	ndhG	GGATTTGCCTGGACCAATAC
		TGACGAGCCACAGAAATTGC
ATCG01130	ycf1.2	AGAGCCACATGGCGAGATTT
		TGGGACCACTCGGGAAATTG
RIP-qPCR		
ATCG00950	23S_104766 and 23S_104856	GATACCTAGGCACCCAGAGAC
		CTACTAAGATGTTTCAGTTCGCCA
ATCG00950	23S_106558	CGGAAGGTTAAGGAAGTTGG
		GGAATTTCGCTACCTTAGGAC
ATCG01080	ndhG	TCGATACGTCATGGTACGGG
		TGACGAGCCACAGAAATTGC
ATCG01130	ycf1.2	ATGTACCAATGGAGCCTGGA
		GGATCAAAGCCATTTCATCGT
ATCG00280	psbC (negative control)	ACTTCCCCACCTAGCCACTT
		AGCCCAAAACTGCAGAAGAA
ATCG00020	psbA (negative control)	TTTCCGGTGCCATTATTCCT
		TCATAAGGACCGCCGTTGTA
ATCG00360	ycf3 (negative control)	CGGATGTCGGCTCAATCTGAAGG
		AGGGGTTTCGTTCTAATGCCCGA
EMSA		
ATCG00950	23S_104856	aagagacaaccuggcgaacugaaac
ATCG01080	ndhG_118454	agaaaaaaaucuguugauaaaugaa
ATMG00190	trnG.1	auuugggaauuucuccauccaucau
Unspecific competitor	For 23S_104856 and ndhG_118454	auucuuauguggcagucucuaguccacuagcuuuug
	For trnG.1	gcaucugaauuucauaaccaaucucgau
ATCG00270	Kim_RNA1	ggaaauccgucgauaucucu
ATCG00270_ mut	Kim_RNA3	ggaccgaaugaucuaucucu

Supplemental information - Chapter 2

Supplementary Material

Response of the organellar and nuclear (post)transcriptomes of Arabidopsis to drought stress

Duorong Xu[1], Qian Tang[1], Ping Xu[2], Anton R Schäffner[2], Dario Leister[1], and Tatjana Kleine[1,*]

*** Correspondence:**
Dr. Tatjana Kleine

Ludwig-Maximilians-Universität München (LMU)
Department Biologie I, Botanik; Großhaderner Str. 2, D-82152
Planegg-Martinsried Phone: +49-89/2180 74554; Fax: +49-89/2180
74599; E-mail: tatjana.kleine@lmu.de

Supplementary Material

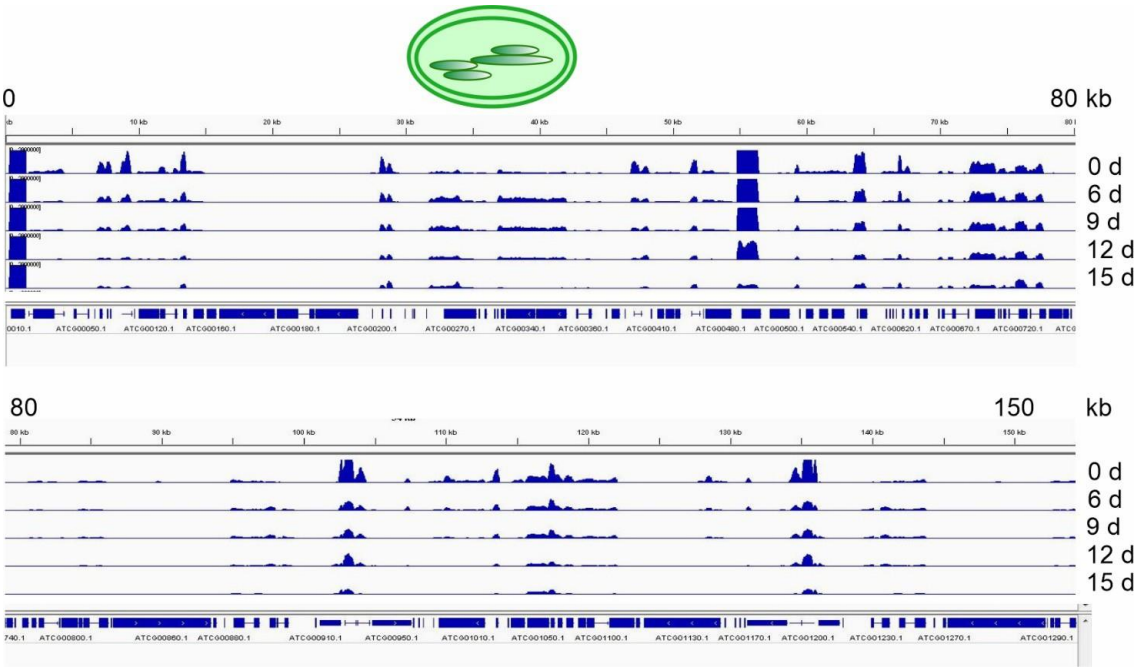

Supplementary Figure 1. Distribution of lncRNA-Seq reads across the chloroplast genome. The normalized read depths of transcripts detected in Col-0 plants under control (0 d) and drought conditions were visualized with the Integrative Genomics Viewer (IGV).

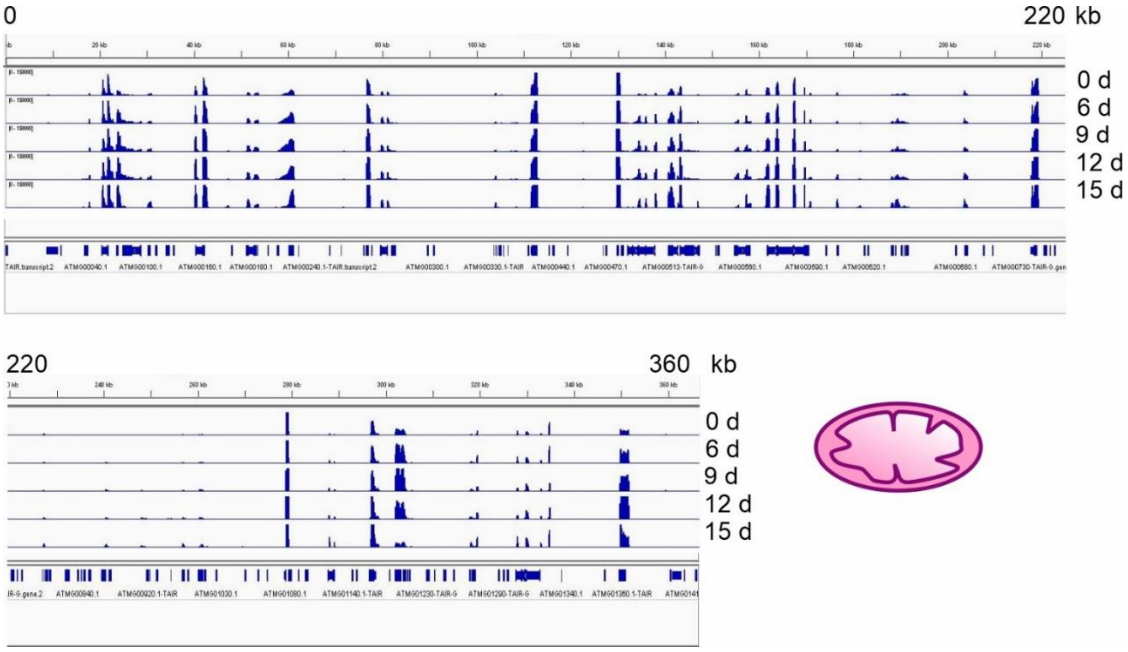

Supplementary Figure 2. Distribution of lncRNA-Seq reads across the mitochondrial genome. The normalized read depths of transcripts detected in Col-0 plants under control (0 d) and drought conditions were visualized with the Integrative Genomics Viewer (IGV).

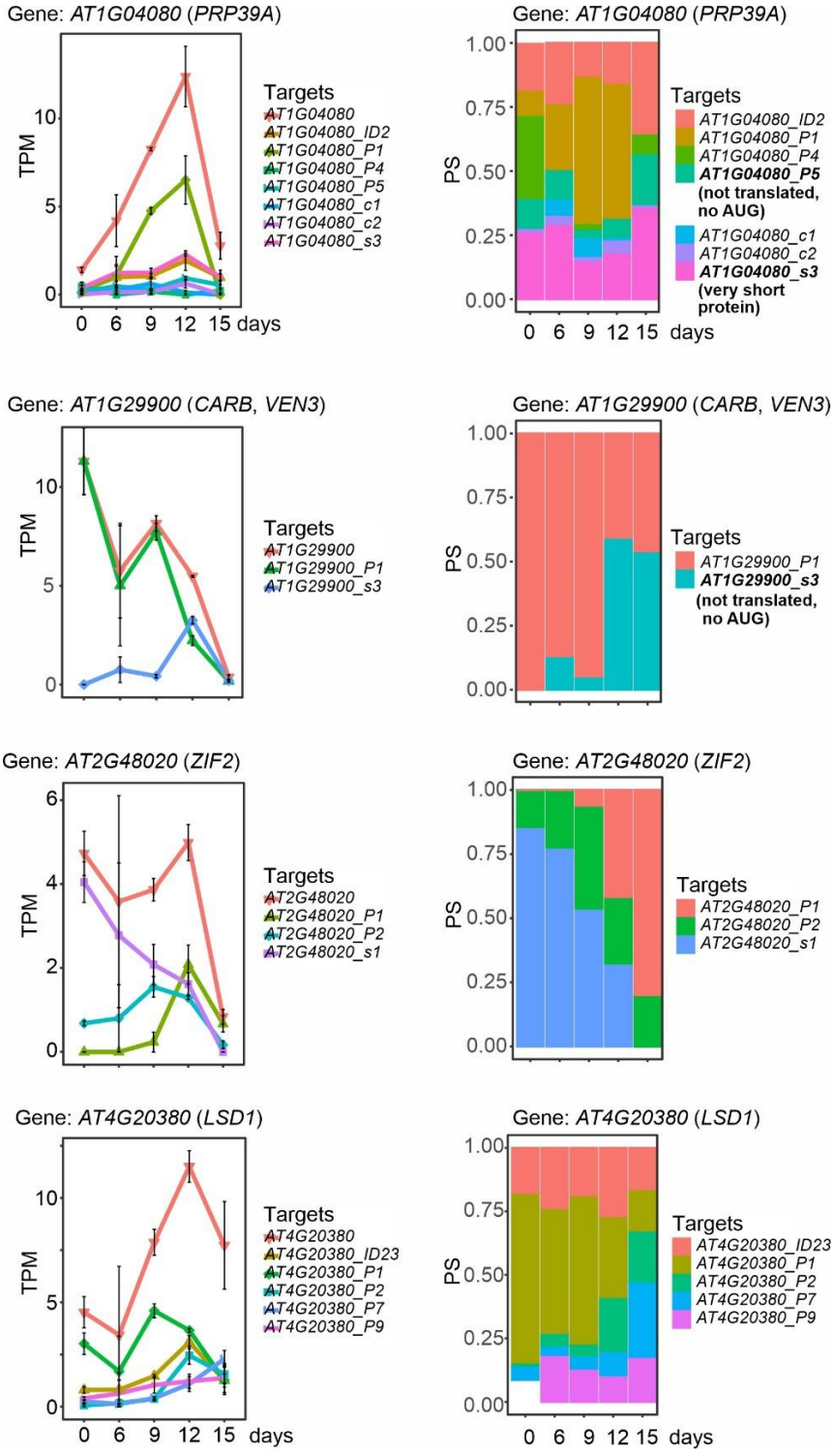

Supplementary Figure 3. Illustrations of further isoform switching (IS) events. Expression profiles of PRP39A, CARB, ZIG2 and LSD1 at the whole-gene level and at the level of detected transcript isoforms are shown. PS, percentage of expressed transcripts spliced; TPM, transcripts per million reads

Supplementary Tables

Supplementary Table 1. Primers used in this study.

Atg number	Description	Primer sequence (from 5' to 3')
qRT-PCR		
AT1G77080	*FLM-RT_F*	TCGCTGTTGTCGTCGTATCTGC
AT1G77080	*FLM-e1-e3-RT_R*	CGGCTTGAACAGCGCTTCTATCTC
AT1G77080	*FLM-e1-e2-RT_R*	CAATGATCTTGGAAATGTCGTCACCG
AT1G77080	*FLM-intr1-RT_R*	GAAGCTTCTATATGGAGAAAGTAA

In separate files:

Supplementary Table 2. Sequencing depth of lncRNA-Seq experiments. Long non-coding RNA sequencing (lncRNA-Seq) was performed with RNA isolated from 3-week-old Col-0 (Col) plants grown under optimal conditions (time-point 0 days; 0d) and after water had been withheld for 6, 9, 12 and 15 days, respectively (6d, 9d, 12d and 15d). Sequences were mapped and analyzed as described in Materials and Methods.

Supplementary Table 3. Genes differentially expressed under drought stress. Long non-coding RNA sequencing (lncRNA-Seq) was performed with RNA isolated from 3-week-old Col-0 (Col) plants grown under optimal conditions (time-point 0 days; 0d) and after water had been withheld for 6, 9, 12 and 15 days, respectively (6d, 9d, 12d and 15d). Sequences were mapped and analyzed with the 3D RNA-Seq pipeline as described in Materials and Methods.

Supplementary Table 4. Drought-stress marker genes. Lists of genes whose transcripts are regulated in the same direction (up or down) after 9, 12 and 15 days of drought stress in our dataset as well as in Kim et al. (2017).

Supplementary Table 5. Gene Ontology (GO) analysis of the nine clusters listed in Figure 1. Biological process (BP) and cellular component (CC) categories were identified with DAVID (Huang da *et al*., 2009) and REVIGO (Supek *et al*., 2011).

Supplementary Table 6. Abundance of chloroplast and mitochondrial transcripts. **(A)** Log_2 fold changes of RNAs encoded by the chloroplast genome. Note that analysis of tRNAs was excluded.

(B) Log_2 fold changes of RNAs encoded by the mitochondrial genome.

Supplementary Table 7. Differentially expressed transcript isoforms under drought stress.

Supplementary Table 8. List of differentially alternatively spliced (DAS) genes under drought stress.

Supplementary Table 9. List of genes that showed isoform switches (ISs) during drought stress.

Acknowledgement

I would like to express my sincere gratitude to everyone who contributed to and supported me throughout my doctoral study journey.

First, I would like to express my sincere thanks to Prof. Dario Leister for providing a well-organized lab environment, which greatly facilitated my experiments and research.

I am deeply grateful to my supervisor, PD Dr. Tatjana Kleine, for her invaluable guidance, support, and encouragement. Your expertise and unwavering support, especially during the challenging phase of changing my research topic, ensured that this work evolved into something both interesting and meaningful.

I would also like to acknowledge the efforts of my thesis committee members, Prof. Christian Schmitz-Linneweber and Prof. Ekkehard Neuhaus, for their thoughtful feedback and advice on the progress of my thesis.

Special thanks go to Dr. Penzler, Jan-Ferdinand, for his kindness in correcting my thesis. I also want to thank Katrin and Michi for their camaraderie and for making the research process both enjoyable and memorable. I am grateful to the gardeners for taking care of my plants, which saved me significant time and energy. I extend my thanks to my colleagues Duorong Xu, Vasil, and all the lab members for their daily help and support.

Beyond the scientific realm, my friends Ting Zhu (朱婷), Yun Yu (余韵), and Ruida Zhang (张睿达) have brought joy and delightful memories to this journey, making it all the more special.

I am also deeply thankful to my family, especially my grandmother Xiurong Wu (吴秀容), my aunt Jingyun Huang (黄锦云), and my parents-in-law Xueping Zhang (张雪萍) and Rongliang Xu (徐荣亮), for their love, trust and emotional encouragement.

Lastly, a heartfelt thank you to my husband, Ping Xu (徐平). The scientific discussions we had, the delicious meals you prepared, and the healing music you played have made this journey both colorful and enjoyable.